Article:
Horne, JE, Brockwell, DJ orcid.org/0000-0002-0802-5937 and Radford, SE orcid.org/0000-0002-3079-8039 (2020) Role of the lipid bilayer in outer membrane protein folding in Gram negative bacteria. Journal of Biological Chemistry. jbc.REV120.011473. ISSN 0021-9258

https://doi.org/10.1074/jbc.rev120.011473

Role of the lipid bilayer in outer-membrane protein folding in Gram-negative bacteria

Jim E. Horne[1,2], David J. Brockwell[1], Sheena E. Radford[1*]

From the [1]Astbury Centre for Structural Molecular Biology, School of Molecular and Cellular Biology, Faculty of Biological Sciences, University of Leeds, Leeds, LS2 9JT, UK; [2]Department of Biochemistry, University of Oxford, Oxford, OX1 3QU, UK

Running Title: *Lipid bilayers and the OM in OMP folding*

*To whom correspondence should be addressed: Sheena E. Radford: Astbury Centre for Structural Molecular Biology, School of Molecular and Cellular Biology, Faculty of Biological Sciences, University of Leeds, Leeds, LS2 9JT, UK; s.e.radford@leeds.ac.uk; Tel. (+44) 113 343 3170

Keywords: β-barrel assembly machinery (BAM) complex, outer membrane, membrane protein folding, protein-lipid interactions, Gram-negative bacteria, lipid membrane, folding kinetics, OMPome, antibiotic resistance, disorderase

ABSTRACT

β-barrel outer membrane proteins (OMPs) represent the major proteinaceous component of the outer membrane (OM) of Gram-negative bacteria. These proteins perform key roles in cell structure and morphology, nutrient acquisition, colonisation and invasion, and protection against external toxic threats such as antibiotics. To become functional, OMPs must fold and insert into a crowded and asymmetric OM that lacks much freely accessible lipid. This feat is accomplished in the absence of an external energy source and is thought to be driven by the high thermodynamic stability of folded OMPs in the OM. With such a stable fold, the challenge that bacteria face in assembling OMPs into the OM is how to overcome the initial energy barrier of membrane insertion. In this review, we highlight the roles of the lipid environment and the OM in modulating the OMP folding landscape and discuss the factors that guide folding *in vitro* and *in vivo*. We particularly focus on the composition, architecture and physical properties of the OM and how an understanding of the folding properties of OMPs *in vitro* can help explain the challenges they encounter during folding *in vivo*. Current models of OMP biogenesis in the cellular environment are still in flux, but the stakes for improving the accuracy of these models are high. Since OMP folding is an essential process in all Gram-negative bacteria, and considering the looming crisis of widespread microbial drug resistance, to bring down the powerful, OMP-supported barrier against antibiotics, we must first understand how bacterial cells build it.

Proteins which span lipid bilayers come in two flavours, either α-helical or β-barrels. While the cytosolic inner membranes (IM) of bacteria and the plasma membrane of eukaryotes are comprised exclusively of α-helical membrane proteins, β-barrel outer membrane proteins (OMPs) are found exclusively in the outer membranes (OM) of diderm bacteria, as well as in bacterially-derived eukaryotic organelles such as mitochondria and chloroplasts. The 'OMPome' (the complement of OMPs encoded for by a genome) of *E. coli* consists of a large number of proteins ranging in barrel size from 8 to 26 β-strands, and including monomers, small assemblies (dimers, trimers etc.), as well as oligomeric structures which can form up to 60-stranded pores (Figure 1). Some OMPs comprise only the integral membrane β-barrel structure, while others have soluble domains in the periplasm or on the extracellular surface of the OM. Some OMPs have low copy number, or can be absent in the OM under 'standard' growth conditions (e.g. the *E. coli* porin OmpN) (1–4), and others are present in large copy number (e.g.

OmpA is estimated to have >100,000 copies in the OM of *E.coli*, while OmpX, OmpC, and OmpF are estimated to have >20,000 copies each) (3–7). The functions of OMPs are also very diverse, including passive pores and ion channels (8–11), antibiotic efflux channels (12–15), nutrient uptake systems (16–18), maintenance of structural integrity (19–21), biogenesis and up-keep of the OM (22–26), host cell adhesion and invasion (27–29), biofilm formation (30–33), and cell defence (34, 35). Despite the enormous diversity of OMPs in *E. coli*, it is perhaps surprising that only two are essential: the 16-stranded BamA and 26-stranded LptD (36) (Figure 1). This is perhaps even more remarkable considering that LptD itself relies on BamA for its assembly (37). LptD's biological role is to insert the lipid component of the outer leaflet of the OM (22, 38). BamA (part of the β-barrel assembly machinery, BAM) is required to fold and insert most (but not all) OMPs into the OM *in vivo* (39) (Table 1). The importance of BAM for the biogenesis of the OM is illustrated by the observation that despite the evolutionary distance between bacteria and eukaryotes, a homologue of BamA, Sam50, is retained in all mitochondria (40). Although only BamA and LptD are essential in *E. coli* under laboratory conditions, it is likely that many more OMPs will be necessary for bacteria to survive, invade new niches, and thrive in diverse environments. Understanding how OMPs fold has been the goal of researchers for the last *ca*. three decades, since the first observations were made that OMPs are capable of folding spontaneously into reconstituted lipid bilayers (41). Initially, the study of the structure and folding mechanisms of OMPs lagged behind those of their α-helical membrane protein counterparts, since the latter are more abundant in eukaryotes, and were considered, initially at least, to be more important from the perspective of human health as half of all approved drugs target α-helical membrane proteins (42, 43). However, in the last 15 years it has become clear that OMPs are ubiquitous and some are essential in bacteria (i.e. BamA and LptD) or in mitochondria (i.e. Sam50 and Tom40) (22, 23, 44–47). Furthermore, the growth in antibiotic-resistant pathogens has highlighted the importance of the OM as a formidable barrier to the entry of antibiotics into bacteria, as well as a site of efflux out (48), and as a shield against recognition of surface epitopes by natural or designed antibodies (49–52). Hence, insights gained from studies of OMP folding and biogenesis are also vital for our understanding of human physiology (53) and will be key in guiding our choice of targets for the generation of new antibiotics and vaccines against Gram-negative bacteria (54). Consequently, a number of academic groups and drug companies have ongoing research projects targeting the essential OMPs BamA (the central β-barrel-containing subunit of BAM) and LptD (50, 52, 55–62), with at least six reports of inhibitors of their function in 2018-2019 alone (63–68).

This review aims to provide a holistic view of our current understanding of the process of OMP biogenesis including (1) the composition, physical, and chemical properties of the OM *in vivo*; (2) current knowledge of the determinants of OMP folding through *in vitro* studies; and (3) how OMP folding depends on parameters such as the lipid composition, physical environment, and the presence/absence of BAM. Although information is drawn from different organisms, we focus on OMPs and the OM of *E. coli*, due to the position of this bacterium as the *de facto* model organism for studying these processes.

Another brick in the wall: building the OM

In order to understand OMP folding and biogenesis, it is first important to review our current understanding of the composition and architecture of the environment in which this process takes place: the complex and crowded bacterial OM.

Lipid types found in the OM

The OM of Gram-negative bacteria is unusual in that it is a highly asymmetric lipid bilayer, comprising an inner leaflet enriched in phospholipids and an outer leaflet containing lipopolysaccharide (LPS) (Figure 2) (69). This is in contrast to the IM in Gram-negative and Gram-positive bacteria which mostly contain phospholipids mixed between both leaflets. In Gram-negative bacteria phospholipids in the OM generally have the canonical structure expected

of a phospholipid, containing two hydrophobic acyl chains, with different length and degree of saturation. These are connected via an ester linkage to a headgroup that can be zwitterionic, positively, or negatively charged (Figure 2). Cardiolipin (CL) is also found in the OM and has the appearance of a phospholipid dimer (Figure 2). LPS is a much bulkier molecule, made up of a variable number of acyl chains (between 4 and 8, depending on the species) (70). The acyl chain can vary in length both within each molecule and between species (e.g. $C_{10:0}$-$C_{14:0}$ in *Bordetella pertussis*, $C_{12:0}$-$C_{14:0}$ in *E. coli*, $C_{14:0}$-$C_{21:0}$ in *Chlamydia trachomatis*, $C_{14:0}$-$C_{28:0}$ in *Agrobacterium tumefaciens*) (71–74). Furthermore, the acyl chains of LPS are usually shorter than those of the average phospholipid and are almost always saturated (75) (Figure 2). The acyl chains in LPS are connected to a disaccharide diphosphate headgroup, which in turn is connected to a conserved 'core' region made up of chained sugar groups, and then finally a highly variable sugar-containing O-antigen region (Figure 2) (76, 77). Together these sugar regions convey a large net negative charge to the outer surface of bacteria (77).

Essentiality of specific lipids

E. coli is remarkably tolerant of modifications in its lipid biosynthesis pathways, with viable strains including bacteria in which synthesis of phosphatidylethanolamine (PE) (78, 79), phosphatidylglycerol (PG) and CL (80, 81), or CL alone (79, 82) is eliminated (see Figure 2 for the structure of common lipid types); phosphatidylcholine (PC) synthesis is induced synthetically (*E. coli* lacks PC in its IM or OM, although this phospholipid is present in some bacterial membranes) (83, 84); gluco- or galacto-lipids are utilised (85); or even archaeal lipids are incorporated into the membrane (86). Although these strains are able to survive under laboratory conditions, their growth and virulence is affected (in some cases severely), stress responses upregulated, and defects of varying acuteness are seen in the structure and permeability of the cell envelope (79, 87). The effect of such changes in lipid composition in the OM on OMP biogenesis has not been investigated in detail for all of these strains. However, in PE deficient strains OmpF folding is impaired in a titratable manner, with complete lack of PE reducing folding yields from ~100% in WT to <15% (79). Lack of CL causes less severe defects, but still reduces OmpF folding yields to ~25% (79) and has also been shown to cause mis-localisation of the OMP IcsA which normally resides at the cell pole in *Shigella flexneri* (87). Interestingly, in *E. coli* lack of CL causes severe distention/detachment of the OM from the IM at the cell poles, and CL and PG have been observed to accumulate at cell poles and division sites (88) suggesting a role for CL in maintaining cell shape and integrity at sites of negative curvature (89). PG null only mutants have not been described as CL utilizes PG for its biosynthesis. However, the creation of viable strains absent in PG synthesis also requires mutations in the major *E. coli* OM lipoprotein Lpp (Braun's lipoprotein) suggesting that lack of PG causes lethality primarily though lethal accumulation of Lpp at the IM (81, 90). The first step in lipoprotein maturation after translocation into the periplasm involves the transfer of a diacyl moiety from PG (91) and its absence presumably stalls maturation at this point. However, the OM lipoproteins LptE and BamD are essential in *E. coli* so the viability of these *lpp* mutant strains suggest alternate maturation pathways or sources of diacylglycerol must exist (92, 93). As BamA and LptD are essential OMPs, the fact that bacteria can still grow and divide in these strains (albeit poorly) suggests that other lipids can moonlight for the loss of PE, PG, or CL; or that there is no absolute need for a particular phospholipid type as a minimum requirement for OMP biogenesis in *E. coli*. Nonetheless, the severe defects observed in these strains show that outside the laboratory all these components are needed for bacterial viability. This highlights that while a stable bilayer is the minimum requirement to fold an OMP, to understand how OMP biogenesis occurs in biologically relevant environments consideration of the complexity of the OM environment is crucial.

Organisation of lipid types within the OM

The *E. coli* OM contains PE, PG, CL, and LPS (Figure 2). These lipid types are divided asymmetrically between the inner and outer leaflets of the OM, with the outer leaflet

containing almost 100% LPS, and the inner leaflet containing ~80% PE, ~15% PG, and ~5% CL (Figures 2 & 3). By contrast the IM also contains ~5% CL with a lower ratio of PE/PG of ~70%/25% (94). Although it is physically possible for phospholipids to flip from the inner leaflet to the outer leaflet, this process is likely to be intrinsically slow (occurring on the order of hours or longer in vesicles *in vitro*) (95, 96). However, this process may be accelerated under conditions of OM/bilayer stress, such as exposure to antimicrobial peptides, detergents, in strains with truncated LPS (see Figure 2), or after loss of OMPs, and is associated with increased permeability of the OM (48, 97–99). Regardless of such events, the asymmetry of the OM is actively maintained in *E. coli* by the Maintenance of Lipid Asymmetry (Mla) system which removes errant phospholipids specifically from the outer leaflet of the OM in order to maintain its barrier function (100–102).

The lipid acyl chain composition is diverse

The acyl chain composition of lipids in the OM of *E. coli* is more variable than that of their headgroups. The acyl chain composition of the OM is dependent on the growth conditions, with acyl chains varying in length from C_{12} to C_{18}, as well as in the degree of saturation or the presence of cyclopropyl modifications (Figure 2) (103–108). Lipidomics has provided insights into the range of acyl groups found in *E. coli* membranes. Early experiments in *E. coli* K1062 reported the presence of $C_{12:0}$, $C_{14:0}$, $C_{16:0}$, $C_{16:1}$, $C_{18:1}$, and cyclo-$C_{19:0}$ acyl chains in phospholipids from the IM and OM (109). Examining total lipid content in *E. coli* K-12 strain LM3118 grown at 37°C and harvested in stationary phase showed that the acyl chains of PE and PG lipids were comprised primarily of $C_{12:0}$, $C_{14:0}$, $C_{16:0}$, $C_{16:1}$, $C_{18:0}$, and $C_{18:1}$ (with $C_{16:0}$ being *ca.* three-times more abundant than the other acyl chains), with a lesser contribution from $C_{15:0}$, cyclo-$C_{17:0}$, and cyclo-$C_{19:0}$ (110, 111). These acyl chains are combined to form a large variety of phospholipid types, most containing at least one unsaturated acyl bond or cyclo-propyl group, although *di*$C_{16:0}$PE, *di*$C_{16:0}$PG, $C_{16:0}C_{14:0}$PG, $C_{16:0}C_{12:0}$PE, *di*$C_{14:0}$PE, and *di*$C_{12:0}$PE lipids were also observed. Despite cyclo-propyl acyl chain-containing lipids being relatively understudied, the most common lipid species detected under these conditions was $C_{16:0}$/cyclo-$C_{17:0}$ (Figure 2). Cyclo-propyl containing lipids are produced in large quantities in stationary phase cultures from the conversion of double bonds in unsaturated chains to cyclo-propyl groups (112, 113). Although the physiological functions of these modifications are unclear, they appear to be related to protection of the bacteria against a variety adverse environmental conditions (113), including acid shock (114, 115), osmotic shock (116), high alcohol concentrations (117), or high temperature (118). Furthermore, OMP folding in *E. coli* occurs primarily during exponential growth (119, 120), while expression is downregulated (121, 122) and OMPs are lost from the OM (123) when bacteria enter stationary phase. Thus, the relevance of this lipid modification for OMP biogenesis may be minor under favourable growth conditions.

Few studies have examined whether significant differences or biases exist between the acyl chain composition of phospholipids in the IM versus the OM of Gram-negative bacteria. Some have reported an enrichment of shorter acyl chains ($C_{12:0}$ and $C_{14:0}$) (109), saturated fatty acids (124), lyso-PE lipids (125), and $C_{16:0}$ acyl chains in the OM, and a depletion of polyunsaturated acyl chains (126), although these biases generally vary with growth conditions and it is unclear to what extent this simply reflects the presence of the lipid A component of the outer leaflet. Regulatory systems which alter the acyl chain composition of lipids specific to the OM are known for LPS, including enzymes which alter the acyl chains attached to lipid A in order to modulate the endotoxicity of this lipid type during growth in a host (69). Modulation of the acyl chain content of lipid A has also been shown to occur in *E. coli* when under selective pressure from an external insult by addition of a bactericidal BamA-specific antibody. This suggests a direct link between modulation of lipid content and a selective pressure to efficiently fold OMPs (63). However, it is not clear whether this change in lipid A reflects a need to aid the function of an essential BAM-client (e.g. LptD), is related to conformational changes in BamA, or is simply a response to a defective permeability barrier.

This diversity of acyl chain types gives *E. coli* a huge pallet of lipids with which it can tailor the biophysical properties of its membranes both globally and locally. This variety may allow it to deal with local minor deformations of the membrane, either due to random thermal fluctuations or the presence of membrane-bound or embedded proteins, as acyl chains can diffuse laterally and occupy the most energetically favourable position dependent on the match between their own physicochemical properties (length and saturation) and those of the membrane environment.

A crowded environment

Although the familiar fluid-mosaic model of membranes found in most textbooks depicts a biological membrane with just a few proteins floating in a 'sea' of lipid, the OM is markedly different, containing instead a much higher fraction of protein by weight, with lipid-to-protein ratios (LPR) (*w*/*w*) estimated to be between 0.14-0.36 (109, 127), corresponding to only 2-4 LPS and 4-10 phospholipid molecules per OMP (128). Estimates based on biochemical studies suggest that as much as 50% of the surface area (SA) of the OM may be occupied by OMPs (7), while AFM studies (127) (Figure 3B), extrapolation from the copy numbers of OMPs measured by proteomics (3, 4), and the above measurements of the LPR suggest that this value may be even higher. For example, a copy number of 100,000 for OmpA would imply ~6-20% of the SA of *E. coli* (dependent on the size of the bacterium) would be occupied by this protein alone. Hence the OM could be considered more like a protein-rich layer solubilised in a relatively small amount of lipid (Figures 3A & B). Despite the low LPR of the OM, the diffusion rates of OMPs in the OM of *E. coli* are similar to those of inner membrane proteins (IMPs), but are, on average, slower (diffusion coefficients of 0.006-0.15 $\mu m^2/s$ for OMPs versus 0.001-0.4 $\mu m^2/s$ for IMPs) (120, 129–141) (Figure 4A). For comparison, the length elongation rate of *E. coli* alone is ~0.006 μm/s (142), while the diffusion coefficient of LPS in the OM of *Salmonella typhimurium* is ~0.00005-0.02 $\mu m^2 s^{-1}$ (for O-antigen containing or truncated 'deep rough' LPS, respectively (Figure 2)) (143, 144), lipid probes in the IM of *E. coli* ~0.8-1.5 $\mu m^2/s$ (133, 145, 146), and the periplasm, cytoplasm, and buffer ~3, 0.4-9, and ~87 $\mu m^2/s$, respectively (130, 139, 147–151) (Figure 4B). What particularly distinguishes OMPs from IMPs is their restricted diffusion areas, with diffusion being confined within clusters in the OM, compared with free diffusion of most IMPs in the IM (120, 137, 152, 153). These observations can be explained by the propensities of OMPs to form clusters (119, 120, 127, 152–159) and/or to interact strongly with LPS or components of the cell envelope (160, 161). OMPs which have a lower tendency to cluster and/or interact with cell envelope components less strongly may exhibit higher diffusion coefficients, but will ultimately become 'corralled' within OMP-LPS domains. On this point, an abundance of clustered OMPs with low mobility may make the OM locally rigid. Indeed, molecular dynamics (MD) simulations have shown that membranes containing 8 to 12-stranded OMPs are much stiffer than membranes containing only DMPC (*di*$C_{14:0}$PC) (128). However, simulations investigating larger length scales have shown that crowding a bilayer with some OMPs (i.e. BtuB), but not others (i.e. OmpF), can reduce the global bending rigidity of a POPE ($C_{16:0}C_{18:1}$PE)/POPC ($C_{16:0}C_{18:1}$PC) membrane (162) – an effect which would explain how a cell with a protein-rich OM could still maintain its shape. An interesting alternative possibility to explain the potentially incompatible concepts of OMP folding and a protein-dense, lipid-poor OM would be to consider the OM as an inhomogeneous mixture of protein and lipid (Figure 3C). The view of OMP monomers or trimers, well-solubilised with lipid would leave little bulk lipid available for nascent OMPs to fold. However, by clustering OMPS together into regions resembling 2D crystals (i.e. forming regions highly enriched with OMPs and little to no lipids – a local LPR closer to 1:1 (mol/mol)) sufficient lipid-rich regions would be created to enable OMP folding and insertion (Figure 3B+C). Regardless of which model is correct, this locally stiff, crowded, and confined environment, with a relative paucity of free lipid, poses a challenging environment into which OMPs must fold.

More than a mix of lipid types

The physical properties of lipid membranes

Lipid bilayers can be characterised by a number of physical, mechanical and chemical parameters, including stored curvature elastic stress (lateral pressure), melting temperature, the bulk lipid phase, the presence of lipid rafts, membrane viscosity, and headgroup charge (163–165) (Figure 5). Many of these properties are inter-related and can be modulated by altering the acyl chain composition and/or the phospholipid headgroup, and by altering the relative amounts of phospholipid, CL, and LPS (166–170). Stored curvature elastic stress makes membranes more rigid and less elastic in terms of their ability to deform or bend. This property can be introduced by the presence of non-bilayer forming lipids in otherwise bilayer-forming membranes (Figure 5). For example, PE lipids create negative curvature, while PG and PC lipids have zero or low spontaneous curvature which allows them to readily form bilayers (171). Doping bilayers containing PC or PG with PE or CL generates a tension in packing of the different lipid types, creating a crowding, or pressure, near the centre of the bilayer where each leaflet meets (Figure 5), which is further altered by the length of the acyl chains (with shorter chains reducing this elastic stress) (171).

The lipid phase of a membrane is also dependent on its lipid composition and on the temperature (Figure 5). Bilayers exist primarily in one of two major states, a solid 'gel' phase in which the acyl chains are tightly packed and the mobility of lipid molecules is low, and a 'liquid' phase, where lipid mobility is higher (172–174). Furthermore, analogous to the familiar phase change of ice to water, lipids in a gel phase membrane can 'melt' to become the liquid phase at a temperature characteristic of the particular lipid type – called the transition temperature, T_m. Lipid mixtures can also adopt a 'liquid-ordered' phase (with the classical pure liquid phase described as 'liquid-disordered'). This liquid-ordered phase contains lipids which are highly mobile, but have well-ordered acyl chains and is often associated with the formation of lipid rafts in cholesterol-containing membranes in eukaryotes (175–177). Although sterol lipids are rare in bacteria, CL may play a similar role in increasing lipid order and there is evidence that CL can participate in the formation of rafts/domains in membranes *in vitro* and *in vivo* (Figure 5) (although it is likely this mechanism is distinct from that of cholesterol) (178, 179). *In silico* CL has been observed to form clusters under patches of LPS in simulations of bacterial OMs in a role that may compensate for packing defects in the outer leaflet of the OM (180, 181).

The physical properties of native lipid extracts

The OM differs from the IM in its highly asymmetric structure, large fraction of proteins by weight, permeability to small molecules (<600 Da), and lack of energisation across it (11, 69, 109, 127, 182). However, relatively little is known about how these unique features of the OM affect its mechanical properties and how this differs from the IM. *E. coli* is known to alter the lipid content of its membranes, particularly the length and degree of saturation of acyl chains, in response to changes in growth temperature. This process, termed 'homeoviscous adaptation' (183), suggests that bacteria actively maintain their membranes at a constant level of 'fluidity', or in a particular phase, that enables them to adjust to different environments. For example, while total lipid extract from *E. coli* K-12 W3110 showed approximately the same headgroup content (with a minor monotonic increase in CL and decrease in PG) when grown at 30 °C, 37 °C, 42 °C, or 45 °C (184), the ratio of saturated over unsaturated acyl chains increased with temperature. This suggests a change to a more 'rigid' mixture of phospholipids at higher growth temperatures in order to balance the increased fluidity caused by the input of thermal energy.

Membrane lipid properties can be probed using fluorescent reporter dyes which partition into membranes (either globally or into specific lipid phases) and alter their excitation or emission properties according to the local lipid environment. Hence, these dyes can be used as reporters of membrane viscosity, degree of hydration, phase, and mobility (185). The fluorophore laurdan partitions into membranes through its acyl tail, while its naphthalene-based headgroup resides in the interfacial region of bilayers where its fluorescence excitation and emission spectra are sensitive to the degree of

hydration of the bilayer allowing it to report on the phase and order of lipids in a bilayer (186). Using laurdan a T_m of *E. coli* total lipid extract of <14 °C was determined for bacteria grown at 30 °C or 37 °C, while the T_m was higher (T_m ~20-22 °C) for bacteria grown at 42 °C, and elevated again (T_m ~27 °C) for bacteria grown at 45 °C (184). This shows that the lipids in *E. coli* are natively in the liquid phase, and their T_m is as much as 20 °C below the growth temperature. However, when the OM and IM are considered separately it becomes clear that 'global' lipid properties do not accurately capture the differences between these two different membranes. Deuterium NMR studies, used to measure the order of acyl chains, found that lipids in an OM preparation of *E. coli* L51 were less fluid than those from the IM, and that the T_m was ~7 °C higher than in the IM (187, 188). Electron spin resonance experiments on IMs and OMs of *E. coli* W1485 doped with a spin-labelled stearic acid probe found the T_m of the OM (26 °C) to be ~13 °C higher than the IM (13 °C) when the bacteria were grown at 37 °C (167). Fluorescence polarisation studies using IM and OM extracts from *E. coli* B doped with parinaric acid also found that the phase transition of the OM was ~15 °C higher than the IM, initiating its phase transition at 40 °C (189).

E. coli membranes in situ

Few studies on the properties of bacterial membrane lipid order (or phase) *in vivo* have been reported to date, but current data suggest that the organisation of the OM is more complicated than that derived using lipid extracts, as described above. Differential scanning calorimetry studies on whole cells of *E. coli* W945 grown at 20 °C or 37 °C observed two reversible transitions, one well below the growth temperature which was suggested to correspond to the IM, and another slightly above the growth temperature which was assigned to the OM (190). Experiments on fixed cells using laurdan and the dye 1,3-diphenyl-1,3,5-hexatriene (DPH) as a probe of local viscosity (185) have shown that *E. coli* membranes are predominantly in the liquid phase. However, these experiments also revealed that these membranes are heterogeneous, and contain at least two distinct phases – one more liquid, and one less so, possibly indicating the presence of distinct lipid domains (191). However, an alternative explanation of these data is that that they reflect a difference between the IM and the OM, since it is not clear to which membrane these probes localise. Indeed, whilst early studies suggested that these dyes (and others, including FM 4-64) localise primarily to the IM (192), it is now known that FM 4-64 partitions specifically into the OM immediately after labelling (19), and DPH may equilibrate between both membranes (193, 194), or be trapped mainly in the first hydrophobic surface encountered (195). Measurements of membrane viscosity using 'molecular rotor' dyes such as BODIPY C10 (viscosity alters the fluorescence lifetime of the probe) showed that the IM of *E. coli* is more viscous than previously believed, with an average viscosity of 980 cP for intact *E. coli*, 950 cP for spheroplasted cells at 37 °C, and 200 cP for large unilamellar vesicles (LUVs) of *E. coli* total lipid extract at 37 °C (146). By contrast, a lower viscosity (~60 cP) was consistently observed for 200 nm LUVs formed from DLPC (diC$_{12:0}$PC), DMPC (diC$_{14:0}$PC), POPC (C$_{16:0}$C$_{18:1}$PC), or DOPC (diC$_{18:1}$PC) in their liquid phase at 37 °C (196) (Figure 4C). Although not yet measured directly, the lower diffusion coefficients of OMPs compared to IMPs (Figure 4A,B) suggests that the viscosity of the OM may be even higher still, and this is a characteristic that model lipid membranes commonly used for OMP folding studies (see below) clearly cannot capture.

The influence of LPS on the mechanical properties of the OM

On the basis of the physicochemical properties of LPS extracts (which generally show T_m values at or above the growth temperature) (197–201), and those of the OM (discussed above), some authors have argued that the OM is more likely to exist in the gel phase at physiological temperatures (48). However, the exact thermotropic response of LPS in the outer leaflet may vary depending on the composition (particularly the presence of H-bond donors and acceptors) and size of the polysaccharide region of the LPS molecules incorporated (48, 200, 202, 203). *In vitro* models of the OM using an asymmetric bilayer

deposited on silicon or lipid-coated gold surfaces showed that the membrane has unusual mixed characteristics with elements of both liquid and gel phase lipids (204, 205). The OM in these studies comprised 'rough' LPS (containing the conserved polysaccharide core but lacking the O-antigen) (Figure 2) in the outer leaflet and phospholipid (DPPC [*di*$C_{16:0}$PC]) in the inner leaflet, with lipid order parameters measured using neutron reflectometry and attenuated total reflection Fourier transform infrared spectroscopy (ATR-FTIR) (204). Two transition midpoints (T_m) were observed, one just below (~36 °C) the physiological growth temperature of *E. coli* (37 °C) for the outer-leaflet of LPS, and the other above the T_m (~39 °C) for the inner-leaflet comprising DPPC (*di*$C_{16:0}$PC) (204). Even though the composition of the inner leaflet lipids and LPS differ *in vivo* from those used in this study, the results suggest that the LPS component of the asymmetric OM may confer greater rigidity to the OM. This agrees with deuterium NMR studies of preparations of *E. coli* OM and IM which found that at a given temperature, phospholipids were more ordered and a larger fraction were in the gel phase in the OM than the IM (188, 206). However, it should be noted that extraction of the OM likely causes mixing of the inner and outer leaflets, reducing the asymmetry (207).

The fluidity of the OM of *E. coli* may also be controlled by temperature-dependent modification of LPS in the outer leaflet. The *lpxT* gene in *E. coli* transfers a phosphate group onto lipid A which may alter the rigidity of the OM and expression of this gene is regulated by an mRNA thermostat (208). LpxT is an IM protein which covalently modifies LPS before it reaches the OM. The protein was shown to be stable between 28 °C to 42 °C, however, its mRNA levels fall dramatically across this same temperature range (208). Another LPS biosynthesis pathway gene, *lpxP*, replaces the $C_{12:0}$ chain in *E. coli* lipid A (which is normally installed by *lpxL*) with a $C_{16:1}$ chain, but expression of this protein is only induced at low temperature (12 °C) and may also be regulated by an mRNA thermostat similar to *lpxT* (209). *Francisella novicida* synthesises lipid A with shorter acyl chains at low growth temperatures (25 °C *cf.* 37 °C), an effect which has been linked to both the differential expression and enzyme activity of the *lpxD2* and *lpxD1* genes (which add different length acyl chains to lipid A) at 25 °C and 37 °C, respectively (210). In *Yersinia pestis*, the *lpxR* gene which is responsible for the removal of acyl chains from lipid A, is inactive at 21 °C (resulting in a hexa-acylated LPS), but functional at 37 °C, resulting in a tetra-acylated LPS in the OM of bacteria grown at this temperature (211). The deacylase enzyme and OMP, PagL, alters lipid A through the removal of acyl chains. The activity of this enzyme in *Pseudomonas aeruginosa* is also affected by growth temperature, with activity falling at low growth temperature (≤ 21 °C) (212). The extent to which these temperature-dependent modifications are a mechanical response to maintain or alter membrane rigidity/fluidity, or an immune-modulating response triggered by the detection of a host environment, or both, remains unclear (213). Despite this, it is likely that the structure and mechanical properties of LPS are important for OMP folding. For example, genetic alterations to the biosynthetic pathway of LPS, which cause changes in its degree of acylation or its sugar headgroup have been shown to cause severe defects in the biogenesis of OMPs (214–216).

The effect of asymmetry

The asymmetric architecture of the OM with an inner leaflet containing canonical phospholipids and an outer leaflet containing LPS with its highly acylated lipid A attached to large sugar groups that protrude into solution, impacts the physical properties of the OM and creates a lipid environment that is very different to that of the IM *in vivo* and vesicles of lipids commonly used in *in vitro* experiments. Representative models of the OM have been built *in silico* and studied using coarse-grained molecular dynamics (CG-MD) and atomistic molecular dynamics (A-MD). A model was built of the *Pseudomonas aeruginosa* PAO1 OM, with an LPS outer leaflet and a DPPE (*di*$C_{16:0}$PE) inner leaflet and studied by A-MD (217). At 37 °C molecules of DPPE in the inner leaflet showed diffusive movement consistent with a liquid phase, whereas LPS in the outer leaflet showed an order of magnitude lower mean-square displacement. Despite this low

lateral mobility, calculation of the lipid order parameters of the acyl tails of LPS indicated they are fluid and not ordered as would be expected for lipids in the gel phase (217). Similar results have been observed in other A-MD simulations of *E. coli* and *P. aeruginosa* OMs with an outer leaflet containing LPS with a short O-antigen region (218, 219) or a 'rough' LPS (219, 220) (Figure 2), and an inner leaflet comprised of a 75/20/5 (mol/mol) mix of PPPE ($C_{16:0}C_{16:1}$PE)/PVPG ($C_{16:0}C_{18:1}$PG)/CL. CG-MD simulations of the *E. coli* OM with a DPPE (*di*$C_{16:0}$PE) inner leaflet and an outer leaflet containing a different ratios of LPS/DPPE (*di*$C_{16:0}$PE) from 10/90 to 100/0 (mol/mol) showed that increasing the fraction of LPS lowered the simulated T_m from 73 °C to 15 °C (221) (for reference, a symmetric bilayer composed solely of DPPE has an experimental T_m of ~64 °C showing inter-leaflet coupling can have hard-to-predict consequences on phase behaviour) (222). A-MD simulations of a model of a *P. aeruginosa* OM containing only lipid A in the outer leaflet and a mix of DPPE (*di*$C_{16:0}$PE), DPPG (*di*$C_{16:0}$PG), DOPE (*di*$C_{18:1}$PE), and DOPG (*di*$C_{18:1}$PG) in the inner leaflet, showed that the acyl chains of lipid A were also consistent with a liquid phase, but were overall less disordered than observed with larger sugar regions – again emphasising the importance of the polysaccharide region of LPS in modulating its packing behaviour (223). Other CG-MD experiments showed *E. coli* asymmetric membranes with a lipid A outer leaflet and a DPPE (*di*$C_{16:0}$PE) inner leaflet had a lower T_m than a 'rough' LPS outer leaflet and DPPE (*di*$C_{16:0}$PE) inner leaflet (~41-46 °C versus ~55 °C) (224), although it is not clear why the T_m values are much higher in these simulations than observed previously from the same group (221). Preparations of the OM and IM from *E. coli* J5 doped with spin label probes showed that membrane order is higher, and lipid mobility lower, in the OM and the magnitude of this difference decreased when a large fraction of LPS is removed (225). Furthermore, in the absence of galactose this strain is unable to synthesise the full polysaccharide region and produces a short 'rough' LPS (Figure 2) (226). The presence of the O-antigen was shown to confer even greater rigidity to the OM extracts than when they contained only truncated 'rough' LPS (225). Deuterium solid-state NMR experiments on multilamellar vesicles containing a mix of partially deuterated DPPC (*di*$C_{16:0}$PC) and 'rough' LPS from *E. coli* J5 or *E. coli* EH100 also found an 'ordering' effect on the acyl chains of DPPC conferred by LPS (227). Despite this ordering of acyl chains, experiments with SUVs composed of *E. coli* B LPS and phospholipid extract doped with spin-labelled PE and PG lipids, and *S. typhimurium* OM lipid preparations doped with a spin-labelled stearic acid probe, found that phospholipids remained freely diffusive and segregated away from LPS (197, 228, 229). The slower diffusion of phospholipids in the inner leaflet of the OM observed in the previous study (which retained its complement of OMPs) (225) may therefore be due to the transient clustering and reduced diffusion of lipids around embedded OMPs (157, 230–232). These *in vitro* studies, although not on fully asymmetric membranes (207), broadly validate the observations of the above *in silico* studies.

Measurement of water permeation in *P. aeruginosa* PAO1 LPS (outer) – DPPE (*di*$C_{16:0}$PE) (inner), *P. aeruginosa* LPS (outer) – PPPE ($C_{16:0}C_{16:1}$PE)/PVPG ($C_{16:0}C_{18:1}$PG)/CL (inner), and *E. coli* LPS (outer) - PPPE/PVPG/CL (inner) asymmetric bilayers by A-MD showed that the outer leaflet is relatively permeable to water when compared with the inner leaflet (with water reaching the terminal methyl groups of lipid A acyl chains) with both 'rough' LPS and LPS containing an O-antigen region (217, 219, 220, 233). This polarity gradient is also apparent through interactions between loop regions of OMPs and charged and polar groups on LPS which have been observed by A-MD and CG-MD (49, 181, 218–220, 224, 234–245), and specific LPS binding sites which have been validated experimentally for trimeric porins such as OmpF (6, 160, 246–249). One area which remains understudied but warrants further investigation is the effect of the acyl tails of lipoproteins in the inner leaflet of the asymmetric OM on membrane properties. The copy number of lipoproteins at the IM is small enough to, presumably, have a negligible effect on the membrane's bulk physicochemical properties. However, at the OM there may be

over 1 million lipoproteins anchored to the inner leaflet, composed primarily of Lpp (Braun's lipoprotein) – one of the most abundant proteins in *E. coli* – and Pal (3, 4, 250, 251). Each lipoprotein is tri-acylated at an N-terminal cysteine (91), and each acyl chain can be approximated to occupy ~0.28 nm^2 in a bilayer (70, 233, 234, 252–256). Assuming a lower bound on the surface area of an average *E. coli* as 3.7 μm^2 and an upper bound of 13 μm^2 (257–259), and the total area occupied by lipoprotein tails similarly bounded between 0.25 μm^2 (3×10^5 proteins) and 1.1 μm^2 (1.3×10^6 proteins) (3, 4), we come to an estimate of 2-30% of the inner leaflet of the OM occupied by these lipid anchors. Lpp and Pal both bind peptidoglycan through their protein domains. This interaction restricts their mobility (and therefore the lateral mobility of their lipid anchors), stiffens the OM, and the protein itself physically occludes the headgroups of the OM inner leaflet lipids (142, 260, 261). The impact that this has on the bilayer properties of the OM requires further study, but the presence of these lipoproteins would act to further reduce the 'accessible' surface for OMPs to bind and initiate folding.

Just as early *in vitro* experiments on synthetic lipid vesicles allowed hypotheses to be generated about the properties of biological membranes, we can look to *in vitro* experimental models of asymmetric phospholipid membranes to infer information about how asymmetry may affect the OM. These systems remain experimentally challenging due to problems with mixing/scrambling of the inner and outer leaflets in both surface-deposited (262, 263) and liposome-based asymmetric membranes (264), as well as difficulties in accurately controlling the composition of the outer leaflet in asymmetric liposome-based studies (265, 266). Nonetheless, such studies have suggested that asymmetry results in coupling between leaflets which alters the physical properties of the bilayer distinctly from those of the same lipid types mixed symmetrically. These include changes to the membrane potential difference, lateral pressure differential, and the packing of lipids (267–271).

Synthesising the data described above from *in vitro* and *in silico* studies allows insights into the view of the membrane encountered by a nascent OMP as it approaches, and is inserted into the OM. As the OMP approaches and moves through the membrane it begins folding on a 'typical' liquid disordered bilayer leaflet where phospholipids are free to diffuse before entering a region of low lateral mobility and increased hydration in the outer leaflet. These gradients of lateral mobility, lipid packing, hydration, and lipid headgroup polarity as an OMP inserts across the membrane normal could help to stabilise the tertiary structure of OMPs, particularly the hydrophilic loop regions (which can be >20 residues in length) (272), and drive the folding of the β-barrel domain to completion. Overall, therefore, the above studies have shown that the physical properties of the OM are highly complex and can vary dependent on the underlying lipid phase and the elastic stress, as well as the presence of OMPs and lipoproteins, and the LPR (146, 185, 273). These parameters, in turn, can be tuned by the lipids incorporated into each leaflet, especially by modifications to the LPS in the outer leaflet of the OM. Hence bacteria have to be adaptable so that they can form and maintain their OM whatever the nature of their environment and the environmental stresses that they encounter.

Membrane-spanning OMPs need to insert through both leaflets of the OM to adopt their native, functional folds, yet how this unique asymmetry and changing lipid content of the OM affects the folding and function of OMPs is currently unknown. We now need to take a deeper look into what we know about OMP folding, starting with the basics and then building more complexity into experimental and theoretical models to allow us to understand how the unusual properties of the OM might influence the process of OMP biogenesis in bacteria.

How do OMPs fold?

30 years of experiments on OMP folding in vitro

Likely due their high thermodynamic stability ($\Delta G°_F$: -10 to -140 $kJ.mol^{-1}$) (274–283), relatively low hydrophobicity (by all-residue average on the Kyte-Doolittle scale most OMPs are hydrophilic due their alternating hydrophobic membrane facing/generally hydrophilic lumen facing pattering), and ease of recombinant expression and purification, OMPs

are unusually tractable models for *in vitro* studies of membrane protein folding. The first published study on the successful folding of OMPs *in vitro* was carried out in 1978, when it was shown that SDS-boiled and denatured OmpA (Figure 6) could be refolded with high yield into LPS (but not into solutions containing total *E. coli* phospholipids, DMPC (*di*$C_{14:0}$PC), or the sugar moiety of LPS) (284). This refolded OmpA was shown to be natively structured since it had regained function (activity in phage receptor binding assays), was protected from protease digestion, and migrated at an anomalous molecular weight in SDS polyacrylamide gels when loaded without boiling (cold SDS-PAGE) (284). Hence, the stage was set for detailed studies of the mechanisms of OMP folding, at least for this, and other small (8 stranded) OMPs.

The next major breakthroughs in our understanding of OMP folding were made in the 1990s when it was shown that OmpA and an unnamed porin could be spontaneously refolded *in vitro* into detergent (octyl glucoside, OG), small unilamellar vesicles (SUVs) of DMPC (*di*$C_{14:0}$PC), or mixed lipid-detergent micelles (octyl-poly-oxyethyleneoxide, C_8POE, and soybean lecithin) in the presence of SDS without the addition of an external energy source or other proteins (285–287). Soon after, several groups began to experiment with the refolding conditions to identify the determinants that allow OMPs to attain their native structure. These studies showed that detergents are required to be above their critical micelle concentration (CMC) for successful OMP folding (288, 289). This highlighted the importance of a surface to initiate folding and showed that simple binding of hydrophobic molecules around an unfolded OMP chain is insufficient to enable folding. Instead, some degree of pre-organisation is required. These studies also showed that folding of OMPs *in vitro* is a remarkably slow process (most OMPs taking on the order of minutes to hours to fold), too slow to be physiologically relevant (the doubling time of *E. coli* is ~20 mins at 37 °C). They also showed that refolding yields are improved by the addition of urea, implying that the OMP folding landscape contains kinetic traps and/or off-pathway intermediates or aggregates which can be suppressed by the addition of chaotrope (288, 290). These experiments also showed that the β-barrel transmembrane fold is extremely stable once formed, with native OMPs being resilient to denaturation by SDS (unless heated to high temperatures), enabling kinetic measurement of folding using cold SDS-PAGE (41, 284, 291). This is due to the high kinetic barrier to unfolding in SDS (on the order of years at 30 °C for OmpA) (285, 292).

Due to their high kinetic and thermodynamic stability, high concentrations of denaturant often fail to unfold OMPs which have been refolded into detergent micelles or lipid bilayers. For example, OmPLA remains enzymatically active in 8M urea and in 6M guanidine-HCl (288). Experiments measuring the activity of OmPLA following refolding into LPS and a range of detergents, showed that the protein can not only re-acquire a stable fold, but also that it regained its phospholipase activity confirming reversible folding to a functional state (288). Thus, OMPs obey Anfinsen's dogma that all the information for a protein to reach its thermodynamically stable native structure is contained in its amino acid sequence (293).

First glimpses of an OMP folding mechanism

The next era of work on OMP folding focussed on attempts to determine the mechanisms of folding, including why the process is so slow, whether partially folded intermediates are formed, the nature of folding transition states, and the role of the protein sequence, lipid composition, and folding factors (including BAM and molecular chaperones) in the folding process. In some of the earliest studies of this kind, Surrey *et al*. (287) measured the kinetics of OmpA folding into SUVs formed from 95% DMPC (*di*$C_{14:0}$PC)/5% DMPG (*di*$C_{14:0}$PG) (mol/mol) at a temperature above the lipid T_m by rapid dilution from urea *in vitro*. The techniques employed and optimised in these early studies of OMP folding form the toolset used for such studies to this day (294). They also reinforced the idea garnered from studies on the folding of water-soluble proteins (295–298) that insights into the mechanisms of folding can be best learned by taking a kinetic approach to dissect each step in the folding pathway. These methods include: (i) monitoring the change in

tryptophan (and/or tyrosine) fluorescence as an OMP folds from aqueous solution into a non-polar membrane (Figure 6 shows the location of aromatic residues on OmpA); (ii) measuring the formation of secondary structure using far UV circular dichroism (CD), and (iii) following the formation of SDS-resistant molecules (presumably containing a correctly folded β-barrel domain) using cold SDS-PAGE (287, 299). This work showed that OmpA folds into lipid bilayers *in vitro* via a multi-phasic mechanism involving rapid hydrophobic collapse that occurs in the experimental dead-time (~1 s), followed by two slower phases occurring in minutes (phase 1) and tens of minutes (phase 2) corresponding to structural rearrangement and concurrent formation of secondary and tertiary structure (Figure 7A) (287). It was also shown that pH affects the yield and rate of OMP folding, with pH values close to the isoelectric point of OmpA (pI ~5.7) increasing the folding rate, but decreasing the folding yield. The average pI of the OMPs shown in Figure 1 is ~5.4 and the environment in which *E. coli* has evolved (the large colon) is mildly acidic (pH 5.5-7.5) (300) suggesting *E. coli* has adapted to favour rapid folding and has systems to handle or circumvent the lower yields. Higher LPRs were also shown to increase the folding rate and yield, consistent with models suggesting that the OMP first binds to the surface of the lipid bilayer before folding and insertion are completed (287, 301–303). Indeed, refolding studies of OmpA into lipids above their T_m confirmed this membrane-binding step with elegant experiments using membranes composed of lipids which had been brominated at different positions along the acyl chain (bromination quenches fluorescence from tryptophan only when in close proximity thereby allowing depth-dependent changes in fluorescence) (304, 305). Earlier data from ATR-FTIR studies showed that this membrane-adsorbed (but not stably integrated) folding intermediate had significant β-sheet content, with β-strands that have still to adopt the orientation found in the native β-barrel (306). Finally, the finding that tryptophan residues located in β-strands, near extracellular loops, or in intracellular turns show similar rates of membrane insertion (judged by tryptophan fluorescence quenching) suggested that folding occurs via a concerted mechanism in which all four hairpins of this 8-stranded OMP move synchronously across the bilayer (301), increasing in tilt angle as the protein becomes fully membrane embedded (306). More recent experiments employing single-Cys single-Trp variants of OmpA labelled at the Cys with Trp-quenching nitroxyl spin labels have shown that despite being concerted, OmpA's β-strands form in a particular order (307), with β-strands initially associating with each other at their 'extracellular' sides like a tipi (i.e. before the 'periplasmic' side forms) (Figure 7A, step 4) and showing that the N- and C-terminal strands are already in close proximity in the membrane-adsorbed state (Figure 7A, step 3), providing evidence against models invoking β-barrel closure as the last step (307). These experiments also failed to detect native β-strand association in aqueous solution, ruling out models in which the OmpA β-barrel 'pre-folds' in solution before inserting as a single unit into the membrane. This complex, multistep process where formation of secondary and tertiary structure is coordinated contrasts markedly with the two-stage mechanism proposed for α-helical membrane proteins in which the formation of α-helices precedes formation of the native tertiary structure (308, 309). The overall general model for spontaneous OMP folding *in vitro* is summarised in Figure 7A.

The role of the membrane in OMP folding

Studies varying the lipid headgroup, acyl chain length, lipid phase, membrane curvature, and elastic curvature stress (the change in lateral pressure across the membrane) (Figure 5) have shown that the properties of the membrane can have dramatic effects on the folding of OMPs. For example, while OMPs such as OmpA and PagP (both 8-stranded, Figure 1) are able to fold into highly curved SUVs comprised of DOPC (diC$_{18:1}$PC) or DMPC (diC$_{14:0}$PC) in minutes, folding is slower or effectively prevented (beyond the timescale employed in the study) when these proteins are folding into LUVs formed from DOPC (diC$_{18:1}$PC) under the same experimental conditions (310). Similar studies have recapitulated these results and shown that the

elastic curvature stress, hydrophobic mismatch (hydrophobic thickness of the OMP versus the bilayer), and membrane curvature (SUV versus LUV) affect OMP folding, emphasising the importance of the physical properties of the lipid environment in determining the folding process (311, 312). The steep decrease in refolding rates observed as the acyl chain length of PC lipids increases (301), and the absence of reports of spontaneous folding into LUVs formed from pure PC lipids with saturated acyl chain lengths >14 carbon units – i.e. >DMPC (*di*$C_{14:0}$PC), can be rationalised by the elastic free energy of the membrane, as this parameter is expected to increase to the fourth power of membrane thickness (313). Membrane thickness is also thought to relate to the incidence of packing defects and thermal fluctuations in the bilayer, with thinner membranes having more defects. Such packing defects may be responsible for the more rapid folding of OMPs into thinner bilayers (313). OMPs have also been shown to be unable to fold into some lipids such as DMPC (*di*$C_{14:0}$PC) and DPPC (*di*$C_{16:0}$PC) in the gel phase, but they fold readily when the same lipids are in the liquid disordered phase, suggesting a significant activation energy barrier for the protein to insert across the bilayer (304, 305). Accordingly, the folding rate and yield of tOmpA (the β-barrel domain of OmpA) and OmpX (8-strands, Figure 1) into micelles (or mixed micelles of different lipid/detergent types) can be increased 10-100-fold by applying a transient 'heat shock' (~70 °C) during folding (314). This heat-shock presumably confers enough thermal energy to rapidly take the unfolded ensemble over the activation energy barrier. It has also been shown that while gel phase lipids (below their T_m) prevent or retard folding, and more rapid folding is observed into lipids in their liquid disordered phase, folding is most rapid at the interface between these phases (i.e. at the T_m) (315). At this temperature regions of gel phase (ordered acyl chains) and liquid phase (disordered acyl chains) lipids coexist (316, 317) and frustration between the packing requirements of these phases is believed to generate packing defects (as shown by an increase in solute permeability) (318–322) which may be responsible for the acceleration of OMP folding. Kinetic modelling experiments have suggested that this phenomenon involves an acceleration in the formation of an early membrane inserted folding intermediate (323).

Together, these data have established the importance of the chemical and physical properties of the membrane environment (lipid head group, acyl chain length, size, and curvature of the membrane vesicle) and the intimate connection between the protein sequence and membrane into which the OMP must fold.

Commonalities in the folding mechanisms of OMPs in vitro

OMP folding intermediates formed by initial adsorption to the lipid bilayer surface have been observed for several small OMPs, including the 8-stranded OmpA (see above), and PagP (303). An extensive mutational study of the folding kinetics and equilibrium stability of single point mutants of PagP revealed the first evidence for the nature of an OMP folding transition state (in DLPC [*di*$C_{12:0}$PC] LUVs), revealing that this species, which is formed subsequent to initial folding on the membrane surface, contains a partially folded β-barrel, in which the C-terminal strands have formed native-like contacts, but the N-terminal strands remain largely unstructured (324). The results from this study also suggested that PagP is tilted in the membrane in the transition state ensemble, reminiscent of CG-MD studies observing the insertion of pre-formed OmpA into a DPPC (*di*$C_{16:0}$PC) bilayer (325). Kinetic analysis of PagP folding also showed that this OMP folds via parallel pathways, with the route taken depending on the nature of the lipid employed (303). Similar results showing parallel folding pathways were also obtained for FomA (302), yet again highlighting the importance of the membrane surface and the physical state of the lipid bilayer in order for OMPs to fold (302, 303).

The view of OMP folding *in vitro* that emerges from these studies show a common first step involving folding on the lipid surface followed by pre-organisation of the approximate structure of the OMP, with translocating aromatic residues anchoring the nascent β-barrel to the membrane, and association of neighbouring β-strands causing a hydrophobic

surface to be displayed toward the membrane. This would, in turn, drive the energetically favourable partitioning of the hydrophobic protein surface deeper into the acyl chains (326). At the same time, hydrogen-bonding between β-strands during insertion may be driven by the energetic penalty associated with displaying the unbonded polar peptide backbone to the non-polar membrane environment. Finally, the association of β-strands in the correct order may be a rate-limiting step for insertion into the bilayer.

BAM: Nature's answer to the challenges of OMP folding

While many OMPs can be folded *in vitro* into SUVs and LUVs composed of short chain lipids, attempts to fold these proteins into liposomes comprised of *E. coli* polar lipid extract results in moderate folding yields for some OMPs (OmpA [8-strands], OmpT [10 strands], and BamA [16-strands]), and poor or no folding for others (OmpX [8 strands], PagP [8 strands], OmpW [8 strands], OmPLA [12 strands], and FadL [14 strands]) (Figure 1) (310, 327). Spontaneous folding of OMPs of many sizes has been observed into DDPC (*di*$C_{10:0}$PC) LUVs (310), but has been shown to be suppressed upon incorporation of lipids with headgroups native to the *E. coli* OM that confer negative spontaneous curvature (PE) or net negative charge (PG) (327). BamA is a 16-stranded essential OMP (Figure 1) and is the most conserved subunit of the multiprotein BAM complex which is involved in the biogenesis of other OMPs. BamA, or a BamA variant lacking most (4 out of 5) of its periplasmic polypeptide transport associated (POTRA) domains, can partially rescue the poor folding efficiency of OMPs into these liposomes (327). These results highlight the vital role of BAM for OMP folding into lipids commensurate with those found *in vivo*, suggesting that spontaneous folding of OMPs into a native lipid bilayer *in vivo* is kinetically unfavourable unless BAM is present.

BAM as a modulator of the physical properties of membranes

Until recently how BAM folds OMPs remained mysterious. The solution of several structures of BamA and BAM, as well as kinetic experiments, are now starting to provide glimpses of how this amazing machinery functions and how it might involve remodelling of the lipid bilayer. MD simulations of BamA and the full BAM complex have shown that the presence of the 16-stranded BamA β-barrel causes thinning and disordering of the membrane in the vicinity of its β1-β16 seam and that BamA can switch between conformations at this interface (328–333) (Figure 8). Other OMPs have been shown to generate variable (i.e. anisotropic) membrane thickness around their circumference experimentally (e.g. BtuB, 22-stranded) (334) and more isotropic bilayer thinning is seen in A-MD and CG-MD simulations in the vicinity of many OMPs (OprH [8-stranded from *P. aeruginosa*], OmpA, LpxR [12-stranded from *S. typhimurium*], Hia [3x4-strands from *Haemophilus influenzae*], OmPLA, NanC, OmpF, LamB, and FhuA) (157, 180, 219, 220, 238, 245, 332, 335). Although the dynamics of lipids surrounding BamA have not yet been studied *in vitro* or *in vivo* (for example, by using spin-labelled lipids), experiments examining the lipids directly surrounding other OMPs have found them to be motionally restricted in the vicinity of the β-barrel, as seen for FomA [8-stranded from *Fusobacterium nucleatum*], OmpA, OmpG, and FhuA (336–338). This has also been observed in CG-MD simulations of OmpA, NanC, OmpF, LamB, and FhuA in a bilayer formed from 75% POPE ($C_{16:0}C_{18:1}$PE) / 25% POPG ($C_{16:0}C_{18:1}$PG) (157). It should be noted, however, that it is not certain that the two parameters of lipid order and motional restriction are always correlated - consider a situation where disordered lipids are corralled by ordered lipids. With current data it is unclear whether the lipid disordering observed around the β1-β16 seam of BamA is purely a consequence of membrane thinning (i.e. a large hydrophobic mismatch) or is accentuated by some other mechanism in this OMP. Evidence for such a reaction cycle that could support a membrane remodelling mechanism for BamA was suggested from crystal structures of BamA in isolation, and from crystal and cryo-EM structures of BamA in the BAM complex. These studies showed that the BamA β-barrel is shorter in the β1-β16 region than in the rest of the barrel,

and that it can explore at least three distinct and potentially membrane-influencing conformations: a closed fully zipped (i.e. hydrogen-bonded along its whole seam) barrel (Figure 8: closed no kink & zipped), a closed partially zipped barrel (Figure 8: closed kink), and an open barrel (Figure 8: open kinked) (61, 328, 330, 339–345). This open conformation was surprising as it would intuitively seem highly energetically unfavourable to break hydrogen-bonds in a hydrophobic environment. However, WT BamA is only capable of forming at most 6-8 backbone hydrogen bonds between its first and last β-strands (Figure 8: closed no kink). MD simulations showed that this fully hydrogen-bonded conformation is unstable and eventually forms the 'partially zipped/closed kink' conformation seen in structures of the full BAM complex (Figure 8: closed kink) where the terminal strand bends back into the barrel lumen leaving just 2-3 hydrogen bonds (333). This partially zipped state may lower the energetic cost of fully opening the BamA barrel (333), leaving at most 1 hydrogen bond between β1 and the periplasmic turn between β15-β16. This periplasmic turn is likely to be important in stabilising this open state as its mutation or truncation is lethal *in vivo* (344). This still requires the breaking of 5-7 hydrogen bonds, but some of this may be compensated by the kinked residues hydrogen bonding to water within the lumen of the BamA barrel. Furthermore, the cost for OMPs to break hydrogen bonds in the membrane may be lower than previously assumed (346) and the outer leaflet of the OM may be more hydrated than a symmetric phospholipid bilayer. These effects could help stabilise the structure of BamA while effecting local changes in packing or stability of the membrane. The importance of this BamA barrel opening was highlighted by the lethality of disulfide-bonds engineered to lock the barrel closed (329) or open (330). Interestingly, folding of OmpT and OmpX via BamA or the full BAM complex *in vitro* is still catalysed in the locked closed state (343, 347). This implies that the structure of BamA alone, with its reduced hydrophobic thickness around β1-β16, may intrinsically accelerate OMP folding by distorting the membrane – even in the absence of the open state. *In vitro*, BamA has been shown to have a greater catalytic effect on tOmpA folding (higher catalytic fold rate enhancement) as the hydrophobic thickness of a bilayer is increased from ~19.5 Å in DLPC (diC$_{12:0}$PC) LUVs to ~23.0 Å in DMPC (diC$_{14:0}$PC) LUVs, showing that hydrophobic mismatch and/or lipid disordering plays an important role in the mechanism of BamA-assisted folding (332). These data illustrate how both structural and biochemical approaches will be required to fully understand the function of the BAM complex.

Recent studies have also shown the importance of BAM and membrane fluidity in folding OMPs *in vivo.* These studies exploited a monoclonal antibody that was found to be bactericidal, binding to extracellular loop 6 of BamA (63). Interestingly, bacteria showing spontaneous resistance to this BAM-mediated toxicity were found to have mutations in the *lpxM* gene. This protein transfers a C14 (myristoyl) chain to penta-acylated LPS, creating hexa-acylated LPS (63). Antibody sensitivity was restored (i.e. bactericidal effects of the antibody were reinstated) when *lpxM* was expressed from a plasmid. Assays of membrane fluidity using a pyrene-based probe showed that membrane fluidity decreased in the resistant strains, and this effect was recapitulated in other conditions that decrease membrane fluidity (high salt, longer LPS sugar region, lower temperature) (50, 63). The levels of OMPs were not reduced in Δ*lpxM* strains in the absence of the antibody. This suggests that there is mechanistic link between BamA/BAM and membrane fluidity, as BAM is most sensitive to inhibition when the membrane is more fluid. Hence BamA activity (as part of the BAM complex) may be lower when the OM is excessively fluid, confirming a link between OMP folding efficiency, BAM activity and membrane fluidity *in vivo*. More generally, it is interesting to consider the role of the lipids that directly surround BAM and how they might interact with it. Most MD studies on BamA have utilised simple lipid mixtures (328–333). However, it is known that membrane proteins can enrich lipids or other proteins around them that match their hydrophobic thickness (348–350). In the context of BAM this may have two consequences. Firstly, shorter chain lipids may be enriched around the β1-β16 seam in order to

reduce the energetic penalty of membrane thinning, with $C_{12:0}$ and $C_{14:0}$ acyl tails found in *E. coli* and also reported to be more abundant in the OM than the IM (109). Secondly, the hydrophobic thickness of substrate OMPs is generally greater than that of BamA. This means immediately after insertion into the region surrounding the BamA β1-β16 seam, the newly folded or folding OMPs will encounter a region of positive hydrophobic mismatch (Figure 5) and it may be energetically favourable for them to diffuse away to regions of greater hydrophobic thickness with a more optimal match to their size (350). This could provide a mechanism for release and local clearance of newly folded OMPs from BAM. Furthermore, although substrate binding to BAM subunits or the POTRA domains of BamA is likely to be important in conformational cycling (351–357), the lateral pressure or fluidity (Figure 5) within the OM might also play a role in controlling opening and closing of the BamA barrel. These dynamics are thought to be essential for its role in catalysing OMP folding *in vivo* (329, 358), and so modulation of the BamA barrel dynamics by the lipid environment may also provide a secondary mechanism of controlling the function of BAM.

A multifaceted mechanism for the BAM complex

Growing evidence points to a mechanism of BAM function in catalysing OMP folding and membrane insertion that involves the templating of C-terminal β-strands of the nascent substrate OMPs onto the β1 strand of BamA (Figures 6, 7 & 8) (359–361). The C-terminal strands of OMPs in bacteria and mitochondria contain a conserved aromatic-rich motif termed the β-signal (Figure 6) which may be important in the recognition of OMP clients by the BAM complex (362, 363). The initial recognition of the OMP's C-terminal strand is thought to then trigger nucleation of further β-hairpins to the growing β-barrel, perhaps favoured by the reduced entropic penalty of folding (as the degrees of freedom of the unfolded chain are reduced). However, the steps following this initial binding event, particularly how the β-barrel of the newly forming OMP folds and inserts into the membrane remain unclear. A role for the lateral gate of BamA in this process was proposed after the first structures of this family of proteins was solved (328, 364, 365). Further experimental evidence suggests four possible models for how this is achieved (Figure 7B): (1) BamA plays a passive role in OMP folding/insertion and merely targets nascent OMPs to a destabilised bilayer in front of its β1-β16 seam. Substrate binding possibly initiates a conformational change in BamA increasing its 'lipid disorderase' activity but folding otherwise proceeds as in the *in vitro* pathway (Figure 7A) (the assisted model) (365); (2) the β-barrel grows laterally into the membrane after templating onto the BamA gate (the budding model) (359, 365); (3) pre-folding / elongation of the OMP occurs in the periplasm after binding to β1 of BamA. A conformational change in BAM then inserts the already-folded β-barrel (the swing/elongation models) (360, 366); or (4) substrates fold against the interior wall of BamA while keeping their N- and C-termini in close proximity ready for β-barrel closure and release into the membrane (the lumen-catalysed model) (361). The last two models are particularly intriguing as they suggest that the hydrophobic surface of the folding OMP is partially exposed to an aqueous or polar environment. How this step could be energetically favourable is not yet clear, but some authors have proposed that the cradle created by the BamA lumen and POTRA domains may aid folding by acting like an entropic cage, analogous to chaperonins such as GroEL/ES (361, 366). This may drive folding by reducing the conformational entropy of the unfolded state, but may also restrict the mobility of water perhaps offsetting some of the cost of exposing hydrophobic residues.

Through its mechanism of β-strand capture, the BAM complex may also act to suppress the reversible off-pathway intermediates in OMP folding that cause kinetic retardation of folding *in vitro* and which may be related to both misfolded monomeric intermediates, as well as aberrant transient inter-molecular interactions (323). Furthermore, these aberrant multimers (so called 'elusive' states as they are not easily observed by SDS-PAGE) are not observed in the absence of a lipid bilayer (323) implicating the OMP-membrane interaction as an important control point where

these states could form. The nature of the terminal stages of folding, including how the OMP is able to partition rapidly into the OM, and how it overcomes the activation energy barrier associated with membrane insertion, remain unresolved. Finally, the enrichment of shorter-chain phospholipids and depletion of OMPs around BamA proposed above would essentially 'clear some space' for folding to proceed (e.g. Figure 3C), providing a mechanism which could overcome the remarkably low LPR of the OM, and an inner leaflet crowded with OMPs and lipoproteins. The proposed formation of 'supercomplexes' that span the periplasm linking the IM SecYEG translocon and the BAM complex at the OM could also provide a direct conduit for OMP biogenesis (367–369). If only limited patches of free lipid exist, it would be important to direct OMPs to these regions of the OM before they misfold or aggregate.

Comparison of folding *in vitro* and *in vivo*

Our current knowledge about the physical constraints of OMP folding into lipid bilayers, the properties of the OM, the folding of OMPs *in vitro*, and the mechanism of BAM action, all point to the membrane as an important interface for pre-organisation of OMPs into an insertion-competent state. Despite clear evidence for the importance of this early folding step, the unusually low LPR of the OM of *E. coli* (which may be as low as 6-14:1) (109, 127, 128), questions the direct interaction of the OMP and the OM during folding *in vivo*. Given this dearth of lipid surface and the observation that the rate of OMP folding falls dramatically with decreasing LPR (287, 302, 303), how do OMPs insert into the OM on a biologically meaningful timescale? Large lipid-rich patches could exist in the OM, but *in vivo* imaging studies have shown that BAM and newly inserted OMPs appear together in protein-rich clusters (119, 120, 152). This means that there are either very few free lipids (Figure 3A) or only small, local, lipid-enriched domains (Figure 3C). Hence, BAM may have evolved to provide an initial nucleation site for OMP folding in a generally lipid-poor environment, and to accelerate this process, particularly for rapidly growing organisms such as *E. coli*. This would also be necessary in order to pack the OM to the high protein density that is observed *in vivo*. Although the recognition of nascent OMPs and the nucleation of β-barrel formation through templating/recognition of the newly folding OMP's β-strands on BamA would provide a rate-enhancement in folding, the dramatic differences of folding rates into detergent micelles (fast) versus LUVs (slow) suggest that the ability of an OMP to navigate its folding pathway to find the native fold is not necessarily a major rate-limiting factor. Instead, it appears that membrane insertion and disruption of lipid packing could play a more significant role in controlling the rate of folding. *In vitro* experiments have shown that the greater the lateral pressure, lipid order, and packing of lipids within a bilayer, the greater the activation energy barrier for folding (311, 312, 327). However, local or transient defects in the packing of lipids in a membrane can allow OMPs to bypass a slower folding pathway and instead fold more rapidly (as shown by studies on the propensity of thinner bilayers and lipids at their T_m to accelerate OMP folding) (310, 315). The physical structure of the OM remains poorly defined but what we know is this: already-folded OMPs are resistant to deformation in the OM, LPS can rigidify the outer leaflet, and *in vivo* measurements suggest that at least some proportion of lipids in the OM are relatively ordered and less mobile. BAM may introduce local defects into this environment (by thinning of the membrane and causing local disorder of the lipids) in order to lower the energy barrier to insertion and thus accelerate OMP folding into this otherwise impenetrable membrane barrier.

Concluding remarks and open questions

The OMP folding problem *in vivo* can be simplified as the interplay between three factors: enzyme (BAM), substrate (OMP), and solvent (lipid). To fully understand OMP folding *in vivo* it is necessary to characterise the relationships between these three dominating factors in order to understand their holistic function. BAM acts to catalyse the folding of OMPs into a lipid bilayer and it may do this both by nucleating the folding of the unfolded OMP substrate (BAM-OMP interaction) and/or by locally disrupting the packing of lipids (BAM-

lipid interaction) to lower the activation energy of folding (OMP-lipid interaction). The evidence for the action of BAM on lipids is currently restricted to *in silico* experiments, although we can imply its importance from *in vitro* studies of the effect of the physical and chemical properties of the bilayer on OMP folding. More studies are now needed to determine the relative importance of this 'disorderase' activity of BAM in ensuring that OMPs can gain access to the highly crowded and lipid-poor OM.

Our current lack of understanding of the physical properties of the OM prevents the generation of accurate models for the mechanism(s) of BAM in the OM; the effect of BAM on the structure and dynamics of the OM lipids (and *vice versa*), and how these changes impact on OMP folding. Although levels of OMPs fall upon depletion of BAM *in vivo*, and OMP insertion kinetics are slowed in the absence of BAM *in vitro*, which OMPs require BAM for folding into the OM *in vivo* is still not known unequivocally. Indeed, some OMPs have been shown to be capable of folding without the aid of BAM, and others are aided by other proteins such as those of the Localisation of lipoproteins (Lol) machinery (Table 1). The asymmetry of the OM, combined with the mixture of lipid types, high fraction of proteins, and the tethering to the peptidoglycan layer, makes the journey taken by a nascent OMP to the OM, and its insertion *in vivo,* an immensely challenging task to replicate *in vitro*. Future *in vitro* work should focus on understanding the OM and OMP folding in a context closer to that found *in vivo*, and also to better understand the effects of suppressor variants on the catalytic activity of BAM, so as to narrow the gap between *in vivo* and *in vitro* insights. At the same time, modern biophysical and biochemical tools are also needed to make these same measurements directly on OMPs in their native context within bacteria. *En route* to this, the use of outer membrane vesicles directly derived from bacteria may provide an excellent stepping stone (370–372).

In summary, despite enormous progress in our understanding of how OMPs fold *in vitro* and in dissecting the interactions and mechanisms of BAM, we still do not fully understand how BAM folds OMPs of different size and sequence, nor do we understand fully the role of the asymmetric OM lipid bilayer in defining this process. OMP folding has moved in the last few years from a question of fundamental importance and interest, to one having direct implications for the development of new antibiotics targeting OM biogenesis. The challenge has thus been set to define how OMPs fold *in vivo* and to solve the remaining mysteries, so that BAM can be targeted to break the OM barrier and render pathogenic bacteria susceptible to attack by new antimicrobial agents.

Acknowledgements: We thank members of the SER and DJB laboratories and our collaborators for many helpful discussions, particularly the OMP team including Bob Schiffrin, Anna Higgins, Paul White, Anton Calabrese, James Whitehouse, Sam Haysom, Matt Iadanza, Matt Watson, Roman Tuma, and Neil Ranson.

Conflict of interest: The authors declare that they have no conflicts of interest with the contents of this article

Author contributions: All authors wrote and revised the manuscript.

References

1. Prilipov, A., Phale, P. S., Koebnik, R., Widmer, C., and Rosenbusch, J. P. (1998) Identification and characterization of two quiescent porin genes, *nmpC* and *ompN*, in *Escherichia coli* BE. *J. Bacteriol.* **180**, 3388–92
2. Fàbrega, A., Rosner, J. L., Martin, R. G., Solé, M., and Vila, J. (2012) SoxS-dependent coregulation of *ompN* and *ydbK* in a multidrug-resistant *Escherichia coli* strain. *FEMS Microbiol. Lett.* **332**, 61–7
3. Li, G.-W., Burkhardt, D., Gross, C., and Weissman, J. S. (2014) Quantifying absolute protein synthesis rates reveals principles underlying allocation of cellular resources. *Cell*. **157**, 624–35
4. Soufi, B., Krug, K., Harst, A., and Macek, B. (2015) Characterization of the *E. coli* proteome and its modifications during growth and ethanol stress. *Front. Microbiol.* **6**, 103
5. Henning, U., Höhn, B., and Sonntag, I. (1973) Cell envelope and shape of *Escherichia coli* K12. The ghost membrane. *Eur. J. Biochem.* **39**, 27–36
6. Rosenbusch, J. P. (1974) Characterization of the major envelope protein from *Escherichia coli*. Regular arrangement on the peptidoglycan and unusual dodecyl sulfate binding. *J. Biol. Chem.* **249**, 8019–29
7. Lugtenberg, B., and Van Alphen, L. (1983) Molecular architecture and functioning of the outer membrane of *Escherichia coli* and other gram-negative bacteria. *Biochim. Biophys. Acta*. **737**, 51–115
8. Ye, J., and van den Berg, B. (2004) Crystal structure of the bacterial nucleoside transporter Tsx. *EMBO J.* **23**, 3187–95
9. Subbarao, G. V., and van den Berg, B. (2006) Crystal structure of the monomeric porin OmpG. *J. Mol. Biol.* **360**, 750–9
10. Wirth, C., Condemine, G., Boiteux, C., Bernèche, S., Schirmer, T., and Peneff, C. M. (2009) NanC crystal structure, a model for outer-membrane channels of the acidic sugar-specific KdgM porin family. *J. Mol. Biol.* **394**, 718–31
11. Vergalli, J., Bodrenko, I. V, Masi, M., Moynié, L., Acosta-Gutiérrez, S., Naismith, J. H., Davin-Regli, A., Ceccarelli, M., van den Berg, B., Winterhalter, M., and Pagès, J.-M. (2019) Porins and small-molecule translocation across the outer membrane of Gram-negative bacteria. *Nat. Rev. Microbiol.* 10.1038/s41579-019-0294-2
12. Xu, C., Lin, X., Ren, H., Zhang, Y., Wang, S., and Peng, X. (2006) Analysis of outer membrane proteome of *Escherichia coli* related to resistance to ampicillin and tetracycline. *Proteomics*. **6**, 462–73
13. Beketskaia, M. S., Bay, D. C., and Turner, R. J. (2014) Outer membrane protein OmpW participates with small multidrug resistance protein member EmrE in quaternary cationic compound efflux. *J. Bacteriol.* **196**, 1908–14
14. Wang, Z., Fan, G., Hryc, C. F., Blaza, J. N., Serysheva, I. I., Schmid, M. F., Chiu, W., Luisi, B. F., and Du, D. (2017) An allosteric transport mechanism for the AcrAB-TolC multidrug efflux pump. *Elife*. **6**, 1–19
15. Fitzpatrick, A. W. P., Llabrés, S., Neuberger, A., Blaza, J. N., Bai, X.-C., Okada, U., Murakami, S., van Veen, H. W., Zachariae, U., Scheres, S. H. W., Luisi, B. F., and Du, D. (2017) Structure of the MacAB-TolC ABC-type tripartite multidrug efflux pump. *Nat. Microbiol.* **2**, 17070
16. Noinaj, N., Guillier, M., Barnard, T. J., and Buchanan, S. K. (2010) TonB-dependent transporters: regulation, structure, and function. *Annu. Rev. Microbiol.* **64**, 43–60
17. Lepore, B. W., Indic, M., Pham, H., Hearn, E. M., Patel, D. R., and van den Berg, B. (2011) Ligand-gated diffusion across the bacterial outer membrane. *Proc. Natl. Acad. Sci. U. S. A.* **108**, 10121–6
18. Aunkham, A., Zahn, M., Kesireddy, A., Pothula, K. R., Schulte, A., Baslé, A., Kleinekathöfer, U., Suginta, W., and van den Berg, B. (2018) Structural basis for chitin acquisition by marine *Vibrio* species. *Nat. Commun.* **9**, 220

19. Rojas, E. R., Billings, G., Odermatt, P. D., Auer, G. K., Zhu, L., Miguel, A., Chang, F., Weibel, D. B., Theriot, J. A., and Huang, K. C. (2018) The outer membrane is an essential load-bearing element in Gram-negative bacteria. *Nature*. **559**, 617–621
20. Samsudin, F., Ortiz-Suarez, M. L., Piggot, T. J., Bond, P. J., and Khalid, S. (2016) OmpA: A flexible clamp for bacterial cell wall attachment. *Structure*. **24**, 2227–2235
21. Vollmer, W., Von Rechenberg, M., and Höltje, J. V. (1999) Demonstration of molecular interactions between the murein polymerase PBP1B, the lytic transglycosylase MltA, and the scaffolding protein MipA of *Escherichia coli*. *J. Biol. Chem.* **274**, 6726–6734
22. Braun, M., and Silhavy, T. J. (2002) Imp/OstA is required for cell envelope biogenesis in *Escherichia coli*. *Mol. Microbiol.* **45**, 1289–302
23. Voulhoux, R., Bos, M. P., Geurtsen, J., Mols, M., and Tommassen, J. (2003) Role of a highly conserved bacterial protein in outer membrane protein assembly. *Science*. **299**, 262–5
24. Bishop, R. E., Gibbons, H. S., Guina, T., Trent, M. S., Miller, S. I., and Raetz, C. R. H. (2000) Transfer of palmitate from phospholipids to lipid A in outer membranes of gram-negative bacteria. *EMBO J.* **19**, 5071–80
25. May, K. L., and Silhavy, T. J. (2018) The *Escherichia coli* phospholipase PldA regulates outer membrane homeostasis via lipid signaling. *MBio*. **9**, 11325–11340
26. Stubenrauch, C. J., and Lithgow, T. (2019) The TAM: A translocation and assembly module of the β-barrel assembly machinery in bacterial outer membranes. *EcoSal Plus*. **8**, 1–7
27. Mecsas, J., Welch, R., Erickson, J. W., and Gross, C. A. (1995) Identification and characterization of an outer membrane protein, OmpX, in *Escherichia coli* that is homologous to a family of outer membrane proteins including Ail of *Yersinia enterocolitica*. *J. Bacteriol.* **177**, 799–804
28. Mulvey, M. A., Lopez-Boado, Y. S., Wilson, C. L., Roth, R., Parks, W. C., Heuser, J., and Hultgren, S. J. (1998) Induction and evasion of host defenses by type 1-piliated uropathogenic *Escherichia coli*. *Science*. **282**, 1494–7
29. Du, M., Yuan, Z., Yu, H., Henderson, N., Sarowar, S., Zhao, G., Werneburg, G. T., Thanassi, D. G., and Li, H. (2018) Handover mechanism of the growing pilus by the bacterial outer-membrane usher FimD. *Nature*. **562**, 444–447
30. Henderson, I. R., and Owen, P. (1999) The major phase-variable outer membrane protein of *Escherichia coli* structurally resembles the immunoglobulin A1 protease class of exported protein and is regulated by a novel mechanism involving Dam and oxyR. *J. Bacteriol.* **181**, 2132–41
31. de Luna, M. das G., Scott-Tucker, A., Desvaux, M., Ferguson, P., Morin, N. P., Dudley, E. G., Turner, S., Nataro, J. P., Owen, P., and Henderson, I. R. (2008) The *Escherichia coli* biofilm-promoting protein Antigen 43 does not contribute to intestinal colonization. *FEMS Microbiol. Lett.* **284**, 237–46
32. Wang, Y., Andole Pannuri, A., Ni, D., Zhou, H., Cao, X., Lu, X., Romeo, T., and Huang, Y. (2016) Structural basis for translocation of a biofilm-supporting exopolysaccharide across the bacterial outer membrane. *J. Biol. Chem.* **291**, 10046–57
33. Acheson, J. F., Derewenda, Z. S., and Zimmer, J. (2019) Architecture of the cellulose synthase outer membrane channel and its association with the periplasmic TPR domain. *Structure*. **27**, 1855-1861.e3
34. Stumpe, S., Schmid, R., Stephens, D. L., Georgiou, G., and Bakker, E. P. (1998) Identification of OmpT as the protease that hydrolyzes the antimicrobial peptide protamine before it enters growing cells of *Escherichia coli*. *J. Bacteriol.* **180**, 4002–6
35. Hwang, B.-Y., Varadarajan, N., Li, H., Rodriguez, S., Iverson, B. L., and Georgiou, G. (2007) Substrate specificity of the *Escherichia coli* outer membrane protease OmpP. *J. Bacteriol.* **189**, 522–30
36. Ruiz, N., Kahne, D., and Silhavy, T. J. (2006) Advances in understanding bacterial outer-membrane biogenesis. *Nat. Rev. Microbiol.* **4**, 57–66
37. Lee, J., Xue, M., Wzorek, J. S., Wu, T., Grabowicz, M., Gronenberg, L. S., Sutterlin, H. A., Davis, R. M., Ruiz, N., Silhavy, T. J., and Kahne, D. E. (2016) Characterization of a stalled complex on

the β-barrel assembly machine. *Proc. Natl. Acad. Sci. U. S. A.* **113**, 8717–22
38. Gu, Y., Stansfeld, P. J., Zeng, Y., Dong, H., Wang, W., and Dong, C. (2015) Lipopolysaccharide is inserted into the outer membrane through an intramembrane hole, a lumen gate, and the lateral opening of LptD. *Structure*. **23**, 496–504
39. Ricci, D. P., and Silhavy, T. J. (2019) Outer membrane protein insertion by the β-barrel assembly machine. *EcoSal Plus*. **8**, 1–9
40. Paschen, S. A., Neupert, W., and Rapaport, D. (2005) Biogenesis of beta-barrel membrane proteins of mitochondria. *Trends Biochem. Sci.* **30**, 575–82
41. Surrey, T., and Jähnig, F. (1992) Refolding and oriented insertion of a membrane protein into a lipid bilayer. *Proc. Natl. Acad. Sci. U. S. A.* **89**, 7457–61
42. Yildirim, M. A., Goh, K.-I., Cusick, M. E., Barabási, A.-L., and Vidal, M. (2007) Drug-target network. *Nat. Biotechnol.* **25**, 1119–26
43. Yin, H., and Flynn, A. D. (2016) Drugging membrane protein interactions. *Annu. Rev. Biomed. Eng.* **18**, 51–76
44. Genevrois, S., Steeghs, L., Roholl, P., Letesson, J.-J., and van der Ley, P. (2003) The Omp85 protein of *Neisseria meningitidis* is required for lipid export to the outer membrane. *EMBO J.* **22**, 1780–9
45. Wiedemann, N., Kozjak, V., Chacinska, A., Schönfisch, B., Rospert, S., Ryan, M. T., Pfanner, N., and Meisinger, C. (2003) Machinery for protein sorting and assembly in the mitochondrial outer membrane. *Nature*. **424**, 565–71
46. Paschen, S. A., Waizenegger, T., Stan, T., Preuss, M., Cyrklaff, M., Hell, K., Rapaport, D., and Neupert, W. (2003) Evolutionary conservation of biogenesis of beta-barrel membrane proteins. *Nature*. **426**, 862–6
47. Kozjak, V., Wiedemann, N., Milenkovic, D., Lohaus, C., Meyer, H. E., Guiard, B., Meisinger, C., and Pfanner, N. (2003) An essential role of Sam50 in the protein sorting and assembly machinery of the mitochondrial outer membrane. *J. Biol. Chem.* **278**, 48520–3
48. Nikaido, H. (2003) Molecular basis of bacterial outer membrane permeability revisited. *Microbiol. Mol. Biol. Rev.* **67**, 593–656
49. Domínguez-Medina, C. C., Pérez-Toledo, M., Schager, A. E., Marshall, J. L., Cook, C. N., Bobat, S., Hwang, H., Chun, B. J., Logan, E., Bryant, J. A., Channell, W. M., Morris, F. C., Jossi, S. E., Alshayea, A., Rossiter, A. E., Barrow, P. A., Horsnell, W. G., MacLennan, C. A., Henderson, I. R., Lakey, J. H., Gumbart, J. C., López-Macías, C., Bavro, V. N., and Cunningham, A. F. (2020) Outer membrane protein size and LPS O-antigen define protective antibody targeting to the *Salmonella* surface. *Nat. Commun.* **11**, 851
50. Storek, K. M., Vij, R., Sun, D., Smith, P. A., Koerber, J. T., and Rutherford, S. T. (2018) The *Escherichia coli* β-barrel assembly machinery is sensitized to perturbations under high membrane fluidity. *J. Bacteriol.* **201**, 1–15
51. Bentley, A. T., and Klebba, P. E. (1988) Effect of lipopolysaccharide structure on reactivity of antiporin monoclonal antibodies with the bacterial cell surface. *J. Bacteriol.* **170**, 1063–8
52. Storek, K. M., Chan, J., Vij, R., Chiang, N., Lin, Z., Bevers, J., Koth, C. M., Vernes, J.-M., Meng, Y. G., Yin, J., Wallweber, H., Dalmas, O., Shriver, S., Tam, C., Schneider, K., Seshasayee, D., Nakamura, G., Smith, P. A., Payandeh, J., Koerber, J. T., Comps-Agrar, L., and Rutherford, S. T. (2019) Massive antibody discovery used to probe structure-function relationships of the essential outer membrane protein LptD. *Elife*. **8**, 1–20
53. Ellenrieder, L., Mårtensson, C. U., and Becker, T. (2015) Biogenesis of mitochondrial outer membrane proteins, problems and diseases. *Biol. Chem.* **396**, 1199–213
54. Tacconelli, E., Carrara, E., Savoldi, A., Harbarth, S., Mendelson, M., Monnet, D. L., Pulcini, C., Kahlmeter, G., Kluytmans, J., Carmeli, Y., Ouellette, M., Outterson, K., Patel, J., Cavaleri, M., Cox, E. M., Houchens, C. R., Grayson, M. L., Hansen, P., Singh, N., Theuretzbacher, U., Magrini, N., and WHO Pathogens Priority List Working Group (2018) Discovery, research, and development of new antibiotics: the WHO priority list of antibiotic-resistant bacteria and

tuberculosis. *Lancet. Infect. Dis.* **18**, 318–327
55. Srinivas, N., Jetter, P., Ueberbacher, B. J., Werneburg, M., Zerbe, K., Steinmann, J., Van der Meijden, B., Bernardini, F., Lederer, A., Dias, R. L. A., Misson, P. E., Henze, H., Zumbrunn, J., Gombert, F. O., Obrecht, D., Hunziker, P., Schauer, S., Ziegler, U., Käch, A., Eberl, L., Riedel, K., DeMarco, S. J., and Robinson, J. A. (2010) Peptidomimetic antibiotics target outer-membrane biogenesis in Pseudomonas aeruginosa. *Science*. **327**, 1010–3
56. Wedege, E., Lie, K., Bolstad, K., Weynants, V. E., Halstensen, A., Herstad, T. K., Kreutzberger, J., Nome, L., Naess, L. M., and Aase, A. (2013) Meningococcal *omp85* in detergent-extracted outer membrane vesicle vaccines induces high levels of non-functional antibodies in mice. *Scand. J. Immunol.* **77**, 452–9
57. Vetterli, S. U., Moehle, K., and Robinson, J. A. (2016) Synthesis and antimicrobial activity against Pseudomonas aeruginosa of macrocyclic β-hairpin peptidomimetic antibiotics containing N-methylated amino acids. *Bioorg. Med. Chem.* **24**, 6332–6339
58. Machutta, C. A., Kollmann, C. S., Lind, K. E., Bai, X., Chan, P. F., Huang, J., Ballell, L., Belyanskaya, S., Besra, G. S., Barros-Aguirre, D., Bates, R. H., Centrella, P. A., Chang, S. S., Chai, J., Choudhry, A. E., Coffin, A., Davie, C. P., Deng, H., Deng, J., Ding, Y., Dodson, J. W., Fosbenner, D. T., Gao, E. N., Graham, T. L., Graybill, T. L., Ingraham, K., Johnson, W. P., King, B. W., Kwiatkowski, C. R., Lelièvre, J., Li, Y., Liu, X., Lu, Q., Lehr, R., Mendoza-Losana, A., Martin, J., McCloskey, L., McCormick, P., O'Keefe, H. P., O'Keeffe, T., Pao, C., Phelps, C. B., Qi, H., Rafferty, K., Scavello, G. S., Steiginga, M. S., Sundersingh, F. S., Sweitzer, S. M., Szewczuk, L. M., Taylor, A., Toh, M. F., Wang, J., Wang, M., Wilkins, D. J., Xia, B., Yao, G., Zhang, J., Zhou, J., Donahue, C. P., Messer, J. A., Holmes, D., Arico-Muendel, C. C., Pope, A. J., Gross, J. W., and Evindar, G. (2017) Prioritizing multiple therapeutic targets in parallel using automated DNA-encoded library screening. *Nat. Commun.* **8**, 16081
59. Vij, R., Lin, Z., Chiang, N., Vernes, J.-M., Storek, K. M., Park, S., Chan, J., Meng, Y. G., Comps-Agrar, L., Luan, P., Lee, S., Schneider, K., Bevers, J., Zilberleyb, I., Tam, C., Koth, C. M., Xu, M., Gill, A., Auerbach, M. R., Smith, P. A., Rutherford, S. T., Nakamura, G., Seshasayee, D., Payandeh, J., and Koerber, J. T. (2018) A targeted boost-and-sort immunization strategy using *Escherichia coli* BamA identifies rare growth inhibitory antibodies. *Sci. Rep.* **8**, 7136
60. Ghequire, M. G. K., Swings, T., Michiels, J., Buchanan, S. K., and De Mot, R. (2018) Hitting with a BAM: Selective killing by lectin-like bacteriocins. *MBio*. **9**, 1–15
61. Kaur, H., Hartmann, J.-B., Jakob, R. P., Zahn, M., Zimmermann, I., Maier, T., Seeger, M. A., and Hiller, S. (2019) Identification of conformation-selective nanobodies against the membrane protein insertase BamA by an integrated structural biology approach. *J. Biomol. NMR*. **73**, 375–384
62. Ghequire, M. G. K., and De Mot, R. (2019) LlpB represents a second subclass of lectin-like bacteriocins. *Microb. Biotechnol.* **12**, 567–573
63. Storek, K. M., Auerbach, M. R., Shi, H., Garcia, N. K., Sun, D., Nickerson, N. N., Vij, R., Lin, Z., Chiang, N., Schneider, K., Wecksler, A. T., Skippington, E., Nakamura, G., Seshasayee, D., Koerber, J. T., Payandeh, J., Smith, P. A., and Rutherford, S. T. (2018) Monoclonal antibody targeting the β-barrel assembly machine of *Escherichia coli* is bactericidal. *Proc. Natl. Acad. Sci. U. S. A.* **115**, 3692–3697
64. Psonis, J. J., Chahales, P., Henderson, N. S., Rigel, N. W., Hoffman, P. S., and Thanassi, D. G. (2019) The small molecule nitazoxanide selectively disrupts BAM-mediated folding of the outer membrane usher protein. *J. Biol. Chem.* **294**, 14357–14369
65. Steenhuis, M., Abdallah, A. M., de Munnik, S. M., Kuhne, S., Sterk, G.-J., van den Berg van Saparoea, B., Westerhausen, S., Wagner, S., van der Wel, N. N., Wijtmans, M., van Ulsen, P., Jong, W. S. P., and Luirink, J. (2019) Inhibition of autotransporter biogenesis by small molecules. *Mol. Microbiol.* **112**, 81–98
66. Luther, A., Urfer, M., Zahn, M., Müller, M., Wang, S., Mondal, M., Vitale, A., Hartmann, J., Sharpe, T., Monte, F. Lo, Kocherla, H., Cline, E., Pessi, G., Rath, P., Modaresi, S. M., Chiquet, P.,

Stiegeler, S., Verbree, C., Remus, T., Schmitt, M., Kolopp, C., Westwood, M., Desjonquères, N., Brabet, E., Hell, S., LePoupon, K., Vermeulen, A., Jaisson, R., Rithié, V., Upert, G., Lederer, A., Zbinden, P., Wach, A., Moehle, K., Zerbe, K., Locher, H. H., Bernardini, F., Dale, G. E., Eberl, L., Wollscheid, B., Hiller, S., Robinson, J. A., and Obrecht, D. (2019) Chimeric peptidomimetic antibiotics against Gram-negative bacteria. *Nature*. **576**, 452–458

67. Imai, Y., Meyer, K. J., Iinishi, A., Favre-Godal, Q., Green, R., Manuse, S., Caboni, M., Mori, M., Niles, S., Ghiglieri, M., Honrao, C., Ma, X., Guo, J. J., Makriyannis, A., Linares-Otoya, L., Böhringer, N., Wuisan, Z. G., Kaur, H., Wu, R., Mateus, A., Typas, A., Savitski, M. M., Espinoza, J. L., O'Rourke, A., Nelson, K. E., Hiller, S., Noinaj, N., Schäberle, T. F., D'Onofrio, A., and Lewis, K. (2019) A new antibiotic selectively kills Gram-negative pathogens. *Nature*. **576**, 459–464
68. Hart, E. M., Mitchell, A. M., Konovalova, A., Grabowicz, M., Sheng, J., Han, X., Rodriguez-Rivera, F. P., Schwaid, A. G., Malinverni, J. C., Balibar, C. J., Bodea, S., Si, Q., Wang, H., Homsher, M. F., Painter, R. E., Ogawa, A. K., Sutterlin, H., Roemer, T., Black, T. A., Rothman, D. M., Walker, S. S., and Silhavy, T. J. (2019) A small-molecule inhibitor of BamA impervious to efflux and the outer membrane permeability barrier. *Proc. Natl. Acad. Sci. U. S. A.* **116**, 21748–21757
69. Henderson, J. C., Zimmerman, S. M., Crofts, A. A., Boll, J. M., Kuhns, L. G., Herrera, C. M., and Trent, M. S. (2016) The power of asymmetry: Architecture and assembly of the Gram-negative outer membrane lipid bilayer. *Annu. Rev. Microbiol.* **70**, 255–78
70. Kim, S., Patel, D. S., Park, S., Slusky, J., Klauda, J. B., Widmalm, G., and Im, W. (2016) Bilayer properties of lipid A from various Gram-negative bacteria. *Biophys. J.* **111**, 1750–1760
71. Kosma, P. (1999) Chlamydial lipopolysaccharide. *Biochim. Biophys. Acta*. **1455**, 387–402
72. Raetz, C. R. H., and Whitfield, C. (2002) Lipopolysaccharide endotoxins. *Annu. Rev. Biochem.* **71**, 635–700
73. Silipo, A., De Castro, C., Lanzetta, R., Molinaro, A., and Parrilli, M. (2004) Full structural characterization of the lipid A components from the *Agrobacterium tumefaciens* strain C58 lipopolysaccharide fraction. *Glycobiology*. **14**, 805–15
74. Albitar-Nehme, S., Basheer, S. M., Njamkepo, E., Brisson, J.-R., Guiso, N., and Caroff, M. (2013) Comparison of lipopolysaccharide structures of *Bordetella pertussis* clinical isolates from pre- and post-vaccine era. *Carbohydr. Res.* **378**, 56–62
75. Zähringer, U., Lindner, B., and Rietschel, E. T. (1994) Molecular structure of lipid A, the endotoxic center of bacterial lipopolysaccharides. *Adv. Carbohydr. Chem. Biochem.* **50**, 211–76
76. Miller, S. I., Ernst, R. K., and Bader, M. W. (2005) LPS, TLR4 and infectious disease diversity. *Nat. Rev. Microbiol.* **3**, 36–46
77. Steimle, A., Autenrieth, I. B., and Frick, J.-S. (2016) Structure and function: Lipid A modifications in commensals and pathogens. *Int. J. Med. Microbiol.* **306**, 290–301
78. DeChavigny, A., Heacock, P. N., and Dowhan, W. (1991) Sequence and inactivation of the pss gene of *Escherichia coli*. Phosphatidylethanolamine may not be essential for cell viability. *J. Biol. Chem.* **266**, 5323–32
79. Rowlett, V. W., Mallampalli, V. K. P. S., Karlstaedt, A., Dowhan, W., Taegtmeyer, H., Margolin, W., and Vitrac, H. (2017) Impact of membrane phospholipid alterations in *Escherichia coli* on cellular function and bacterial stress adaptation. *J. Bacteriol.* **199**, 1–22
80. Kikuchi, S., Shibuya, I., and Matsumoto, K. (2000) Viability of an *Escherichia coli pgsA* null mutant lacking detectable phosphatidylglycerol and cardiolipin. *J. Bacteriol.* **182**, 371–6
81. Matsumoto, K. (2001) Dispensable nature of phosphatidylglycerol in *Escherichia coli*: dual roles of anionic phospholipids. *Mol. Microbiol.* **39**, 1427–33
82. Tan, B. K., Bogdanov, M., Zhao, J., Dowhan, W., Raetz, C. R. H., and Guan, Z. (2012) Discovery of a cardiolipin synthase utilizing phosphatidylethanolamine and phosphatidylglycerol as substrates. *Proc. Natl. Acad. Sci. U. S. A.* **109**, 16504–9
83. Chen, F., Zhao, Q., Cai, X., Lv, L., Lin, W., Yu, X., Li, C., Li, Y., Xiong, M., and Wang, X.-G.

(2009) Phosphatidylcholine in membrane of *Escherichia coli* changes bacterial antigenicity. *Can. J. Microbiol.* **55**, 1328–34
84. Geiger, O., López-Lara, I. M., and Sohlenkamp, C. (2013) Phosphatidylcholine biosynthesis and function in bacteria. *Biochim. Biophys. Acta*. **1831**, 503–13
85. Wikström, M., Kelly, A. A., Georgiev, A., Eriksson, H. M., Klement, M. R., Bogdanov, M., Dowhan, W., and Wieslander, A. (2009) Lipid-engineered Escherichia coli membranes reveal critical lipid headgroup size for protein function. *J. Biol. Chem.* **284**, 954–65
86. Caforio, A., Siliakus, M. F., Exterkate, M., Jain, S., Jumde, V. R., Andringa, R. L. H., Kengen, S. W. M., Minnaard, A. J., Driessen, A. J. M., and van der Oost, J. (2018) Converting *Escherichia coli* into an archaebacterium with a hybrid heterochiral membrane. *Proc. Natl. Acad. Sci. U. S. A.* **115**, 3704–3709
87. Rossi, R. M., Yum, L., Agaisse, H., and Payne, S. M. (2017) Cardiolipin synthesis and outer membrane localization are required for *Shigella flexneri* virulence. *MBio*. **8**, 1–16
88. Oliver, P. M., Crooks, J. A., Leidl, M., Yoon, E. J., Saghatelian, A., and Weibel, D. B. (2014) Localization of anionic phospholipids in *Escherichia coli* cells. *J. Bacteriol.* **196**, 3386–98
89. Koppelman, C. M., Den Blaauwen, T., Duursma, M. C., Heeren, R. M., and Nanninga, N. (2001) *Escherichia coli* minicell membranes are enriched in cardiolipin. *J. Bacteriol.* **183**, 6144–7
90. Suzuki, M., Hara, H., and Matsumoto, K. (2002) Envelope disorder of *Escherichia coli* cells lacking phosphatidylglycerol. *J. Bacteriol.* **184**, 5418–25
91. Nakayama, H., Kurokawa, K., and Lee, B. L. (2012) Lipoproteins in bacteria: structures and biosynthetic pathways. *FEBS J.* **279**, 4247–68
92. Grabowicz, M., and Silhavy, T. J. (2017) Redefining the essential trafficking pathway for outer membrane lipoproteins. *Proc. Natl. Acad. Sci. U. S. A.* **114**, 4769–4774
93. Grabowicz, M. (2018) Lipoprotein transport: Greasing the machines of outer membrane biogenesis: Re-examining lipoprotein transport mechanisms among diverse Gram-negative bacteria while exploring new discoveries and questions. *Bioessays*. **40**, e1700187
94. McMorran, L. M., Brockwell, D. J., and Radford, S. E. (2014) Mechanistic studies of the biogenesis and folding of outer membrane proteins *in vitro* and *in vivo*: what have we learned to date? *Arch. Biochem. Biophys.* **564**, 265–80
95. Bai, J., and Pagano, R. E. (1997) Measurement of spontaneous transfer and transbilayer movement of BODIPY-labeled lipids in lipid vesicles. *Biochemistry*. **36**, 8840–8
96. Nakano, M., Fukuda, M., Kudo, T., Matsuzaki, N., Azuma, T., Sekine, K., Endo, H., and Handa, T. (2009) Flip-flop of phospholipids in vesicles: kinetic analysis with time-resolved small-angle neutron scattering. *J. Phys. Chem. B*. **113**, 6745–8
97. Vaara, M., and Vaara, T. (1983) Polycations as outer membrane-disorganizing agents. *Antimicrob. Agents Chemother.* **24**, 114–22
98. Paul, S., Chaudhuri, K., Chatterjee, A. N., and Das, J. (1992) Presence of exposed phospholipids in the outer membrane of *Vibrio cholerae*. *J. Gen. Microbiol.* **138**, 755–61
99. Contreras, F.-X., Sánchez-Magraner, L., Alonso, A., and Goñi, F. M. (2010) Transbilayer (flip-flop) lipid motion and lipid scrambling in membranes. *FEBS Lett.* **584**, 1779–86
100. Malinverni, J. C., and Silhavy, T. J. (2009) An ABC transport system that maintains lipid asymmetry in the gram-negative outer membrane. *Proc. Natl. Acad. Sci. U. S. A.* **106**, 8009–14
101. Abellón-Ruiz, J., Kaptan, S. S., Baslé, A., Claudi, B., Bumann, D., Kleinekathöfer, U., and van den Berg, B. (2017) Structural basis for maintenance of bacterial outer membrane lipid asymmetry. *Nat. Microbiol.* **2**, 1616–1623
102. Powers, M. J., and Trent, M. S. (2019) Intermembrane transport: Glycerophospholipid homeostasis of the Gram-negative cell envelope. *Proc. Natl. Acad. Sci. U. S. A.* **116**, 17147–17155
103. Ingram, L. O. (1977) Changes in lipid composition of *Escherichia coli* resulting from growth with organic solvents and with food additives. *Appl. Environ. Microbiol.* **33**, 1233–6
104. McGarrity, J. T., and Armstrong, J. B. (1981) The effect of temperature and other growth conditions on the fatty acid composition of *Escherichia coli*. *Can. J. Microbiol.* **27**, 835–40

105. Ingram, L. O. (1982) Regulation of fatty acid composition in *Escherichia coli*: a proposed common mechanism for changes induced by ethanol, chaotropic agents, and a reduction of growth temperature. *J. Bacteriol.* **149**, 166–72
106. Arneborg, N., Salskov-Iversen, A., and Mathiasen, T. (1993) The effect of growth rate and other growth conditions on the lipid composition of *Escherichia coli*. *Appl. Microbiol. Biotechnol.* **39**, 353–357
107. Gidden, J., Denson, J., Liyanage, R., Ivey, D. M., and Lay, J. O. (2009) Lipid compositions in *Escherichia coli* and *Bacillus subtilis* during growth as determined by MALDI-TOF and TOF/TOF mass spectrometry. *Int. J. Mass Spectrom.* **283**, 178–184
108. Jeucken, A., Molenaar, M. R., van de Lest, C. H. A., Jansen, J. W. A., Helms, J. B., and Brouwers, J. F. (2019) A comprehensive functional characterization of *Escherichia coli* lipid genes. *Cell Rep.* **27**, 1597-1606.e2
109. Overath, P., Brenner, M., Gulik-Krzywicki, T., Shechter, E., and Letellier, L. (1975) Lipid phase transitions in cytoplasmic and outer membranes of *Escherichia coli*. *Biochim. Biophys. Acta*. **389**, 358–69
110. Oursel, D., Loutelier-Bourhis, C., Orange, N., Chevalier, S., Norris, V., and Lange, C. M. (2007) Identification and relative quantification of fatty acids in *Escherichia coli* membranes by gas chromatography/mass spectrometry. *Rapid Commun. Mass Spectrom.* **21**, 3229–33
111. Oursel, D., Loutelier-Bourhis, C., Orange, N., Chevalier, S., Norris, V., and Lange, C. M. (2007) Lipid composition of membranes of *Escherichia coli* by liquid chromatography/tandem mass spectrometry using negative electrospray ionization. *Rapid Commun. Mass Spectrom.* **21**, 1721–8
112. Wang, A. -Y, and Cronan, J. E. (1994) The growth phase-dependent synthesis of cyclopropane fatty acids in *Escherichia coli* is the result of an RpoS(KatF)-dependent promoter plus enzyme instability. *Mol. Microbiol.* **11**, 1009–17
113. Grogan, D. W., and Cronan, J. E. (1997) Cyclopropane ring formation in membrane lipids of bacteria. *Microbiol. Mol. Biol. Rev.* **61**, 429–41
114. Chang, Y. Y., and Cronan, J. E. (1999) Membrane cyclopropane fatty acid content is a major factor in acid resistance of *Escherichia coli*. *Mol. Microbiol.* **33**, 249–59
115. Kim, B. H., Kim, S., Kim, H. G., Lee, J., Lee, I. S., and Park, Y. K. (2005) The formation of cyclopropane fatty acids in *Salmonella enterica* serovar Typhimurium. *Microbiology*. **151**, 209–18
116. Asakura, H., Ekawa, T., Sugimoto, N., Momose, Y., Kawamoto, K., Makino, S.-I., Igimi, S., and Yamamoto, S. (2012) Membrane topology of *Salmonella* invasion protein SipB confers osmotolerance. *Biochem. Biophys. Res. Commun.* **426**, 654–8
117. Grandvalet, C., Assad-García, J. S., Chu-Ky, S., Tollot, M., Guzzo, J., Gresti, J., and Tourdot-Maréchal, R. (2008) Changes in membrane lipid composition in ethanol- and acid-adapted *Oenococcus oeni* cells: characterization of the cfa gene by heterologous complementation. *Microbiology*. **154**, 2611–9
118. Annous, B. A., Kozempel, M. F., and Kurantz, M. J. (1999) Changes in membrane fatty acid composition of *Pediococcus* sp. strain NRRL B-2354 in response to growth conditions and its effect on thermal resistance. *Appl. Environ. Microbiol.* **65**, 2857–62
119. Ursell, T. S., Trepagnier, E. H., Huang, K. C., and Theriot, J. A. (2012) Analysis of surface protein expression reveals the growth pattern of the Gram-negative outer membrane. *PLoS Comput. Biol.* **8**, e1002680
120. Rassam, P., Copeland, N. A., Birkholz, O., Tóth, C., Chavent, M., Duncan, A. L., Cross, S. J., Housden, N. G., Kaminska, R., Seger, U., Quinn, D. M., Garrod, T. J., Sansom, M. S. P., Piehler, J., Baumann, C. G., and Kleanthous, C. (2015) Supramolecular assemblies underpin turnover of outer membrane proteins in bacteria. *Nature*. **523**, 333–6
121. Johansen, J., Rasmussen, A. A., Overgaard, M., and Valentin-Hansen, P. (2006) Conserved small non-coding RNAs that belong to the sigmaE regulon: role in down-regulation of outer membrane proteins. *J. Mol. Biol.* **364**, 1–8
122. Guillier, M., Gottesman, S., and Storz, G. (2006) Modulating the outer membrane with small

RNAs. *Genes Dev.* **20**, 2338–48
123. Allen, R. J., and Scott, G. K. (1979) Biosynthesis and turnover of outer-membrane proteins in *Escherichia coli* ML308-225. *Biochem. J.* **182**, 407–12
124. Lugtenberg, E. J. J., and Peters, R. (1976) Distribution of lipids in cytoplasmic and outer membranes of *Escherichia coli* K12. *Biochim. Biophys. Acta*. **441**, 38–47
125. White, D. A., Lennarz, W. J., and Schnaitman, C. A. (1972) Distribution of lipids in the wall and cytoplasmic membrane subfractions of the cell envelope of *Escherichia coli*. *J. Bacteriol.* **109**, 686–90
126. Ishinaga, M., Kanamoto, R., and Kito, M. (1979) Distribution of phospholipid molecular species in outer and cytoplasmic membrane of *Escherichia coli*. *J. Biochem.* **86**, 161–5
127. Jarosławski, S., Duquesne, K., Sturgis, J. N., and Scheuring, S. (2009) High-resolution architecture of the outer membrane of the Gram-negative bacteria *Roseobacter denitrificans*. *Mol. Microbiol.* **74**, 1211–22
128. Lessen, H. J., Fleming, P. J., Fleming, K. G., and Sodt, A. J. (2018) Building blocks of the outer membrane: Calculating a general elastic energy model for β-barrel membrane proteins. *J. Chem. Theory Comput.* **14**, 4487–4497
129. Oddershede, L., Dreyer, J. K., Grego, S., Brown, S., and Berg-Sørensen, K. (2002) The motion of a single molecule, the λ-receptor, in the bacterial outer membrane. *Biophys. J.* **83**, 3152–3161
130. Kumar, M., Mommer, M. S., and Sourjik, V. (2010) Mobility of cytoplasmic, membrane, and DNA-binding proteins in *Escherichia coli*. *Biophys. J.* **98**, 552–9
131. Ritchie, K., Lill, Y., Sood, C., Lee, H., and Zhang, S. (2013) Single-molecule imaging in live bacteria cells. *Philos. Trans. R. Soc. Lond. B. Biol. Sci.* **368**, 20120355
132. Oh, D., Yu, Y., Lee, H., Wanner, B. L., and Ritchie, K. (2014) Dynamics of the serine chemoreceptor in the *Escherichia coli* inner membrane: A high-speed single-molecule tracking study. *Biophys. J.* **106**, 145–153
133. Oswald, F., Varadarajan, A., Lill, H., Peterman, E. J. G., and Bollen, Y. J. M. (2016) MreB-dependent organization of the *E. coli* cytoplasmic membrane controls membrane protein diffusion. *Biophys. J.* **110**, 1139–49
134. Gibbs, K. A., Isaac, D. D., Xu, J., Hendrix, R. W., Silhavy, T. J., and Theriot, J. A. (2004) Complex spatial distribution and dynamics of an abundant *Escherichia coli* outer membrane protein, LamB. *Mol. Microbiol.* **53**, 1771–83
135. Spector, J., Zakharov, S., Lill, Y., Sharma, O., Cramer, W. A., and Ritchie, K. (2010) Mobility of BtuB and OmpF in the *Escherichia coli* outer membrane: implications for dynamic formation of a translocon complex. *Biophys. J.* **99**, 3880–6
136. Rothenberg, E., Sepúlveda, L. A., Skinner, S. O., Zeng, L., Selvin, P. R., and Golding, I. (2011) Single-virus tracking reveals a spatial receptor-dependent search mechanism. *Biophys. J.* **100**, 2875–82
137. Kleanthous, C., Rassam, P., and Baumann, C. G. (2015) Protein-protein interactions and the spatiotemporal dynamics of bacterial outer membrane proteins. *Curr. Opin. Struct. Biol.* **35**, 109–15
138. Deich, J., Judd, E. M., McAdams, H. H., and Moerner, W. E. (2004) Visualization of the movement of single histidine kinase molecules in live *Caulobacter* cells. *Proc. Natl. Acad. Sci. U. S. A.* **101**, 15921–6
139. Mullineaux, C. W., Nenninger, A., Ray, N., and Robinson, C. (2006) Diffusion of green fluorescent protein in three cell environments in *Escherichia coli*. *J. Bacteriol.* **188**, 3442–8
140. Leake, M. C., Chandler, J. H., Wadhams, G. H., Bai, F., Berry, R. M., and Armitage, J. P. (2006) Stoichiometry and turnover in single, functioning membrane protein complexes. *Nature*. **443**, 355–8
141. Leake, M. C., Greene, N. P., Godun, R. M., Granjon, T., Buchanan, G., Chen, S., Berry, R. M., Palmer, T., and Berks, B. C. (2008) Variable stoichiometry of the TatA component of the twin-arginine protein transport system observed by *in vivo* single-molecule imaging. *Proc. Natl. Acad.*

Sci. U. S. A. **105**, 15376–81
142. Szczepaniak, J., Holmes, P., Rajasekar, K., Kaminska, R., Samsudin, F., Inns, P. G., Rassam, P., Khalid, S., Murray, S. M., Redfield, C., and Kleanthous, C. (2020) The lipoprotein Pal stabilises the bacterial outer membrane during constriction by a mobilisation-and-capture mechanism. *Nat. Commun.* **11**, 1305
143. Mühlradt, P. F., Menzel, J., Golecki, J. R., and Speth, V. (1974) Lateral mobility and surface density of lipopolysaccharide in the outer membrane of *Salmonella typhimurium*. *Eur. J. Biochem.* **43**, 533–9
144. Schindler, M., Osborn, M. J., and Koppel, D. E. (1980) Lateral diffusion of lipopolysaccharide in the outer membrane of *Salmonella typhimurium*. *Nature*. **285**, 261–3
145. Nenninger, A., Mastroianni, G., Robson, A., Lenn, T., Xue, Q., Leake, M. C., and Mullineaux, C. W. (2014) Independent mobility of proteins and lipids in the plasma membrane of *Escherichia coli*. *Mol. Microbiol.* **92**, 1142–53
146. Mika, J. T., Thompson, A. J., Dent, M. R., Brooks, N. J., Michiels, J., Hofkens, J., and Kuimova, M. K. (2016) Measuring the viscosity of the *Escherichia coli* plasma membrane using molecular rotors. *Biophys. J.* **111**, 1528–1540
147. Elowitz, M. B., Surette, M. G., Wolf, P. E., Stock, J. B., and Leibler, S. (1999) Protein mobility in the cytoplasm of *Escherichia coli*. *J. Bacteriol.* **181**, 197–203
148. Cluzel, P., Surette, M., and Leibler, S. (2000) An ultrasensitive bacterial motor revealed by monitoring signaling proteins in single cells. *Science*. **287**, 1652–5
149. Konopka, M. C., Shkel, I. A., Cayley, S., Record, M. T., and Weisshaar, J. C. (2006) Crowding and confinement effects on protein diffusion *in vivo*. *J. Bacteriol.* **188**, 6115–23
150. Potma, E. O., de Boeij, W. P., Bosgraaf, L., Roelofs, J., van Haastert, P. J., and Wiersma, D. A. (2001) Reduced protein diffusion rate by cytoskeleton in vegetative and polarized dictyostelium cells. *Biophys. J.* **81**, 2010–9
151. Terry, B. R., Matthews, E. K., and Haseloff, J. (1995) Molecular characterisation of recombinant green fluorescent protein by fluorescence correlation microscopy. *Biochem. Biophys. Res. Commun.* **217**, 21–7
152. Gunasinghe, S. D., Shiota, T., Stubenrauch, C. J., Schulze, K. E., Webb, C. T., Fulcher, A. J., Dunstan, R. A., Hay, I. D., Naderer, T., Whelan, D. R., Bell, T. D. M., Elgass, K. D., Strugnell, R. A., and Lithgow, T. (2018) The WD40 protein BamB mediates coupling of BAM complexes into assembly precincts in the bacterial outer membrane. *Cell Rep.* **23**, 2782–2794
153. Lill, Y., Jordan, L. D., Smallwood, C. R., Newton, S. M., Lill, M. A., Klebba, P. E., and Ritchie, K. (2016) Confined mobility of TonB and FepA in *Escherichia coli* membranes. *PLoS One*. **11**, e0160862
154. Gold, V. A. M., Ieva, R., Walter, A., Pfanner, N., van der Laan, M., and Kühlbrandt, W. (2014) Visualizing active membrane protein complexes by electron cryotomography. *Nat. Commun.* **5**, 4129
155. Casuso, I., Khao, J., Chami, M., Paul-Gilloteaux, P., Husain, M., Duneau, J.-P., Stahlberg, H., Sturgis, J. N., and Scheuring, S. (2012) Characterization of the motion of membrane proteins using high-speed atomic force microscopy. *Nat. Nanotechnol.* **7**, 525–9
156. Yamashita, H., Taoka, A., Uchihashi, T., Asano, T., Ando, T., and Fukumori, Y. (2012) Single-molecule imaging on living bacterial cell surface by high-speed AFM. *J. Mol. Biol.* **422**, 300–9
157. Goose, J. E., and Sansom, M. S. P. (2013) Reduced lateral mobility of lipids and proteins in crowded membranes. *PLoS Comput. Biol.* **9**, e1003033
158. Chavent, M., Duncan, A. L., Rassam, P., Birkholz, O., Hélie, J., Reddy, T., Beliaev, D., Hambly, B., Piehler, J., Kleanthous, C., and Sansom, M. S. P. (2018) How nanoscale protein interactions determine the mesoscale dynamic organisation of bacterial outer membrane proteins. *Nat. Commun.* **9**, 2846
159. Smit, J., and Nikaido, H. (1978) Outer membrane of gram-negative bacteria. XVIII. Electron microscopic studies on porin insertion sites and growth of cell surface of *Salmonella typhimurium*.

J. Bacteriol. **135**, 687–702
160. Arunmanee, W., Pathania, M., Solovyova, A. S., Le Brun, A. P., Ridley, H., Baslé, A., van den Berg, B., and Lakey, J. H. (2016) Gram-negative trimeric porins have specific LPS binding sites that are essential for porin biogenesis. *Proc. Natl. Acad. Sci. U. S. A.* **113**, E5034-43
161. Verhoeven, G. S., Dogterom, M., and den Blaauwen, T. (2013) Absence of long-range diffusion of OmpA in *E. coli* is not caused by its peptidoglycan binding domain. *BMC Microbiol.* **13**, 66
162. Fowler, P. W., Hélie, J., Duncan, A., Chavent, M., Koldsø, H., and Sansom, M. S. P. (2016) Membrane stiffness is modified by integral membrane proteins. *Soft Matter*. **12**, 7792–7803
163. Heberle, F. A., and Feigenson, G. W. (2011) Phase separation in lipid membranes. *Cold Spring Harb. Perspect. Biol.* **3**, 1–13
164. Bigay, J., and Antonny, B. (2012) Curvature, lipid packing, and electrostatics of membrane organelles: defining cellular territories in determining specificity. *Dev. Cell*. **23**, 886–95
165. Budin, I., de Rond, T., Chen, Y., Chan, L. J. G., Petzold, C. J., and Keasling, J. D. (2018) Viscous control of cellular respiration by membrane lipid composition. *Science*. **362**, 1186–1189
166. Jackson, M. B., and Cronan, J. E. (1978) An estimate of the minimum amount of fluid lipid required for the growth of *Escherichia coli*. *Biochim. Biophys. Acta*. **512**, 472–9
167. Janoff, A. S., Haug, A., and McGroarty, E. J. (1979) Relationship of growth temperature and thermotropic lipid phase changes in cytoplasmic and outer membranes from *Escherichia coli* K12. *Biochim. Biophys. Acta*. **555**, 56–66
168. Nakayama, H., Mitsui, T., Nishihara, M., and Kito, M. (1980) Relation between growth temperature of *E. coli* and phase transition temperatures of its cytoplasmic and outer membranes. *Biochim. Biophys. Acta*. **601**, 1–10
169. Janoff, A. S., Gupte, S., and McGroarty, E. J. (1980) Correlation between temperature range of growth and structural transitions in membranes and lipids of *Escherichia coli* K12. *Biochim. Biophys. Acta*. **598**, 641–6
170. Souzu, H. (1982) *Escherichia coli* B membrane stability related to cell growth phase. Measurement of temperature dependent physical state change of the membrane over a wide range. *Biochim. Biophys. Acta*. **691**, 161–70
171. van den Brink-van der Laan, E., Killian, J. A., and de Kruijff, B. (2004) Nonbilayer lipids affect peripheral and integral membrane proteins via changes in the lateral pressure profile. *Biochim. Biophys. Acta*. **1666**, 275–88
172. Kranenburg, M., and Smit, B. (2005) Phase behavior of model lipid bilayers. *J. Phys. Chem. B*. **109**, 6553–63
173. Brown, D. A., and London, E. (1998) Structure and origin of ordered lipid domains in biological membranes. *J. Membr. Biol.* **164**, 103–14
174. M'Baye, G., Mély, Y., Duportail, G., and Klymchenko, A. S. (2008) Liquid ordered and gel phases of lipid bilayers: fluorescent probes reveal close fluidity but different hydration. *Biophys. J.* **95**, 1217–25
175. Quinn, P. J., and Wolf, C. (2009) The liquid-ordered phase in membranes. *Biochim. Biophys. Acta*. **1788**, 33–46
176. Mouritsen, O. G. (2010) The liquid-ordered state comes of age. *Biochim. Biophys. Acta*. **1798**, 1286–8
177. Sodt, A. J., Sandar, M. L., Gawrisch, K., Pastor, R. W., and Lyman, E. (2014) The molecular structure of the liquid-ordered phase of lipid bilayers. *J. Am. Chem. Soc.* **136**, 725–32
178. Boscia, A. L., Treece, B. W., Mohammadyani, D., Klein-Seetharaman, J., Braun, A. R., Wassenaar, T. A., Klösgen, B., and Tristram-Nagle, S. (2014) X-ray structure, thermodynamics, elastic properties and MD simulations of cardiolipin/dimyristoylphosphatidylcholine mixed membranes. *Chem. Phys. Lipids*. **178**, 1–10
179. Bramkamp, M., and Lopez, D. (2015) Exploring the existence of lipid rafts in bacteria. *Microbiol. Mol. Biol. Rev.* **79**, 81–100
180. Shearer, J., and Khalid, S. (2018) Communication between the leaflets of asymmetric membranes

revealed from coarse-grain molecular dynamics simulations. *Sci. Rep.* **8**, 1805
181. Shearer, J., Jefferies, D., and Khalid, S. (2019) Outer membrane proteins OmpA, FhuA, OmpF, EstA, BtuB, and OmpX have unique lipopolysaccharide fingerprints. *J. Chem. Theory Comput.* **15**, 2608–2619
182. Thanassi, D. G., Stathopoulos, C., Karkal, A., and Li, H. (2005) Protein secretion in the absence of ATP: the autotransporter, two-partner secretion and chaperone/usher pathways of gram-negative bacteria (review). *Mol. Membr. Biol.* **22**, 63–72
183. Sinensky, M. (1974) Homeoviscous adaptation--a homeostatic process that regulates the viscosity of membrane lipids in *Escherichia coli*. *Proc. Natl. Acad. Sci. U. S. A.* **71**, 522–5
184. Velázquez, J. B., and Fernández, M. S. (2006) GPS, the slope of Laurdan generalized polarization spectra, in the study of phospholipid lateral organization and *Escherichia coli* lipid phases. *Arch. Biochem. Biophys.* **455**, 163–74
185. Demchenko, A. P., Mély, Y., Duportail, G., and Klymchenko, A. S. (2009) Monitoring biophysical properties of lipid membranes by environment-sensitive fluorescent probes. *Biophys. J.* **96**, 3461–70
186. Leung, S. S. W., Brewer, J., Bagatolli, L. A., and Thewalt, J. L. (2019) Measuring molecular order for lipid membrane phase studies: Linear relationship between Laurdan generalized polarization and deuterium NMR order parameter. *Biochim. Biophys. acta. Biomembr.* **1861**, 183053
187. Davis, J. H., Nichol, C. P., Weeks, G., and Bloom, M. (1979) Study of the cytoplasmic and outer membranes of *Escherichia coli* by deuterium magnetic resonance. *Biochemistry*. **18**, 2103–12
188. Nichol, C. P., Davis, J. H., Weeks, G., and Bloom, M. (1980) Quantitative study of the fluidity of *Escherichia coli* membranes using deuterium magnetic resonance. *Biochemistry*. **19**, 451–7
189. Souzu, H. (1986) Fluorescence polarization studies on *Escherichia coli* membrane stability and its relation to the resistance of the cell to freeze-thawing. I. Membrane stability in cells of differing growth phase. *Biochim. Biophys. Acta*. **861**, 353–60
190. Melchior, D. L., and Steim, J. M. (1976) Thermotropic transitions in biomembranes. *Annu. Rev. Biophys. Bioeng.* **5**, 205–38
191. Vanounou, S., Pines, D., Pines, E., Parola, A. H., and Fishov, I. (2002) Coexistence of domains with distinct order and polarity in fluid bacterial membranes. *Photochem. Photobiol.* **76**, 1–11
192. Fishov, I., and Woldringh, C. L. (1999) Visualization of membrane domains in *Escherichia coli*. *Mol. Microbiol.* **32**, 1166–72
193. Sperka-Gottlieb, C. D. M., Hermetter, A., Paltauf, F., and Daum, G. (1988) Lipid topology and physical properties of the outer mitochondrial membrane of the yeast, *Saccharomyces cerevisiae*. *Biochim. Biophys. Acta*. **946**, 227–34
194. Liu, P., Duan, W., Wang, Q., and Li, X. (2010) The damage of outer membrane of *Escherichia coli* in the presence of TiO2 combined with UV light. *Colloids Surf. B. Biointerfaces*. **78**, 171–6
195. Wu, C.-H., Bialecka-Fornal, M., and Newman, D. K. (2015) Methylation at the C-2 position of hopanoids increases rigidity in native bacterial membranes. *Elife*. **4**, 1–18
196. Wu, Y., Stefl, M., Olzyńska, A., Hof, M., Yahioglu, G., Yip, P., Casey, D. R., Ces, O., Humpolíčková, J., and Kuimova, M. K. (2013) Molecular rheometry: direct determination of viscosity in Lo and Ld lipid phases via fluorescence lifetime imaging. *Phys. Chem. Chem. Phys.* **15**, 14986–93
197. Nikaido, H., Takeuchi, Y., Ohnishi, S. I., and Nakae, T. (1977) Outer membrane of *Salmonella typhimurium*. Electron spin resonance studies. *Biochim. Biophys. Acta*. **465**, 152–64
198. Labischinski, H., Barnickel, G., Bradaczek, H., Naumann, D., Rietschel, E. T., and Giesbrecht, P. (1985) High state of order of isolated bacterial lipopolysaccharide and its possible contribution to the permeation barrier property of the outer membrane. *J. Bacteriol.* **162**, 9–20
199. Brandenburg, K., and Blume, A. (1987) Investigations into the thermotropic phase behaviour of natural membranes extracted from gram-negative bacteria and artificial membrane systems made from lipopolysaccharides and free lipid A. *Thermochim. Acta*. **119**, 127–142
200. Brandenburg, K., and Seydel, U. (1990) Investigation into the fluidity of lipopolysaccharide and

free lipid A membrane systems by Fourier-transform infrared spectroscopy and differential scanning calorimetry. *Eur. J. Biochem.* **191**, 229–36
201. Conde-Álvarez, R., Arce-Gorvel, V., Iriarte, M., Manček-Keber, M., Barquero-Calvo, E., Palacios-Chaves, L., Chacón-Díaz, C., Chaves-Olarte, E., Martirosyan, A., von Bargen, K., Grilló, M.-J., Jerala, R., Brandenburg, K., Llobet, E., Bengoechea, J. A., Moreno, E., Moriyón, I., and Gorvel, J.-P. (2012) The lipopolysaccharide core of *Brucella abortus* acts as a shield against innate immunity recognition. *PLoS Pathog.* **8**, e1002675
202. Brandenburg, K., and Seydel, U. (1984) Physical aspects of structure and function of membranes made from lipopolysaccharides and free lipid A. *Biochim. Biophys. Acta - Biomembr.* **775**, 225–238
203. Seydel, U., Koch, M. H. J., and Brandenburg, K. (1993) Structural polymorphisms of rough mutant lipopolysaccharides Rd to Ra from *Salmonella minnesota*. *J. Struct. Biol.* **110**, 232–43
204. Paracini, N., Clifton, L. A., Skoda, M. W. A., and Lakey, J. H. (2018) Liquid crystalline bacterial outer membranes are critical for antibiotic susceptibility. *Proc. Natl. Acad. Sci. U. S. A.* **115**, E7587–E7594
205. Hughes, A. V, Patel, D. S., Widmalm, G., Klauda, J. B., Clifton, L. A., and Im, W. (2019) Physical properties of bacterial outer membrane models: Neutron reflectometry & molecular simulation. *Biophys. J.* **116**, 1095–1104
206. Gally, H. U., Pluschke, G., Overath, P., and Seelig, J. (1980) Structure of *Escherichia coli* membranes. Fatty acyl chain order parameters of inner and outer membranes and derived liposomes. *Biochemistry*. **19**, 1638–43
207. Mühlradt, P. F., and Golecki, J. R. (1975) Asymmetrical distribution and artifactual reorientation of lipopolysaccharide in the outer membrane bilayer of *Salmonella typhimurium*. *Eur. J. Biochem.* **51**, 343–52
208. Sciandrone, B., Forti, F., Perego, S., Falchi, F., and Briani, F. (2019) Temperature-dependent regulation of the *Escherichia coli lpxT* gene. *Biochim. Biophys. acta. Gene Regul. Mech.* **1862**, 786–795
209. Carty, S. M., Sreekumar, K. R., and Raetz, C. R. H. (1999) Effect of cold shock on lipid A biosynthesis in *Escherichia coli*. Induction at 12 degrees C of an acyltransferase specific for palmitoleoyl-acyl carrier protein. *J. Biol. Chem.* **274**, 9677–85
210. Li, Y., Powell, D. A., Shaffer, S. A., Rasko, D. A., Pelletier, M. R., Leszyk, J. D., Scott, A. J., Masoudi, A., Goodlett, D. R., Wang, X., Raetz, C. R. H., and Ernst, R. K. (2012) LPS remodeling is an evolved survival strategy for bacteria. *Proc. Natl. Acad. Sci. U. S. A.* **109**, 8716–21
211. Reinés, M., Llobet, E., Dahlström, K. M., Pérez-Gutiérrez, C., Llompart, C. M., Torrecabota, N., Salminen, T. A., and Bengoechea, J. A. (2012) Deciphering the acylation pattern of *Yersinia enterocolitica* lipid A. *PLoS Pathog.* **8**, e1002978
212. Ernst, R. K., Adams, K. N., Moskowitz, S. M., Kraig, G. M., Kawasaki, K., Stead, C. M., Trent, M. S., and Miller, S. I. (2006) The *Pseudomonas aeruginosa* lipid A deacylase: selection for expression and loss within the cystic fibrosis airway. *J. Bacteriol.* **188**, 191–201
213. Needham, B. D., and Trent, M. S. (2013) Fortifying the barrier: the impact of lipid A remodelling on bacterial pathogenesis. *Nat. Rev. Microbiol.* **11**, 467–81
214. Schnaitman, C. A., and Klena, J. D. (1993) Genetics of lipopolysaccharide biosynthesis in enteric bacteria. *Microbiol. Rev.* **57**, 655–82
215. Missiakas, D., Betton, J. M., and Raina, S. (1996) New components of protein folding in extracytoplasmic compartments of *Escherichia coli* SurA, FkpA and Skp/OmpH. *Mol. Microbiol.* **21**, 871–884
216. Klein, G., Lindner, B., Brabetz, W., Brade, H., and Raina, S. (2009) *Escherichia coli* K-12 suppressor-free mutants lacking early glycosyltransferases and late acyltransferases: minimal lipopolysaccharide structure and induction of envelope stress response. *J. Biol. Chem.* **284**, 15369–89
217. López, C. A., Zgurskaya, H., and Gnanakaran, S. (2020) Molecular characterization of the outer

membrane of *Pseudomonas aeruginosa*. *Biochim. Biophys. acta. Biomembr.* **1862**, 183151
218. Patel, D. S., Re, S., Wu, E. L., Qi, Y., Klebba, P. E., Widmalm, G., Yeom, M. S., Sugita, Y., and Im, W. (2016) Dynamics and interactions of OmpF and LPS: Influence on pore accessibility and ion permeability. *Biophys. J.* **110**, 930–8
219. Lee, J., Patel, D. S., Kucharska, I., Tamm, L. K., and Im, W. (2017) Refinement of OprH-LPS interactions by molecular simulations. *Biophys. J.* **112**, 346–355
220. Wu, E. L., Fleming, P. J., Yeom, M. S., Widmalm, G., Klauda, J. B., Fleming, K. G., and Im, W. (2014) *E. coli* outer membrane and interactions with OmpLA. *Biophys. J.* **106**, 2493–502
221. Ma, H., Irudayanathan, F. J., Jiang, W., and Nangia, S. (2015) Simulating Gram-negative bacterial outer membrane: A coarse grain model. *J. Phys. Chem. B*. **119**, 14668–82
222. Petrov, A. G., Gawrisch, K., Brezesinski, G., Klose, G., and Möps, A. (1982) Optical detection of phase transitions in simple and mixed lipid-water phases. *Biochim. Biophys. Acta*. **690**, 1–7
223. Li, A., Schertzer, J. W., and Yong, X. (2018) Molecular dynamics modeling of *Pseudomonas aeruginosa* outer membranes. *Phys. Chem. Chem. Phys.* **20**, 23635–23648
224. Ma, H., Khan, A., and Nangia, S. (2018) Dynamics of OmpF trimer formation in the bacterial outer membrane of *Escherichia coli*. *Langmuir*. **34**, 5623–5634
225. Rottem, S., and Leive, L. (1977) Effect of variations in lipopolysaccharide on the fluidity of the outer membrane of *Escherichia coli*. *J. Biol. Chem.* **252**, 2077–81
226. Müller-Loennies, S., Holst, O., and Brade, H. (1994) Chemical structure of the core region of *Escherichia coli* J-5 lipopolysaccharide. *Eur. J. Biochem.* **224**, 751–60
227. Bello, G., Bodin, A., Lawrence, M. J., Barlow, D., Mason, A. J., Barker, R. D., and Harvey, R. D. (2016) The influence of rough lipopolysaccharide structure on molecular interactions with mammalian antimicrobial peptides. *Biochim. Biophys. Acta*. **1858**, 197–209
228. Takeuchi, Y., and Nikaido, H. (1981) Persistence of segregated phospholipid domains in phospholipid-lipopolysaccharide mixed bilayers: studies with spin-labeled phospholipids. *Biochemistry*. **20**, 523–9
229. Takeuchi, Y., and Nikaido, H. (1984) Physical interaction between lipid A and phospholipids: a study with spin-labeled phospholipids. *Rev. Infect. Dis.* **6**, 488–92
230. Niemelä, P. S., Miettinen, M. S., Monticelli, L., Hammaren, H., Bjelkmar, P., Murtola, T., Lindahl, E., and Vattulainen, I. (2010) Membrane proteins diffuse as dynamic complexes with lipids. *J. Am. Chem. Soc.* **132**, 7574–5
231. Javanainen, M., Hammaren, H., Monticelli, L., Jeon, J., Miettinen, M. S., Martinez-Seara, H., Metzler, R., and Vattulainen, I. (2013) Anomalous and normal diffusion of proteins and lipids in crowded lipid membranes. *Faraday Discuss.* **161**, 397–417; discussion 419-59
232. Guigas, G., and Weiss, M. (2016) Effects of protein crowding on membrane systems. *Biochim. Biophys. Acta*. **1858**, 2441–2450
233. Kirschner, K. N., Lins, R. D., Maass, A., and Soares, T. A. (2012) A glycam-based force field for simulations of lipopolysaccharide membranes: Parametrization and validation. *J. Chem. Theory Comput.* **8**, 4719–31
234. Ortiz-Suarez, M. L., Samsudin, F., Piggot, T. J., Bond, P. J., and Khalid, S. (2016) Full-length OmpA: Structure, function, and membrane interactions predicted by molecular dynamics simulations. *Biophys. J.* **111**, 1692–1702
235. Balusek, C., and Gumbart, J. C. (2016) Role of the native outer-membrane environment on the transporter BtuB. *Biophys. J.* **111**, 1409–1417
236. Matthias, K. A., Strader, M. B., Nawar, H. F., Gao, Y. S., Lee, J., Patel, D. S., Im, W., and Bash, M. C. (2017) Heterogeneity in non-epitope loop sequence and outer membrane protein complexes alters antibody binding to the major porin protein PorB in serogroup B *Neisseria meningitidis*. *Mol. Microbiol.* **105**, 934–953
237. Lee, J., Pothula, K. R., Kleinekathöfer, U., and Im, W. (2018) Simulation study of Occk5 functional properties in *Pseudomonas aeruginosa* outer membranes. *J. Phys. Chem. B*. **122**, 8185–8192

238. Saunders, G. M., Bruce Macdonald, H. E., Essex, J. W., and Khalid, S. (2018) Prediction of the closed conformation and insights into the mechanism of the membrane enzyme LpxR. *Biophys. J.* **115**, 1445–1456
239. Kesireddy, A., Pothula, K. R., Lee, J., Patel, D. S., Pathania, M., van den Berg, B., Im, W., and Kleinekathöfer, U. (2019) Modeling of specific lipopolysaccharide binding sites on a Gram-negative porin. *J. Phys. Chem. B*. **123**, 5700–5708
240. Samsudin, F., and Khalid, S. (2019) Movement of arginine through OprD: The energetics of permeation and the role of lipopolysaccharide in directing arginine to the protein. *J. Phys. Chem. B*. **123**, 2824–2832
241. Lundquist, K. P., and Gumbart, J. C. (2020) Presence of substrate aids lateral gate separation in LptD. *Biochim. Biophys. acta. Biomembr.* **1862**, 183025
242. Kurisu, G., Zakharov, S. D., Zhalnina, M. V., Bano, S., Eroukova, V. Y., Rokitskaya, T. I., Antonenko, Y. N., Wiener, M. C., and Cramer, W. A. (2003) The structure of BtuB with bound colicin E3 R-domain implies a translocon. *Nat. Struct. Biol.* **10**, 948–54
243. Straatsma, T. P., and Soares, T. A. (2009) Characterization of the outer membrane protein OprF of Pseudomonas aeruginosa in a lipopolysaccharide membrane by computer simulation. *Proteins*. **74**, 475–88
244. Piggot, T. J., Holdbrook, D. A., and Khalid, S. (2013) Conformational dynamics and membrane interactions of the *E. coli* outer membrane protein FecA: a molecular dynamics simulation study. *Biochim. Biophys. Acta*. **1828**, 284–93
245. Holdbrook, D. A., Piggot, T. J., Sansom, M. S. P., and Khalid, S. (2013) Stability and membrane interactions of an autotransport protein: MD simulations of the Hia translocator domain in a complex membrane environment. *Biochim. Biophys. Acta*. **1828**, 715–23
246. Schindler, H., and Rosenbusch, J. P. (1978) Matrix protein from *Escherichia coli* outer membranes forms voltage-controlled channels in lipid bilayers. *Proc. Natl. Acad. Sci. U. S. A.* **75**, 3751–5
247. Rocque, W. J., Coughlin, R. T., and McGroarty, E. J. (1987) Lipopolysaccharide tightly bound to porin monomers and trimers from *Escherichia coli* K-12. *J. Bacteriol.* **169**, 4003–10
248. Holzenburg, A., Engel, A., Kessler, R., Manz, H. J., Lustig, A., and Aebi, U. (1989) Rapid isolation of OmpF porin-LPS complexes suitable for structure-function studies. *Biochemistry*. **28**, 4187–93
249. Ferguson, A. D., Welte, W., Hofmann, E., Lindner, B., Holst, O., Coulton, J. W., and Diederichs, K. (2000) A conserved structural motif for lipopolysaccharide recognition by procaryotic and eucaryotic proteins. *Structure*. **8**, 585–92
250. DiRienzo, J. M., Nakamura, K., and Inouye, M. (1978) The outer membrane proteins of Gram-negative bacteria: biosynthesis, assembly, and functions. *Annu. Rev. Biochem.* **47**, 481–532
251. Loos, M. S., Ramakrishnan, R., Vranken, W., Tsirigotaki, A., Tsare, E.-P., Zorzini, V., Geyter, J. De, Yuan, B., Tsamardinos, I., Klappa, M., Schymkowitz, J., Rousseau, F., Karamanou, S., and Economou, A. (2019) Structural basis of the subcellular topology landscape of *Escherichia coli*. *Front. Microbiol.* **10**, 1–22
252. Rand, R. P., Fuller, N., Parsegian, V. A., and Rau, D. C. (1988) Variation in hydration forces between neutral phospholipid bilayers: evidence for hydration attraction. *Biochemistry*. **27**, 7711–22
253. Petrache, H. I., Dodd, S. W., and Brown, M. F. (2000) Area per lipid and acyl length distributions in fluid phosphatidylcholines determined by (2)H NMR spectroscopy. *Biophys. J.* **79**, 3172–92
254. Rappolt, M., Hickel, A., Bringezu, F., and Lohner, K. (2003) Mechanism of the lamellar/inverse hexagonal phase transition examined by high resolution x-ray diffraction. *Biophys. J.* **84**, 3111–22
255. Leekumjorn, S., and Sum, A. K. (2007) Molecular studies of the gel to liquid-crystalline phase transition for fully hydrated DPPC and DPPE bilayers. *Biochim. Biophys. Acta - Biomembr.* **1768**, 354–365
256. Piggot, T. J., Holdbrook, D. A., and Khalid, S. (2011) Electroporation of the *E. coli* and *S. aureus* membranes: molecular dynamics simulations of complex bacterial membranes. *J. Phys. Chem. B*.

115, 13381–8
257. Pierucci, O. (1978) Dimensions of *Escherichia coli* at various growth rates: model for envelope growth. *J. Bacteriol.* **135**, 559–74
258. Trueba, F. J., and Woldringh, C. L. (1980) Changes in cell diameter during the division cycle of *Escherichia coli*. *J. Bacteriol.* **142**, 869–78
259. Reshes, G., Vanounou, S., Fishov, I., and Feingold, M. (2008) Timing the start of division in *E. coli*: a single-cell study. *Phys. Biol.* **5**, 046001
260. Mathelié-Guinlet, M., Asmar, A. T., Collet, J., and Dufrêne, Y. F. (2020) Lipoprotein Lpp regulates the mechanical properties of the *E. coli* cell envelope. *Nat. Commun.* **11**, 1789
261. Rao, S., Bates, G. T., Matthews, C. R., Newport, T. D., Vickery, O. N., and Stansfeld, P. J. (2020) Characterizing membrane association and periplasmic transfer of bacterial lipoproteins through molecular dynamics simulations. *Structure*. 10.1016/j.str.2020.01.012
262. Clifton, L. A., Skoda, M. W. A., Daulton, E. L., Hughes, A. V., Le Brun, A. P., Lakey, J. H., and Holt, S. A. (2013) Asymmetric phospholipid: lipopolysaccharide bilayers; a Gram-negative bacterial outer membrane mimic. *J. R. Soc. Interface*. **10**, 20130810
263. Clifton, L. A., Skoda, M. W. A., Le Brun, A. P., Ciesielski, F., Kuzmenko, I., Holt, S. A., and Lakey, J. H. (2015) Effect of divalent cation removal on the structure of Gram-negative bacterial outer membrane models. *Langmuir*. **31**, 404–12
264. Markones, M., Fippel, A., Kaiser, M., Drechsler, C., Hunte, C., and Heerklotz, H. (2020) Stairway to asymmetry: Five steps to lipid-asymmetric proteoliposomes. *Biophys. J.* **118**, 294–302
265. Markones, M., Drechsler, C., Kaiser, M., Kalie, L., Heerklotz, H., and Fiedler, S. (2018) Engineering asymmetric lipid vesicles: Accurate and convenient control of the outer leaflet lipid composition. *Langmuir*. **34**, 1999–2005
266. Drechsler, C., Markones, M., Choi, J.-Y., Frieling, N., Fiedler, S., Voelker, D. R., Schubert, R., and Heerklotz, H. (2018) Preparation of asymmetric liposomes using a phosphatidylserine decarboxylase. *Biophys. J.* **115**, 1509–1517
267. Gurtovenko, A. A., and Vattulainen, I. (2008) Membrane potential and electrostatics of phospholipid bilayers with asymmetric transmembrane distribution of anionic lipids. *J. Phys. Chem. B*. **112**, 4629–34
268. Esteban-Martín, S., Risselada, H. J., Salgado, J., and Marrink, S. J. (2009) Stability of asymmetric lipid bilayers assessed by molecular dynamics simulations. *J. Am. Chem. Soc.* **131**, 15194–202
269. Park, S., Beaven, A. H., Klauda, J. B., and Im, W. (2015) How tolerant are membrane simulations with mismatch in area per lipid between leaflets? *J. Chem. Theory Comput.* **11**, 3466–77
270. Heberle, F. A., Marquardt, D., Doktorova, M., Geier, B., Standaert, R. F., Heftberger, P., Kollmitzer, B., Nickels, J. D., Dick, R. A., Feigenson, G. W., Katsaras, J., London, E., and Pabst, G. (2016) Subnanometer structure of an asymmetric model membrane: Interleaflet coupling influences domain properties. *Langmuir*. **32**, 5195–200
271. Doktorova, M., and Weinstein, H. (2018) Accurate in silico modeling of asymmetric bilayers based on biophysical principles. *Biophys. J.* **115**, 1638–1643
272. Franklin, M. W., and Slusky, J. S. G. (2018) Tight turns of outer membrane proteins: An analysis of sequence, structure, and hydrogen bonding. *J. Mol. Biol.* **430**, 3251–3265
273. Steinkühler, J., Sezgin, E., Urbančič, I., Eggeling, C., and Dimova, R. (2019) Mechanical properties of plasma membrane vesicles correlate with lipid order, viscosity and cell density. *Commun. Biol.* **2**, 337
274. Mogensen, J. E., Kleinschmidt, J. H., Schmidt, M. A., and Otzen, D. E. (2005) Misfolding of a bacterial autotransporter. *Protein Sci.* **14**, 2814–27
275. Chaturvedi, D., and Mahalakshmi, R. (2018) Folding determinants of transmembrane β-barrels using engineered OMP chimeras. *Biochemistry*. **57**, 1987–1996
276. Hong, H., Park, S., Jiménez, R. H. F., Rinehart, D., and Tamm, L. K. (2007) Role of aromatic side chains in the folding and thermodynamic stability of integral membrane proteins. *J. Am. Chem. Soc.* **129**, 8320–7

277. Sanchez, K. M., Gable, J. E., Schlamadinger, D. E., and Kim, J. E. (2008) Effects of tryptophan microenvironment, soluble domain, and vesicle size on the thermodynamics of membrane protein folding: lessons from the transmembrane protein OmpA. *Biochemistry*. **47**, 12844–52
278. Andersen, K. K., Wang, H., and Otzen, D. E. (2012) A kinetic analysis of the folding and unfolding of OmpA in urea and guanidinium chloride: single and parallel pathways. *Biochemistry*. **51**, 8371–83
279. Pocanschi, C. L., Popot, J.-L., and Kleinschmidt, J. H. (2013) Folding and stability of outer membrane protein A (OmpA) from *Escherichia coli* in an amphipathic polymer, amphipol A8-35. *Eur. Biophys. J.* **42**, 103–18
280. Moon, C. P., and Fleming, K. G. (2011) Side-chain hydrophobicity scale derived from transmembrane protein folding into lipid bilayers. *Proc. Natl. Acad. Sci. U. S. A.* **108**, 10174–7
281. Moon, C. P., Kwon, S., and Fleming, K. G. (2011) Overcoming hysteresis to attain reversible equilibrium folding for outer membrane phospholipase A in phospholipid bilayers. *J. Mol. Biol.* **413**, 484–94
282. McDonald, S. K., and Fleming, K. G. (2016) Aromatic side chain water-to-lipid transfer free energies show a depth dependence across the membrane normal. *J. Am. Chem. Soc.* **138**, 7946–50
283. Chaturvedi, D., and Mahalakshmi, R. (2013) Methionine mutations of outer membrane protein X influence structural stability and beta-barrel unfolding. *PLoS One*. **8**, e79351
284. Schweizer, M., Hindennach, I., Garten, W., and Henning, U. (1978) Major proteins of the *Escherichia coli* outer cell envelope membrane. Interaction of protein II with lipopolysaccharide. *Eur. J. Biochem.* **82**, 211–7
285. Dornmair, K., Kiefer, H., and Jähnig, F. (1990) Refolding of an integral membrane protein. OmpA of *Escherichia coli*. *J. Biol. Chem.* **265**, 18907–11
286. Garavito, R. M., and Rosenbusch, J. P. (1986) Isolation and crystallization of bacterial porin. *Methods Enzymol.* **125**, 309–28
287. Surrey, T., and Jähnig, F. (1995) Kinetics of folding and membrane insertion of a beta-barrel membrane protein. *J. Biol. Chem.* **270**, 28199–203
288. Dekker, N., Merck, K., Tommassen, J., and Verheij, H. M. (1995) *In vitro* folding of *Escherichia coli* outer-membrane phospholipase A. *Eur. J. Biochem.* **232**, 214–9
289. Kleinschmidt, J. H., Wiener, M. C., and Tamm, L. K. (1999) Outer membrane protein A of *E. coli* folds into detergent micelles, but not in the presence of monomeric detergent. *Protein Sci.* **8**, 2065–71
290. Ebie Tan, A., Burgess, N. K., DeAndrade, D. S., Marold, J. D., and Fleming, K. G. (2010) Self-association of unfolded outer membrane proteins. *Macromol. Biosci.* **10**, 763–7
291. Schnaitman, C. A. (1973) Outer membrane proteins of *Escherichia coli*. I. Effect of preparative conditions on the migration of protein in polyacrylamide gels. *Arch. Biochem. Biophys.* **157**, 541–52
292. Ohnishi, S., and Kameyama, K. (2001) Escherichia coli OmpA retains a folded structure in the presence of sodium dodecyl sulfate due to a high kinetic barrier to unfolding. *Biochim. Biophys. Acta*. **1515**, 159–66
293. Anfinsen, C. B. (1973) Principles that govern the folding of protein chains. *Science*. **181**, 223–30
294. Horne, J. E., and Radford, S. E. (2016) A growing toolbox of techniques for studying β-barrel outer membrane protein folding and biogenesis. *Biochem. Soc. Trans.* **44**, 802–9
295. Clark, A. C. (2008) Protein folding: are we there yet? *Arch. Biochem. Biophys.* **469**, 1–3
296. Bartlett, A. I., and Radford, S. E. (2009) An expanding arsenal of experimental methods yields an explosion of insights into protein folding mechanisms. *Nat. Struct. Mol. Biol.* **16**, 582–8
297. Gruebele, M., Dave, K., and Sukenik, S. (2016) Globular protein folding *in vitro* and *in vivo*. *Annu. Rev. Biophys.* **45**, 233–51
298. Muñoz, V., and Cerminara, M. (2016) When fast is better: protein folding fundamentals and mechanisms from ultrafast approaches. *Biochem. J.* **473**, 2545–59
299. Kleinschmidt, J. H., and Tamm, L. K. (1996) Folding intermediates of a beta-barrel membrane

protein. Kinetic evidence for a multi-step membrane insertion mechanism. *Biochemistry*. **35**, 12993–3000
300. Nugent, S. G., Kumar, D., Rampton, D. S., and Evans, D. F. (2001) Intestinal luminal pH in inflammatory bowel disease: possible determinants and implications for therapy with aminosalicylates and other drugs. *Gut*. **48**, 571–7
301. Kleinschmidt, J. H., and Tamm, L. K. (2002) Secondary and tertiary structure formation of the beta-barrel membrane protein OmpA is synchronized and depends on membrane thickness. *J. Mol. Biol.* **324**, 319–30
302. Pocanschi, C. L., Apell, H.-J., Puntervoll, P., Høgh, B., Jensen, H. B., Welte, W., and Kleinschmidt, J. H. (2006) The major outer membrane protein of *Fusobacterium nucleatum* (FomA) folds and inserts into lipid bilayers via parallel folding pathways. *J. Mol. Biol.* **355**, 548–61
303. Huysmans, G. H. M., Radford, S. E., Baldwin, S. A., and Brockwell, D. J. (2012) Malleability of the folding mechanism of the outer membrane protein PagP: parallel pathways and the effect of membrane elasticity. *J. Mol. Biol.* **416**, 453–64
304. Kleinschmidt, J. H., and Tamm, L. K. (1999) Time-resolved distance determination by tryptophan fluorescence quenching: probing intermediates in membrane protein folding. *Biochemistry*. **38**, 4996–5005
305. Kleinschmidt, J. H., den Blaauwen, T., Driessen, A. J., and Tamm, L. K. (1999) Outer membrane protein A of *Escherichia coli* inserts and folds into lipid bilayers by a concerted mechanism. *Biochemistry*. **38**, 5006–16
306. Rodionova, N. A., Tatulian, S. A., Surrey, T., Jähnig, F., and Tamm, L. K. (1995) Characterization of two membrane-bound forms of OmpA. *Biochemistry*. **34**, 1921–9
307. Kleinschmidt, J. H., Bulieris, P. V., Qu, J., Dogterom, M., and den Blaauwen, T. (2011) Association of neighboring β-strands of outer membrane protein A in lipid bilayers revealed by site-directed fluorescence quenching. *J. Mol. Biol.* **407**, 316–32
308. Popot, J. L., and Engelman, D. M. (2000) Helical membrane protein folding, stability, and evolution. *Annu. Rev. Biochem.* **69**, 881–922
309. Engelman, D. M., Chen, Y., Chin, C.-N., Curran, A. R., Dixon, A. M., Dupuy, A. D., Lee, A. S., Lehnert, U., Matthews, E. E., Reshetnyak, Y. K., Senes, A., and Popot, J.-L. (2003) Membrane protein folding: beyond the two stage model. *FEBS Lett.* **555**, 122–5
310. Burgess, N. K., Dao, T. P., Stanley, A. M., and Fleming, K. G. (2008) Beta-barrel proteins that reside in the *Escherichia coli* outer membrane *in vivo* demonstrate varied folding behavior *in vitro*. *J. Biol. Chem.* **283**, 26748–58
311. Hong, H., and Tamm, L. K. (2004) Elastic coupling of integral membrane protein stability to lipid bilayer forces. *Proc. Natl. Acad. Sci. U. S. A.* **101**, 4065–70
312. Pocanschi, C. L., Patel, G. J., Marsh, D., and Kleinschmidt, J. H. (2006) Curvature elasticity and refolding of OmpA in large unilamellar vesicles. *Biophys. J.* **91**, L75-7
313. Marsh, D., Shanmugavadivu, B., and Kleinschmidt, J. H. (2006) Membrane elastic fluctuations and the insertion and tilt of beta-barrel proteins. *Biophys. J.* **91**, 227–32
314. Maurya, S. R., Chaturvedi, D., and Mahalakshmi, R. (2013) Modulating lipid dynamics and membrane fluidity to drive rapid folding of a transmembrane barrel. *Sci. Rep.* **3**, 1989
315. Danoff, E. J., and Fleming, K. G. (2015) Membrane defects accelerate outer membrane β-barrel protein folding. *Biochemistry*. **54**, 97–9
316. Nielsen, L. K., Bjørnholm, T., and Mouritsen, O. G. (2000) Fluctuations caught in the act. *Nature*. **404**, 352
317. Enders, O., Ngezahayo, A., Wiechmann, M., Leisten, F., and Kolb, H.-A. (2004) Structural calorimetry of main transition of supported DMPC bilayers by temperature-controlled AFM. *Biophys. J.* **87**, 2522–31
318. Blok, M. C., van der Neut-Kok, E. C., van Deenen, L. L., and de Gier, J. (1975) The effect of chain length and lipid phase transitions on the selective permeability properties of liposomes.

Biochim. Biophys. Acta. **406**, 187–96
319. Blok, M. C., van Deenen, L. L., and De Gier, J. (1976) Effect of the gel to liquid crystalline phase transition on the osmotic behaviour of phosphatidylcholine liposomes. *Biochim. Biophys. Acta*. **433**, 1–12
320. van Hoogevest, P., de Gier, J., and de Kruijff, B. (1984) Determination of the size of the packing defects in dimyristoylphosphatidylcholine bilayers, present at the phase transition temperature. *FEBS Lett.* **171**, 160–164
321. Hays, L. M., Crowe, J. H., Wolkers, W., and Rudenko, S. (2001) Factors affecting leakage of trapped solutes from phospholipid vesicles during thermotropic phase transitions. *Cryobiology*. **42**, 88–102
322. Heimburg, T. (2007) Permeability. in *Thermal Biophysics of Membranes*, pp. 289–300, Wiley-VCH Verlag GmbH & Co. KGaA, Weinheim, Germany, 10.1002/9783527611591.ch17
323. Danoff, E. J., and Fleming, K. G. (2017) Novel kinetic intermediates populated along the folding pathway of the transmembrane β-barrel OmpA. *Biochemistry*. **56**, 47–60
324. Huysmans, G. H. M., Baldwin, S. A., Brockwell, D. J., and Radford, S. E. (2010) The transition state for folding of an outer membrane protein. *Proc. Natl. Acad. Sci. U. S. A.* **107**, 4099–104
325. Bond, P. J., and Sansom, M. S. P. (2006) Insertion and assembly of membrane proteins via simulation. *J. Am. Chem. Soc.* **128**, 2697–704
326. Moon, C. P., Zaccai, N. R., Fleming, P. J., Gessmann, D., and Fleming, K. G. (2013) Membrane protein thermodynamic stability may serve as the energy sink for sorting in the periplasm. *Proc. Natl. Acad. Sci. U. S. A.* **110**, 4285–90
327. Gessmann, D., Chung, Y. H., Danoff, E. J., Plummer, A. M., Sandlin, C. W., Zaccai, N. R., and Fleming, K. G. (2014) Outer membrane β-barrel protein folding is physically controlled by periplasmic lipid head groups and BamA. *Proc. Natl. Acad. Sci. U. S. A.* **111**, 5878–83
328. Noinaj, N., Kuszak, A. J., Gumbart, J. C., Lukacik, P., Chang, H., Easley, N. C., Lithgow, T., and Buchanan, S. K. (2013) Structural insight into the biogenesis of β-barrel membrane proteins. *Nature*. **501**, 385–90
329. Noinaj, N., Kuszak, A. J., Balusek, C., Gumbart, J. C., and Buchanan, S. K. (2014) Lateral opening and exit pore formation are required for BamA function. *Structure*. **22**, 1055–62
330. Gu, Y., Li, H., Dong, H., Zeng, Y., Zhang, Z., Paterson, N. G., Stansfeld, P. J., Wang, Z., Zhang, Y., Wang, W., and Dong, C. (2016) Structural basis of outer membrane protein insertion by the BAM complex. *Nature*. **531**, 64–9
331. Fleming, P. J., Patel, D. S., Wu, E. L., Qi, Y., Yeom, M. S., Sousa, M. C., Fleming, K. G., and Im, W. (2016) BamA POTRA domain interacts with a native lipid membrane surface. *Biophys. J.* **110**, 2698–2709
332. Schiffrin, B., Calabrese, A. N., Higgins, A. J., Humes, J. R., Ashcroft, A. E., Kalli, A. C., Brockwell, D. J., and Radford, S. E. (2017) Effects of periplasmic chaperones and membrane thickness on BamA-catalyzed outer-membrane protein folding. *J. Mol. Biol.* **429**, 3776–3792
333. Lundquist, K., Bakelar, J., Noinaj, N., and Gumbart, J. C. (2018) C-terminal kink formation is required for lateral gating in BamA. *Proc. Natl. Acad. Sci. U. S. A.* **115**, E7942–E7949
334. Ellena, J. F., Lackowicz, P., Mongomery, H., and Cafiso, D. S. (2011) Membrane thickness varies around the circumference of the transmembrane protein BtuB. *Biophys. J.* **100**, 1280–7
335. Holdbrook, D. A., Huber, R. G., Piggot, T. J., Bond, P. J., and Khalid, S. (2016) Dynamics of crowded vesicles: Local and global responses to membrane composition. *PLoS One*. **11**, e0156963
336. Ramakrishnan, M., Pocanschi, C. L., Kleinschmidt, J. H., and Marsh, D. (2004) Association of spin-labeled lipids with beta-barrel proteins from the outer membrane of *Escherichia coli*. *Biochemistry*. **43**, 11630–6
337. Anbazhagan, V., Qu, J., Kleinschmidt, J. H., and Marsh, D. (2008) Incorporation of outer membrane protein OmpG in lipid membranes: protein-lipid interactions and beta-barrel orientation. *Biochemistry*. **47**, 6189–98
338. Anbazhagan, V., Vijay, N., Kleinschmidt, J. H., and Marsh, D. (2008) Protein-lipid interactions

with *Fusobacterium nucleatum* major outer membrane protein FomA: spin-label EPR and polarized infrared spectroscopy. *Biochemistry*. **47**, 8414–23
339. Ni, D., Wang, Y., Yang, X., Zhou, H., Hou, X., Cao, B., Lu, Z., Zhao, X., Yang, K., and Huang, Y. (2014) Structural and functional analysis of the β-barrel domain of BamA from *Escherichia coli*. *FASEB J.* **28**, 2677–85
340. Albrecht, R., Schütz, M., Oberhettinger, P., Faulstich, M., Bermejo, I., Rudel, T., Diederichs, K., and Zeth, K. (2014) Structure of BamA, an essential factor in outer membrane protein biogenesis. *Acta Crystallogr. D. Biol. Crystallogr.* **70**, 1779–89
341. Bakelar, J., Buchanan, S. K., and Noinaj, N. (2016) The structure of the β-barrel assembly machinery complex. *Science*. **351**, 180–6
342. Han, L., Zheng, J., Wang, Y., Yang, X., Liu, Y., Sun, C., Cao, B., Zhou, H., Ni, D., Lou, J., Zhao, Y., and Huang, Y. (2016) Structure of the BAM complex and its implications for biogenesis of outer-membrane proteins. *Nat. Struct. Mol. Biol.* **23**, 192–6
343. Iadanza, M. G., Higgins, A. J., Schiffrin, B., Calabrese, A. N., Brockwell, D. J., Ashcroft, A. E., Radford, S. E., and Ranson, N. A. (2016) Lateral opening in the intact β-barrel assembly machinery captured by cryo-EM. *Nat. Commun.* **7**, 12865
344. Gu, Y., Zeng, Y., Wang, Z., and Dong, C. (2017) BamA β16C strand and periplasmic turns are critical for outer membrane protein insertion and assembly. *Biochem. J.* **474**, 3951–3961
345. Hartmann, J.-B., Zahn, M., Burmann, I. M., Bibow, S., and Hiller, S. (2018) Sequence-specific solution NMR assignments of the β-barrel insertase BamA to monitor its conformational ensemble at the atomic level. *J. Am. Chem. Soc.* **140**, 11252–11260
346. Lessen, H. J., Majumdar, A., and Fleming, K. G. (2020) Backbone hydrogen bond energies in membrane proteins are insensitive to large changes in local water concentration. *J. Am. Chem. Soc.* **142**, 6227–6235
347. Doerner, P. A., and Sousa, M. C. (2017) Extreme dynamics in the BamA β-barrel seam. *Biochemistry*. **56**, 3142–3149
348. Marsh, D. (2008) Energetics of hydrophobic matching in lipid-protein interactions. *Biophys. J.* **94**, 3996–4013
349. Yin, F., and Kindt, J. T. (2012) Hydrophobic mismatch and lipid sorting near OmpA in mixed bilayers: atomistic and coarse-grained simulations. *Biophys. J.* **102**, 2279–87
350. Katira, S., Mandadapu, K. K., Vaikuntanathan, S., Smit, B., and Chandler, D. (2016) Pre-transition effects mediate forces of assembly between transmembrane proteins. *Elife*. **5**, e13150
351. Ricci, D. P., Hagan, C. L., Kahne, D., and Silhavy, T. J. (2012) Activation of the *Escherichia coli* β-barrel assembly machine (Bam) is required for essential components to interact properly with substrate. *Proc. Natl. Acad. Sci. U. S. A.* **109**, 3487–91
352. Rigel, N. W., Schwalm, J., Ricci, D. P., and Silhavy, T. J. (2012) BamE modulates the *Escherichia coli* beta-barrel assembly machine component BamA. *J. Bacteriol.* **194**, 1002–8
353. Rigel, N. W., Ricci, D. P., and Silhavy, T. J. (2013) Conformation-specific labeling of BamA and suppressor analysis suggest a cyclic mechanism for β-barrel assembly in *Escherichia coli*. *Proc. Natl. Acad. Sci. U. S. A.* **110**, 5151–6
354. McCabe, A. L., Ricci, D., Adetunji, M., and Silhavy, T. J. (2017) Conformational changes that coordinate the activity of BamA and BamD allowing β-barrel assembly. *J. Bacteriol.* **199**, 1–11
355. Lee, J., Sutterlin, H. A., Wzorek, J. S., Mandler, M. D., Hagan, C. L., Grabowicz, M., Tomasek, D., May, M. D., Hart, E. M., Silhavy, T. J., and Kahne, D. (2018) Substrate binding to BamD triggers a conformational change in BamA to control membrane insertion. *Proc. Natl. Acad. Sci. U. S. A.* **115**, 2359–2364
356. Hart, E. M., Gupta, M., Wühr, M., and Silhavy, T. J. (2019) The synthetic phenotype of ΔbamB ΔbamE double mutants results from a lethal jamming of the Bam complex by the lipoprotein RcsF. *MBio*. **10**, 1–12
357. Tata, M., and Konovalova, A. (2019) Improper coordination of BamA and BamD results in Bam complex jamming by a lipoprotein substrate. *MBio*. **10**, 1–10

358. Warner, L. R., Gatzeva-Topalova, P. Z., Doerner, P. A., Pardi, A., and Sousa, M. C. (2017) Flexibility in the periplasmic domain of BamA is important for function. *Structure*. **25**, 94–106
359. Höhr, A. I. C., Lindau, C., Wirth, C., Qiu, J., Stroud, D. A., Kutik, S., Guiard, B., Hunte, C., Becker, T., Pfanner, N., and Wiedemann, N. (2018) Membrane protein insertion through a mitochondrial β-barrel gate. *Science*. **359**, eaah6834
360. Doyle, M. T., and Bernstein, H. D. (2019) Bacterial outer membrane proteins assemble via asymmetric interactions with the BamA β-barrel. *Nat. Commun.* **10**, 3358
361. Lee, J., Tomasek, D., Santos, T. M., May, M. D., Meuskens, I., and Kahne, D. (2019) Formation of a β-barrel membrane protein is catalyzed by the interior surface of the assembly machine protein BamA. *Elife*. 10.7554/eLife.49787
362. Kutik, S., Stojanovski, D., Becker, L., Becker, T., Meinecke, M., Krüger, V., Prinz, C., Meisinger, C., Guiard, B., Wagner, R., Pfanner, N., and Wiedemann, N. (2008) Dissecting membrane insertion of mitochondrial beta-barrel proteins. *Cell*. **132**, 1011–24
363. Paramasivam, N., Habeck, M., and Linke, D. (2012) Is the C-terminal insertional signal in Gram-negative bacterial outer membrane proteins species-specific or not? *BMC Genomics*. **13**, 510
364. Gruss, F., Zähringer, F., Jakob, R. P., Burmann, B. M., Hiller, S., and Maier, T. (2013) The structural basis of autotransporter translocation by TamA. *Nat. Struct. Mol. Biol.* **20**, 1318–20
365. Noinaj, N., Rollauer, S. E., and Buchanan, S. K. (2015) The β-barrel membrane protein insertase machinery from Gram-negative bacteria. *Curr. Opin. Struct. Biol.* **31**, 35–42
366. Schiffrin, B., Brockwell, D. J., and Radford, S. E. (2017) Outer membrane protein folding from an energy landscape perspective. *BMC Biol.* **15**, 123
367. Wang, Y., Wang, R., Jin, F., Liu, Y., Yu, J., Fu, X., and Chang, Z. (2016) A supercomplex spanning the inner and outer membranes mediates the biogenesis of β-barrel outer membrane proteins in bacteria. *J. Biol. Chem.* **291**, 16720–9
368. Alvira, S., Watkins, D. W., Troman, L., Lorriman, J., Daum, B., Gold, V. A. M., and Collinson, I. (2019) Trans-membrane association of the Sec and BAM complexes for bacterial outer-membrane biogenesis. *bioRxiv*. doi.org/10.1101/589077
369. Carlson, M. L., Stacey, R. G., Young, J. W., Wason, I. S., Zhao, Z., Rattray, D. G., Scott, N., Kerr, C. H., Babu, M., Foster, L. J., and Duong Van Hoa, F. (2019) Profiling the *Escherichia coli* membrane protein interactome captured in Peptidisc libraries. *Elife*. **8**, 1–26
370. Thoma, J., Manioglu, S., Kalbermatter, D., Bosshart, P. D., Fotiadis, D., and Müller, D. J. (2018) Protein-enriched outer membrane vesicles as a native platform for outer membrane protein studies. *Commun. Biol.* **1**, 23
371. Thoma, J., Sun, Y., Ritzmann, N., and Müller, D. J. (2018) POTRA domains, extracellular lid, and membrane composition modulate the conformational stability of the β-barrel assembly factor BamA. *Structure*. **26**, 987-996.e3
372. Thoma, J., and Burmann, B. M. (2020) High-resolution in situ NMR spectroscopy of bacterial envelope proteins in outer membrane vesicles. *Biochemistry*. 10.1021/acs.biochem.9b01123
373. Hagan, C. L., Kim, S., and Kahne, D. (2010) Reconstitution of outer membrane protein assembly from purified components. *Science*. **328**, 890–2
374. Hagan, C. L., Westwood, D. B., and Kahne, D. (2013) Bam lipoproteins assemble BamA *in vitro*. *Biochemistry*. **52**, 6108–13
375. Patel, G. J., and Kleinschmidt, J. H. (2013) The lipid bilayer-inserted membrane protein BamA of *Escherichia coli* facilitates insertion and folding of outer membrane protein A from its complex with Skp. *Biochemistry*. **52**, 3974–86
376. Hussain, S., and Bernstein, H. D. (2018) The Bam complex catalyzes efficient insertion of bacterial outer membrane proteins into membrane vesicles of variable lipid composition. *J. Biol. Chem.* **293**, 2959–2973
377. Ieva, R., and Bernstein, H. D. (2009) Interaction of an autotransporter passenger domain with BamA during its translocation across the bacterial outer membrane. *Proc. Natl. Acad. Sci. U. S. A.* **106**, 19120–5

378. Sauri, A., Soprova, Z., Wickström, D., de Gier, J.-W., Van der Schors, R. C., Smit, A. B., Jong, W. S. P., and Luirink, J. (2009) The Bam (Omp85) complex is involved in secretion of the autotransporter haemoglobin protease. *Microbiology*. **155**, 3982–91
379. Bodelón, G., Marín, E., and Fernández, L. A. (2009) Role of periplasmic chaperones and BamA (YaeT/Omp85) in folding and secretion of intimin from enteropathogenic *Escherichia coli* strains. *J. Bacteriol.* **191**, 5169–79
380. Norell, D., Heuck, A., Tran-Thi, T.-A., Götzke, H., Jacob-Dubuisson, F., Clausen, T., Daley, D. O., Braun, V., Müller, M., and Fan, E. (2014) Versatile *in vitro* system to study translocation and functional integration of bacterial outer membrane proteins. *Nat. Commun.* **5**, 5396
381. Roman-Hernandez, G., Peterson, J. H., and Bernstein, H. D. (2014) Reconstitution of bacterial autotransporter assembly using purified components. *Elife*. **3**, e04234
382. Klein, K., Sonnabend, M. S., Frank, L., Leibiger, K., Franz-Wachtel, M., Macek, B., Trunk, T., Leo, J. C., Autenrieth, I. B., Schütz, M., and Bohn, E. (2019) Deprivation of the periplasmic chaperone SurA reduces virulence and restores antibiotic susceptibility of multidrug-resistant Pseudomonas aeruginosa. *Front. Microbiol.* **10**, 100
383. Ruiz, N., Falcone, B., Kahne, D., and Silhavy, T. J. (2005) Chemical conditionality: a genetic strategy to probe organelle assembly. *Cell*. **121**, 307–17
384. Wu, T., Malinverni, J., Ruiz, N., Kim, S., Silhavy, T. J., and Kahne, D. (2005) Identification of a multicomponent complex required for outer membrane biogenesis in *Escherichia coli*. *Cell*. **121**, 235–45
385. Ryan, K. R., Taylor, J. A., and Bowers, L. M. (2010) The BAM complex subunit BamE (SmpA) is required for membrane integrity, stalk growth and normal levels of outer membrane {beta}-barrel proteins in *Caulobacter crescentus*. *Microbiology*. **156**, 742–56
386. Werner, J., and Misra, R. (2005) YaeT (Omp85) affects the assembly of lipid-dependent and lipid-independent outer membrane proteins of *Escherichia coli*. *Mol. Microbiol.* **57**, 1450–9
387. Palomino, C., Marín, E., and Fernández, L. Á. (2011) The fimbrial usher FimD follows the SurA-BamB pathway for its assembly in the outer membrane of *Escherichia coli*. *J. Bacteriol.* **193**, 5222–30
388. Chimalakonda, G., Ruiz, N., Chng, S.-S., Garner, R. A., Kahne, D., and Silhavy, T. J. (2011) Lipoprotein LptE is required for the assembly of LptD by the beta-barrel assembly machine in the outer membrane of *Escherichia coli*. *Proc. Natl. Acad. Sci. U. S. A.* **108**, 2492–7
389. Volokhina, E. B., Beckers, F., Tommassen, J., and Bos, M. P. (2009) The beta-barrel outer membrane protein assembly complex of *Neisseria meningitidis*. *J. Bacteriol.* **191**, 7074–85
390. Collin, S., Guilvout, I., Chami, M., and Pugsley, A. P. (2007) YaeT-independent multimerization and outer membrane association of secretin PulD. *Mol. Microbiol.* **64**, 1350–7
391. Hoang, H. H., Nickerson, N. N., Lee, V. T., Kazimirova, A., Chami, M., Pugsley, A. P., and Lory, S. (2011) Outer membrane targeting of *Pseudomonas aeruginosa* proteins shows variable dependence on the components of Bam and Lol machineries. *MBio*. **2**, 1–8
392. Huysmans, G. H. M., Guilvout, I., Chami, M., Nickerson, N. N., and Pugsley, A. P. (2015) Lipids assist the membrane insertion of a BAM-independent outer membrane protein. *Sci. Rep.* **5**, 1–15
393. Dunstan, R. A., Hay, I. D., Wilksch, J. J., Schittenhelm, R. B., Purcell, A. W., Clark, J., Costin, A., Ramm, G., Strugnell, R. A., and Lithgow, T. (2015) Assembly of the secretion pores GspD, Wza and CsgG into bacterial outer membranes does not require the Omp85 proteins BamA or TamA. *Mol. Microbiol.* **97**, 616–29
394. Kazmierczak, B. I., Mielke, D. L., Russel, M., and Model, P. (1994) pIV, a filamentous phage protein that mediates phage export across the bacterial cell envelope, forms a multimer. *J. Mol. Biol.* **238**, 187–98
395. Nickerson, N. N., Abby, S. S., Rocha, E. P. C., Chami, M., and Pugsley, A. P. (2012) A single amino acid substitution changes the self-assembly status of a Type IV piliation secretin. *J. Bacteriol.* **194**, 4951–8
396. Yang, J., and Zhang, Y. (2015) I-TASSER server: new development for protein structure and

function predictions. *Nucleic Acids Res.* **43**, W174-81
397. Chorev, D. S., Baker, L. A., Wu, D., Beilsten-Edmands, V., Rouse, S. L., Zeev-Ben-Mordehai, T., Jiko, C., Samsudin, F., Gerle, C., Khalid, S., Stewart, A. G., Matthews, S. J., Grünewald, K., and Robinson, C. V. (2018) Protein assemblies ejected directly from native membranes yield complexes for mass spectrometry. *Science*. **362**, 829–834
398. Booth, P. J., and Curnow, P. (2009) Folding scene investigation: membrane proteins. *Curr. Opin. Struct. Biol.* **19**, 8–13
399. Robert, V., Volokhina, E. B., Senf, F., Bos, M. P., Van Gelder, P., and Tommassen, J. (2006) Assembly factor Omp85 recognizes its outer membrane protein substrates by a species-specific C-terminal motif. *PLoS Biol.* **4**, e377
400. Arora, A., Abildgaard, F., Bushweller, J. H., and Tamm, L. K. (2001) Structure of outer membrane protein A transmembrane domain by NMR spectroscopy. *Nat. Struct. Biol.* **8**, 334–8
401. Ishida, H., Garcia-Herrero, A., and Vogel, H. J. (2014) The periplasmic domain of *Escherichia coli* outer membrane protein A can undergo a localized temperature dependent structural transition. *Biochim. Biophys. Acta*. **1838**, 3014–24
402. Baltoumas, F. A., Hamodrakas, S. J., and Iconomidou, V. A. (2019) The gram-negative outer membrane modeler: Automated building of lipopolysaccharide-rich bacterial outer membranes in four force fields. *J. Comput. Chem.* **40**, 1727–1734

FOOTNOTES

[1] The abbreviations used are:

A-MD, atomistic molecular dynamics; **BAM**, β-barrel assembly machinery; **C_8POE**, octyl-poly-oxyethyleneoxide; **CD**, circular dichroism; **CG-MD**, coarse-grained molecular dynamics; **CL**, cardiolipin; **CMC**, critical micelle concentration; **cryo-EM**, cryogenic electron microscopy; **DDPC**, 1,2-didecanoyl-sn-glycero-3-phosphocholine; **DLPC**, 1,2-dilauroyl-sn-glycero-3-phosphocholine; **DMPC**, 1,2-dimyristoyl-sn-glycero-3-phosphocholine; **DMPG**, 1,2-dimyristoyl-sn-glycero-3-phosphoglycerol; **DOPC**, 1,2-dioleoyl-sn-glycero-3-phosphocholine; **DOPE**, 1,2-dioleoyl-sn-glycero-3-phosphoethanolamine; **DOPG**, 1,2-dioleoyl-sn-glycero-3-phosphoglycerol; **DPH**, 1,3-diphenyl-1,3,5-hexatriene; **DPPC**, 1,2-dipalmitoyl-sn-glycero-3-phosphocholine ; **DPPE**, 1,2-dipalmitoyl-sn-glycero-3-phosphoethanolamine; **DPPG**, 1,2-dipalmitoyl-sn-glycero-3-phosphoglycerol; **IM**, inner membrane; **IMPs,** inner membrane proteins; **LPR**, lipid-to-protein ratio; **LPS,** lipopolysaccharide; **LUV**, large unilamellar vesicle; **MD**, molecular dynamics; **OG,** octyl glucoside; **OM,** outer membrane; **OMP,** outer membrane protein; **PC**, phosphatidylcholine; **PE**, phosphatidylethanolamine; **PG**, phosphatidylglycerol; **POPC,** 1-palmitoyl-2-oleoyl-sn-glycero-3-phosphocholine; **POPE,** 1-palmitoyl-2-oleoyl-sn-glycero-3-phosphoethanolamine; **POPG,** 1-palmitoyl-2-oleoyl-sn-glycero-3-phosphoglycerol; **POTRA domain**, polypeptide transport associated domain; **PPPE,** 1-palmitoyl-2-palmitoleoyl-sn-glycero-3-phosphoethanolamine; **PVPG,** 1-palmitoyl-2-vacenoyl-sn-glycero-3-phosphoglycerol; **SDS-PAGE**, sodium dodecyl sulfate polyacrylamide gel electrophoresis; **SUV**, small unilamellar vesicle; $\boldsymbol{T_m}$, transition temperature; **tOmpA**, the β-barrel domain of OmpA; **UV**, ultraviolet.

Funding to JEH was provided by the Biological and Biotechnology Research Council (BBSRC) (BB/M01151/1). SER and DJB acknowledge BBSRC (BB/K000659/1, BB/T000635/1 and BB/N007603/1) and MRC (MR/P018491/1) for funding their work on BAM and OMPs.

Tables and Table Legends

OMP(s)	Family	Number of β-strands	Organism	Reference
BAM-catalysis involved				
OmpA, OmpX, OmpT, OmPLA, OmpG	*Varied small barrels*	8-14	*E. coli**	(310, 327, 343, 373–376)
various	Autotransporters	12	*E. coli*	(360, 376–381)
OprD	Outer membrane porin	18	*Pseudomonas aeruginosa*	(382)
LamB	Sugar porin	18	*E. coli*	(383, 384)
various	TonB-dependent receptors	22	*Caulobacter crescentus*	(120, 385)
TolC	Outer membrane factor	3x4 (12)	*E. coli*	(386)
FimD‡	Fimbrial usher	24	*E. coli*	(387)
LptD	LPS assembly	26	*E. coli*	(37, 355, 361, 383, 388)
PilQ‡	Type IV pilus secretin	14x4 (56)	*Neisseria meningitidis*	(23, 389)
BAM-independent folding				
PulD‡, XcpQ‡, GspD‡	T2SS secretin	15x4 (60)	*Klebsiella oxytoca, Pseudomonas aeruginosa, E. coli*	(390–393)
pIV‡	Phage secretin	?	Phage f1	(394, 395)
CsgG‡†	Curli secretion	9x4 (36)	*E. coli*	(393)

Table 1. Summary of BAM-dependent and BAM-independent OMPs in the OM of different bacteria.
A list of studies which present evidence a link is present (BAM-catalysis involved) or absent (BAM-independent folding) between the biogenesis of a particular OMP and the presence of the BAM complex. This list includes *in vivo* studies and *in vitro* folding studies performed with polar lipid extract from *E. coli.* *****, these studies were all performed *in vitro*. ‡, these proteins are often assembled as part of larger protein machineries or export/import pathways and may also include their own targeting and assembly factors. †, also contains an N-terminal lipid anchor.

Figures and Figure Legnds

Figure 1

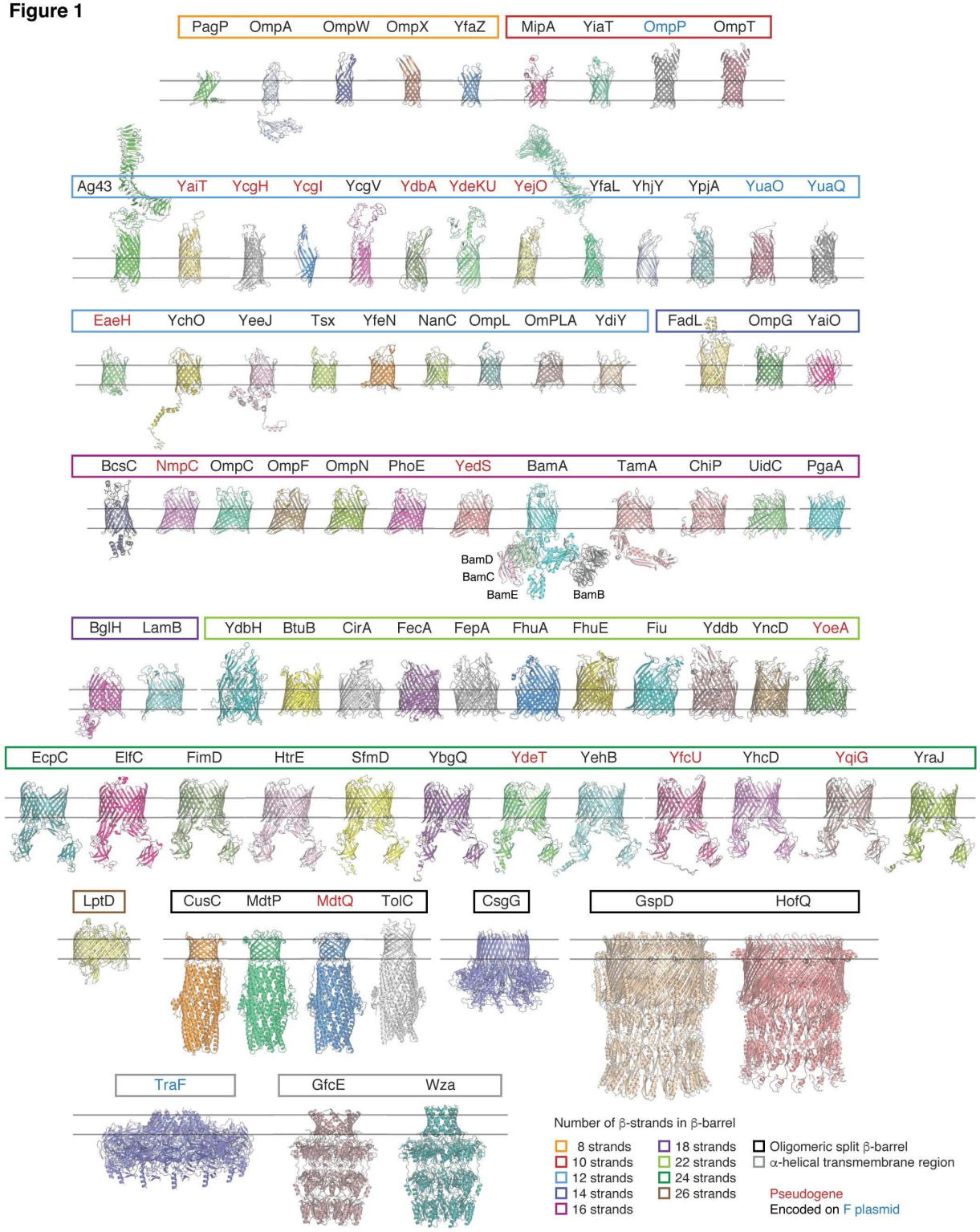

Figure 1. Structures of transmembrane proteins found in the OM of *E. coli* K-12 MG1655. A list of all known and predicted transmembrane proteins in the OM of *E. coli* K-12 strain MG1655 was manually

curated, creating the "OMP-ome". The Protein Data Bank (https://www.rcsb.org/) was then searched for solved structures of these proteins or close homologues. Where no high-resolution solved 3D structures were available, homology models were generated using the I-TASSER server (https://zhanglab.ccmb.med.umich.edu/I-TASSER/) (396). For two proteins, NfrA (the N4 bacteriophage receptor), and FlgH (the flagellar L-ring protein), no homology models could be generated. Predictions for YaiO, YcgI, YdbH, and YhjY generated deformed or broken barrels (possibly due to a lack of homology to existing structures) but their predictions are displayed to indicate their approximate structure. Extracellular domains of autotransporters have only been shown where accurate models could be built or crystal structures were available. OMPs are grouped here by the number of β-strands and then by protein family. The non-OMP subunits of the BAM complex are labelled beneath the central BamA subunit. Protein names are in red if they represent pseudogenes (inactivated by mutation in this strain) and blue if they are encoded on the F plasmid. The colour of the box surrounding the protein names represents the number of β-strands in the β-barrel. Light blue = 8, dark blue = 10, light green = 12, dark green = 14, light red = 16, red = 18, light orange = 22, orange = 24, pink = 26, black = oligomeric split β-barrel, grey = α-helical transmembrane region. Structures were aligned on each other by their β-barrel domains and rendered individually in PyMol 2.X (Schrödinger, LLC). A list of the proteins with their associated family and PDB code can be found in Table S1.

Figure 2

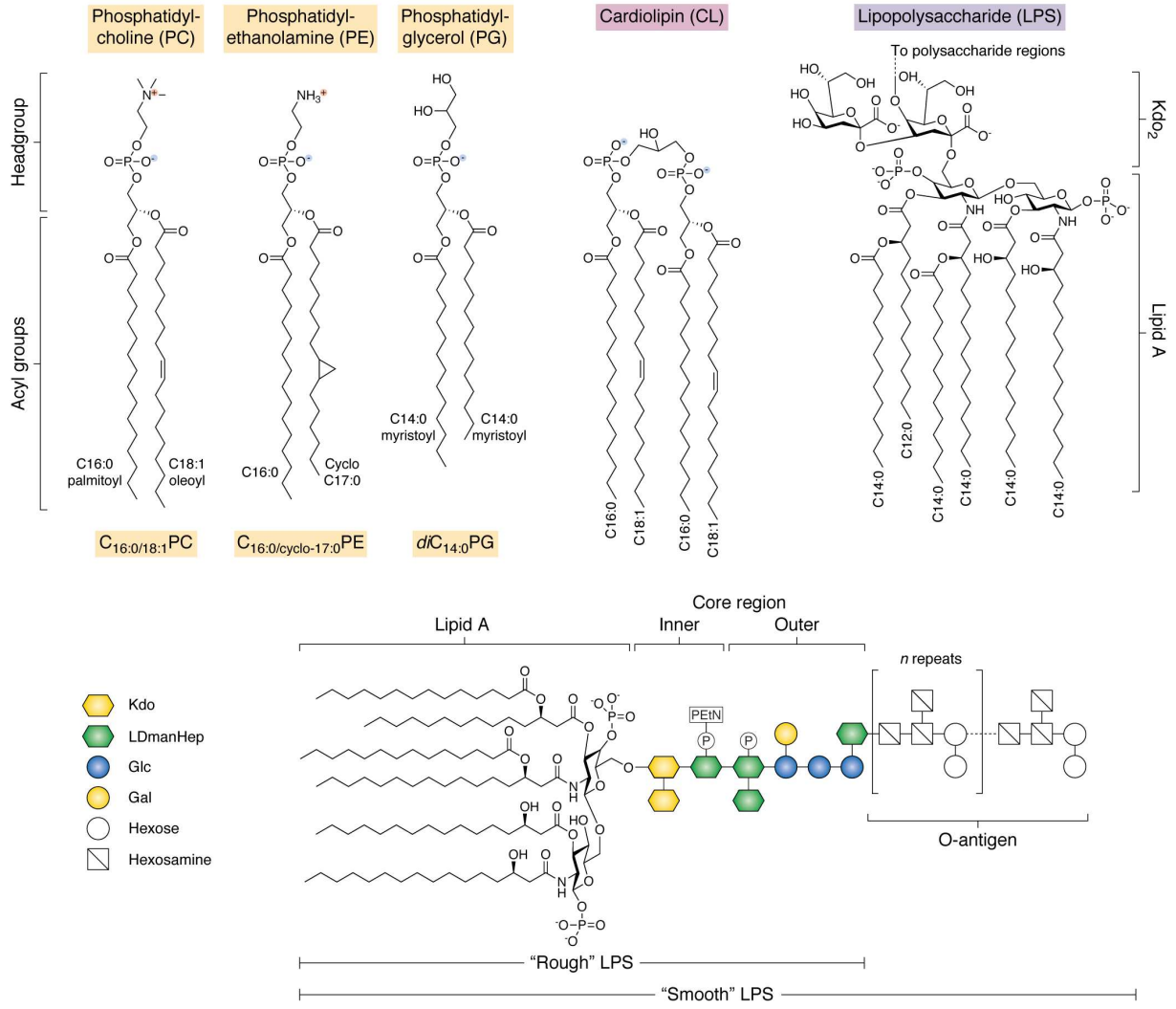

Figure 2. Common lipid types found in bacterial outer membranes and/or used in *in vitro* studies of OMP folding. (Top) Schematic of the generic structure of phospholipids and LPS. Bacterial lipids can be conceptualized as having two 'domains': a polar headgroup, and a hydrophobic acyl tail region. In phospholipids, the acyl tails are connected by an ester linkage to a phosphate group and a variable headgroup region. Phosphatidylcholine (PC) and phosphatidylethanolamine (PE) are zwitterionic while phosphatidylglycerol (PG) carries a net negative charge. Note that PC lipids are not commonly found in bacterial membranes but are often used for OMP folding studies *in vitro* due to their net neutral charge and propensity to form bilayers. Cardiolipin comprises two acyl tail regions connected by phosphate groups via a glycerol linkage and carries a net double negative charge. Lipopolysaccharide (LPS) is found exclusively in the OM of Gram-negative bacteria and varies considerably between species in both the number and length of acyl tails in the lipid A region, and the sugar composition in the polysaccharide region (shown below). Here the most common structure of Lipid A-Kdo_2 for *E. coli* K-12 LPS is shown in full. (Bottom) The architecture of a generic LPS is shown. The lipid A and core region are consistent with LPS found in *E. coli* K-12, however, this strain does not naturally produce an O-antigen whilst many environmental and clinical strains do. Strains lacking the O-antigen region are said to contain 'rough' LPS and this can further be divided into subtypes dependent on truncations in the core region. The most

extreme of these which is still viable at 37 °C under laboratory growth conditions is ‘deep rough’ LPS, containing only lipid A-Kdo_2. The O-antigen region is highly variable within species and can contain as many as 40 glycan repeats. Kdo, keto-deoxyoctulosonate; LDmanHep, L-glycero-D-manno-heptose; Glc, glucose; Gal, galactose; P, phosphate group; PEtN, phosphorylethanolamine.

Figure 3

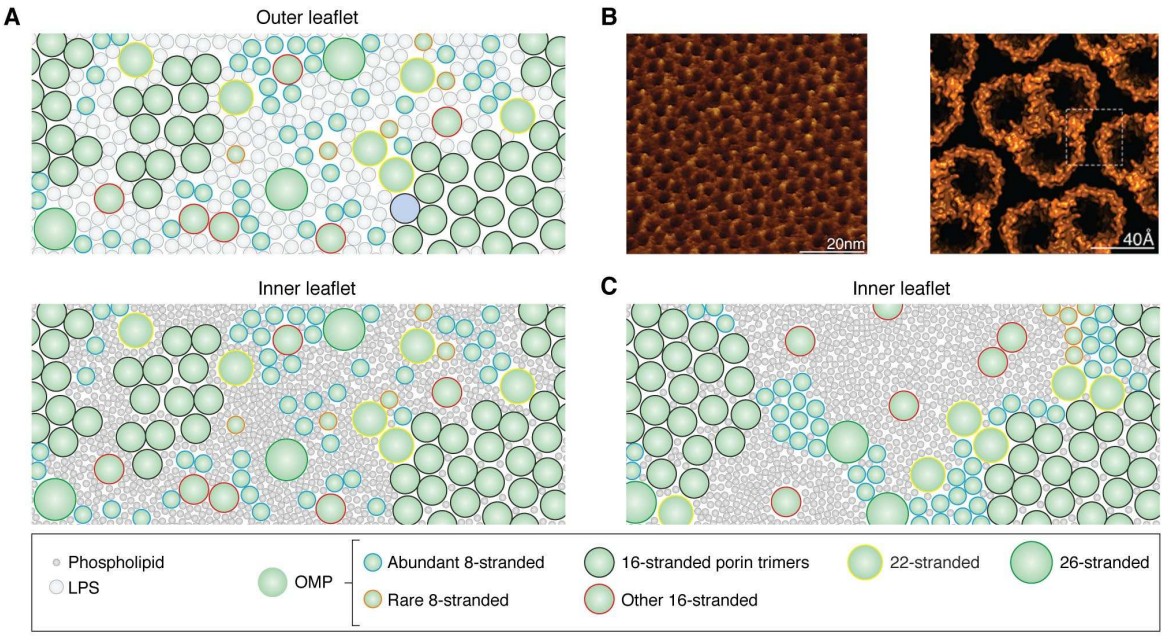

Figure 3. Model depicting the structural organisation of the *E. coli* OM. Schematic displaying the degree of crowding in the OM. (A) View of an imagined OM showing the dense packing of different size OMPs in monomers, dimers, and trimers interspersed with LPS in the outer leaflet (top) and phospholipids in the inner leaflet (bottom). Lipids are represented as grey circles with a diameter proportional to their surface area: phospholipids (dark grey) proportional to the headgroup size of PE/PG, LPS (light grey) proportional the size of lipid A. Different OMPs are represented as idealised circles with diameters proportional to their number of strands. Blue outline = abundant 8-stranded, orange outline = rare 8-stranded, black = 16-stranded porin trimers, red = other 16-stranded, yellow = 22-stranded, green = 26-stranded.The overall LPR in this schematic is ~9:1, with ~2 LPS and ~7 phospholipids per OMP, consistent with estimates for the LPR of the *E. coli* OM. (B) *Left:* High resolution AFM image of OM extracts from *Roseobacter dentrificans* imaged from the periplasmic side showing a dense lattice of porin trimers. *Right*: Atomic model of the packing of porin trimers derived from the AFM data. Reproduced with permission from Jarosawski *et al.* (2009) (127). (C) View of an imagined OM with the same LPR as in (A) but assuming a more extreme clustering of most OMPs. Only the inner leaflet is shown. Despite having the same LPR values, the buried surface area of the clustered OMPs frees up more lipid to form larger bulk lipid domains.

Figure 4

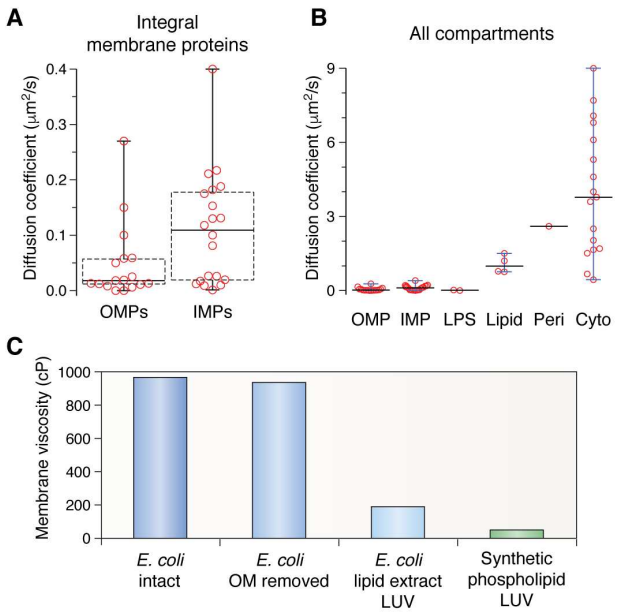

Figure 4. Comparison of physical properties of bacterial membranes. (A) Box plots showing the range of diffusion coefficients reported for OMPs and IMPs (see main text for sources). Boxes show interquartile range calculated by the Tukey method with the median indicated as a bold horizontal line. Whiskers show the minimum and maximum values. (B) Comparison of the diffusion coefficients of membrane proteins with other components of bacteria. Whiskers are only shown for components which have three or more values reported in the literature. All values are reported from *in vivo* studies. LPS = diffusion of LPS molecules in *S. typhimurium*. Lipid = diffusion rate of a fluorescent lipid reporter probe in *E. coli* membranes. Peri = diffusion of soluble protein in the *E. coli* periplasm. Cyto = diffusion of soluble protein in the *E. coli* cytoplasm. (C) Viscosities of different membrane environments as measured by the use of fluorescent BODIPY C10 lipid reporter probes. *E. coli* data from Mika et al. (146) and synthetic phospholipid data from Wu et al. (196). BODIPY C10 specifically incorporates into the IM of *E. coli* and removal of the OM minimally affects the measured viscosity. Synthetic phospholipid 200nm LUVs were comprised of DLPC, DMPC, POPC, or DOPC. cP, centipoise.

Figure 5

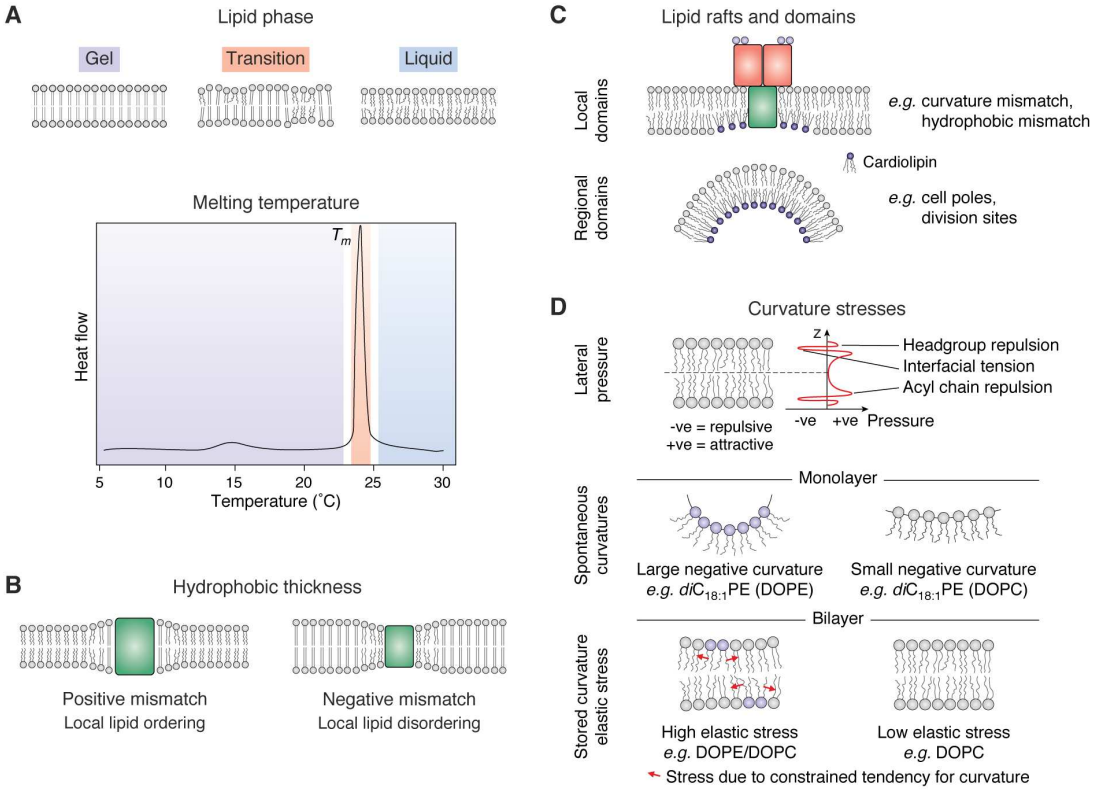

Figure 5. Physical and mechanical properties of a lipid bilayer. (A) Top: the phase of a lipid bilayer depends on the temperature, with the lipids being in an ordered (gel) phase below the transition temperature (T_m) and in a (liquid) disordered phase above the T_m. At the transition temperature, frustration between packing of regions of gel and liquid phase cause defects to occur at these boundaries. Bottom: a typical differential scanning calorimetry curve illustrating the thermal response of a DMPC (diC$_{14:0}$PC) bilayer with the regions of each phase coloured as above. (B) The hydrophobic thickness of a membrane depends on the lipid acyl chain length. However, when an OMP becomes embedded in a lipid bilayer, the membrane responds by trying to 'match' the hydrophobic thickness of the protein to that of the membrane in order to minimise the energetic penalty of exposing polar lipid headgroups to a hydrophobic OMP surface, or hydrophobic acyl tails to polar OMP loops. (C) Mixtures of lipids can separate forming 'rafts' or domains dependent on the physical conditions and lipid type. CL has a high propensity for negative curvature and has been shown to be enriched at cell poles and division sites where the membrane constricts. CL has also been observed to bind to membrane protein complexes such as the BAM complex (397) and cluster under patches of LPS in MD simulations (180, 181), suggesting it may help stabilise bilayer packing defects (which might be induced by LPS) and stabilise regions of large hydrophobic mismatch (for example around embedded proteins such as BamA). (D) Schematic describing stored curvature elastic stress and how this depends on lipid type. Schematic adapted from Booth & Curnow (398). Attractive and repulsive interactions driven by the packing of lipids creates a pressure differential along the normal of the membrane that must be overcome to deform or alter lipid packing. Incorporation of lipids which have a tendency towards negative curvature (due to the relative size of the headgroup versus the acyl chain, e.g. PE lipids) into a bilayer formed from lipids with a neutral or low curvature tendency (e.g. PC lipids) generates a stress force within the bilayer due to the opposing tendencies for bilayer formation of these lipids.

Figure 6

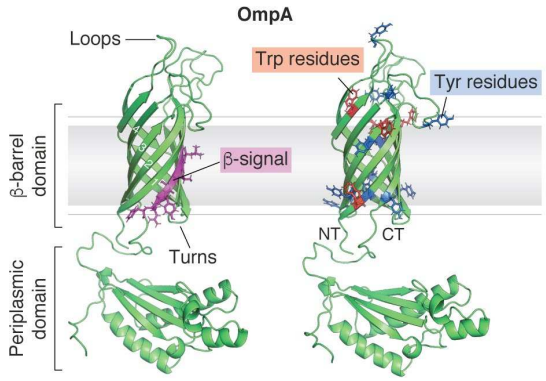

Figure 6. The structure and architecture of OmpA. The 8-stranded β-barrel OmpA has been used for many studies of OMP folding *in vitro*. It comprises a transmembrane β-barrel domain and a soluble periplasmic peptidoglycan-binding domain. Neighbouring β-strands are connected on their extracellular side by a long disordered 'loop' and on the periplasmic side by a short 'turn'. OMP β-strands are usually numbered N-terminal (NT) to C-terminal (CT) and the C-terminal β-strand often contains a conserved motif of Gly-X-X-Ar-X-Ar (where Ar = any aromatic residue), indicated in purple on OmpA, thought to be important for recognition by BAM (363, 399). Many OMPs contain an enrichment in aromatic Trp and Tyr residues in their β-barrel domain, particularly at the interfacial region between the lipid headgroups (approximate position indicated by the grey line) and acyl tails (approximate position indicated by the grey box) known as an 'aromatic girdle'. Trp (red) and Tyr (blue) residues found in the β-barrel domain of OmpA are indicated above. This model of OmpA was created in PyMol 2.X (Schrödinger, LLC) by fusing the NMR structures of the *E. coli* OmpA β-barrel (PDB: 1G90) (400) and its periplasmic domain (PDB: 2MQE) (401).

Figure 7

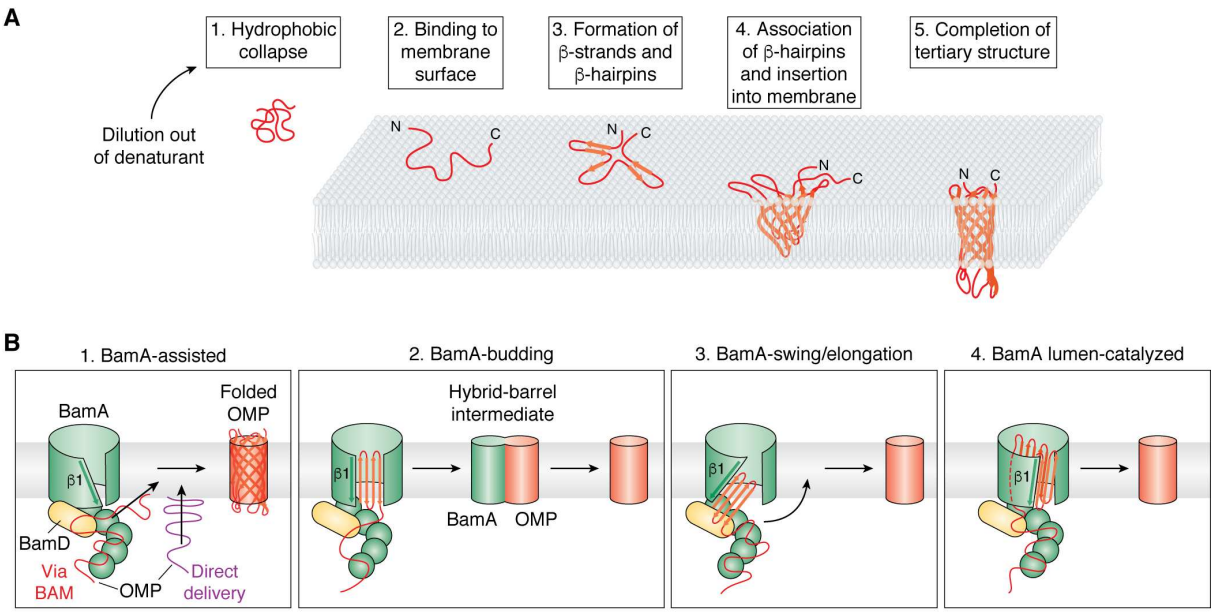

Figure 7. Mechanisms of OMP folding *in vitro* and *in vivo*. (A) Mechanism of spontaneous OMP folding *in vitro* as described for OmpA. *In vitro* studies have shed light on the folding pathway of model OMPs, particularly OmpA, after dilution out of high concentrations of denaturant in the presence of a lipid bilayer. Adapted from Danoff & Fleming (323). 1) immediately after dilution out of denaturant the chain undergoes hydrophobic collapse; 2) the polypeptide chain then binds to the surface of a membrane; 3) the nascent OMP then begins to form secondary structure as it brings together neighbouring β-strands to form β-hairpins while still mostly exposed to the aqueous environment; 4) these β-hairpins associate and begin to insert into the acyl tail region of the membrane; 5) the tertiary structure of the barrel is complete with the final step likely being a slower equilibration of side chains and extrusion of hydrophilic loops from the barrel lumen. (B) Proposed mechanisms of BAM-catalysed folding of OMPs *in vivo*. The nascent OMP is shown in red or purple, BamA is shown in green, and BamD is shown in yellow (other subunits have been omitted for clarity). **1, BamA-assisted)** substrate OMPs are delivered to BAM or directly to the membrane by periplasmic chaperones. These nascent OMPs then fold spontaneously into a region of destabilised membrane in front of the lateral gate of BamA, essentially following the same pathway as described in panel (A). **2, BamA-budding)** Binding/recognition of the OMP occurs on BAM before β-strands are added a β-hairpin at a time between β1-β16 of BamA, forming a semi-symmetric hybrid-barrel intermediate. Once all β-hairpins are added this folded OMP then buds off from BamA. **3, BamA-swing/elongation)** Binding/recognition of the OMP occurs on BAM and folding starts with templating of the C-terminal β-strand of a nascent OMP against β1 of BamA. Folding proceeds in the periplasm through the stepwise addition of the more β-strands. Once all β-strands have been added, a conformational change in BamA 'swings' the folded β-barrel into the membrane. **4, BamA lumen-catalyzed)** This model begins as described in 3) with templating against BamA β1. However, formation of further β-strands is catalysed against the lumen wall of BamA with a conserved motif in loop 6 of BamA (not shown) possibly stabilising this interaction. In all these models, BamD (yellow) may play an important role in substrate recognition and/or the conformational cycle.

Figure 8

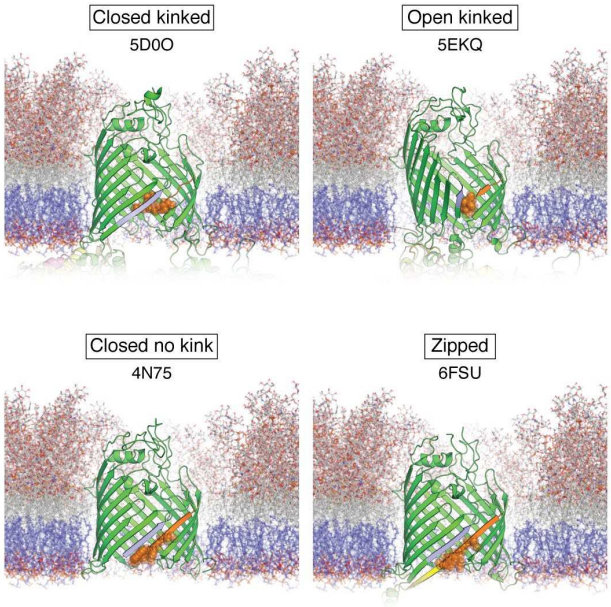

Figure 8. Conformations of the BamA lipid-facing lateral gate. Example structures of *E. coli* BamA adopting different conformations around the location of the β1-β16 seam/gate. BamA has been observed in both gate open and closed states with the open state observed in the presence of other BAM subunits but not in structures of BamA in isolation. Furthermore, in all structures of the full BAM complex β16 of BamA adopts a kinked conformation at a highly conserved glycine (G807) in both the open (PDB: 5EKQ - BamACDE) (341) and closed (PDB: 5D0O - BamABCDE) (330) states of the gate. Residues N427-G433 (β1) are highlighted in light blue, residues F802-W810 (β16) are indicated in orange, the kink is further highlighted with spheres (I806–W810). This kink is also observed in structures of BamA from *Salmonella enterica* (PDB: 5OR1) (344) and *Neisseria gonorrhoeae* (PDB: 4K3B) (328) (not shown) and in the BamA homologue, TamA, which also plays a role in OMP assembly (PDB: 4N74 & 4C00) (364) (not shown). BamA with a closed gate and no kink has been observed in isolation (PDB: 4N75 – BamAΔ1-427) (339), and in a hybrid BamA containing a C-terminal 9-residue extension (coloured yellow) comprised of part of turn 3 and β7 from OmpX which may represent a mimic of an OMP-BamA folding intermediate (PDB: 6FSU) (345). Structures are represented in an asymmetric bilayer with a mixture of phospholipids with 14-18 carbon acyl chains (shown in violet) in the inner leaflet and *E. coli* rough LPS in the outer leaflet (acyl chains in white). Note the different hydrophobic thickness between each leaflet. Asymmetric bilayer built using the GNOMM server (402).